50272-101

REPORT DOCUMENTATION PAGE	1. REPORT NO. NCEER-94-0015	2.	3. PB95-181996

4. Title and Subtitle
Generation of Hazard-Consistent Fragility Curves for Seismic Loss Estimation Studies

5. Report Date
June 14, 1994

6.

7. Author(s)
H.H.M. Hwang and J-R. Huo

8. Performing Organization Rept. No.

9. Performing Organization Name and Address
Memphis State University
Center for Earthquake Research and Information
Memphis, Tennessee 38152

10. Project/Task/Work Unit No.

11. Contract(C) or Grant(G) No.
(C) BCS-90-25010
NEC-91029
(G)

12. Sponsoring Organization Name and Address
National Center for Earthquake Engineering Research
State University of new York at Buffalo
Red Jacket Quadrangle
Buffalo, New York 14261

13. Type of Report & Period Covered
Technical report

14.

15. Supplementary Notes
This research was conducted at Memphis State University and was partially supported by the National Science Foundation under Grant No. BCS 90-25010 and the New York State Science and Technology Foundation under Grant No. NEC-91029.

16. Abstract (Limit: 200 words)

This report presents an analytical method for generating fragility curves and corresponding damage probability matrix for structures subject to earthquakes. In the proposed method, seismic hazards, local soil conditions, and nonlinear building behavior are systematically considered, and all the uncertainties in seismic, site, and structural parameters are taken into account. For an illustration, the proposed method is used to generate fragility curves and damage probability matrix for Smith Hall on the main campus of the University of Memphis, which is located close to the New Madrid seismic zone. The expected damage cost is also estimated based on the 1993 replacement value of the building.

17. Document Analysis a. Descriptors

b. Identifiers/Open-Ended Terms
Fragility curves. Loss estimates. Damage probability matrices. Memphis, Tennessee New Madrid seismic zone. Central United States. Probabilistic seismic hazard analysis. Nonlinear site response analysis. Local soil conditions. Soil profiles. Damage indices. Nonlinear response analysis. Earthquake engineering.

c. COSATI Field/Group

18. Availability Statement	19. Security Class (This Report)	21. No. of Pages
Release unlimited	Unclassified	172
	20. Security Class (This Page)	22. Price
	Unclassified	

(See ANSI-Z39.18) See Instructions on Reverse OPTIONAL FORM 272 (4-77) (Formerly NTIS-35) Department of Commerce

NATIONAL CENTER FOR EARTHQUAKE ENGINEERING RESEARCH

State University of New York at Buffalo

PB95-181996

Generation of Hazard-Consistent Fragility Curves for Seismic Loss Estimation Studies

by

H.H.M. Hwang and J-R. Huo

Memphis State University

Center for Earthquake Research and Informaiton

Memphis, Tennessee 38152

Technical Report NCEER-94-0015

June 14, 1994

This research was conducted at Memphis State University and was partially supported by the National Science Foundation under Grant No. BCS 90-25010 and the New York State Science and Technology Foundation under Grant No. NEC-91029.

NOTICE

PB95-181996

Generation of Hazard-Consistent Fragility Curves for Seismic Loss Estimation Studies

by

H.H.M. Hwang[1] and J-R. Huo[2]

June 14, 1994

Technical Report NCEER-94-0015

NCEER Task Numbers 91-4121 and 92-4001A

NSF Master Contract Number BCS 90-25010
and
NYSSTF Grant Number NEC-91029

1 Professor, Center for Earthquake Research and Information, Memphis State University
2 Visiting Scholar, Center for Earthquake Research and Information, Memphis State University

NATIONAL CENTER FOR EARTHQUAKE ENGINEERING RESEARCH
State University of New York at Buffalo
Red Jacket Quadrangle, Buffalo, NY 14261

PREFACE

The National Center for Earthquake Engineering Research (NCEER) was established to expand and disseminate knowledge about earthquakes, improve earthquake-resistant design, and implement seismic hazard mitigation procedures to minimize loss of lives and property. The emphasis is on structures in the eastern and central United States and lifelines throughout the country that are found in zones of low, moderate, and high seismicity.

NCEER's research and implementation plan in years six through ten (1991-1996) comprises four interlocked elements, as shown in the figure below. Element I, Basic Research, is carried out to support projects in the Applied Research area. Element II, Applied Research, is the major focus of work for years six through ten. Element III, Demonstration Projects, have been planned to support Applied Research projects, and will be either case studies or regional studies. Element IV, Implementation, will result from activity in the four Applied Research projects, and from Demonstration Projects.

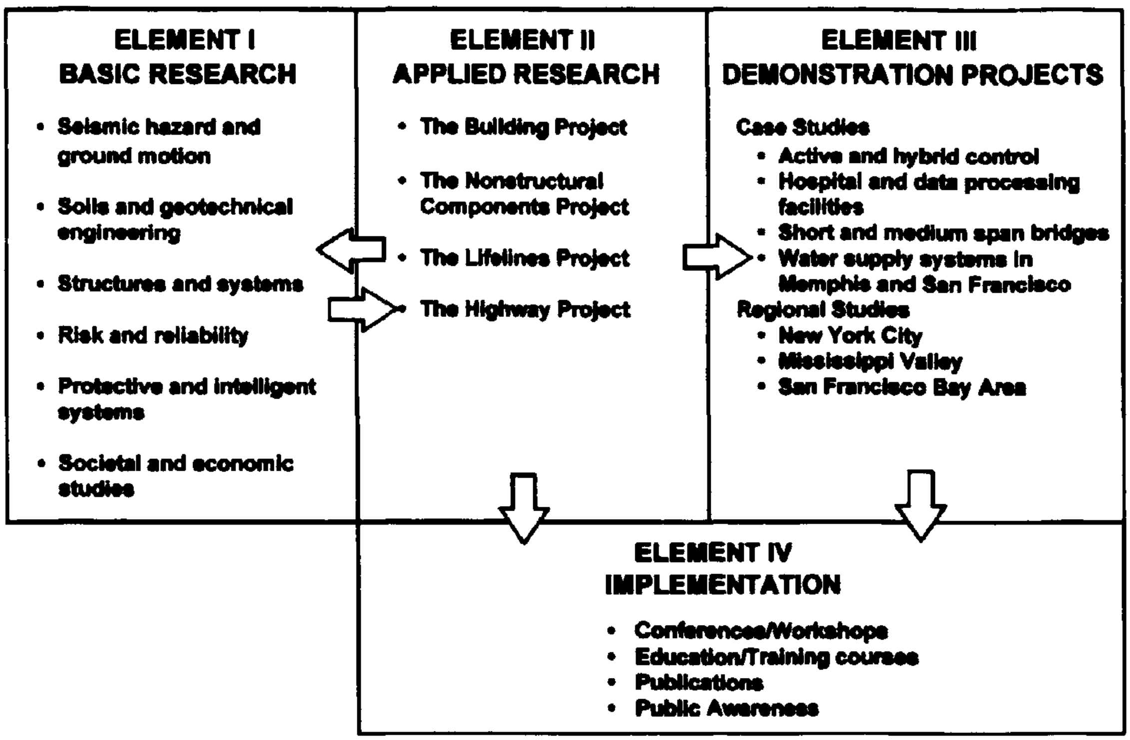

Research in the **Building Project** focuses on the evaluation and retrofit of buildings in regions of moderate seismicity. Emphasis is on lightly reinforced concrete buildings, steel semi-rigid frames, and masonry walls or infills. The research involves small- and medium-scale shake table tests and full-scale component tests at several institutions. In a parallel effort, analytical models and computer programs are being developed to aid in the prediction of the response of these buildings to various types of ground motion.

Two of the short-term products of the **Building Project** will be a monograph on the evaluation of lightly reinforced concrete buildings and a state-of-the-art report on unreinforced masonry.

The **risk and reliability program** constitutes one of the important areas of research in the **Building Project**. The program is concerned with reducing the uncertainty in current models which characterize and predict seismically induced ground motion, and resulting structural damage and system unserviceability. The goal of the program is to provide analytical and empirical procedures to bridge the gap between traditional earthquake engineering and socioeconomic considerations for the most cost-effective seismic hazard mitigation. Among others, the following tasks are being carried out:

1. Study seismic damage and develop fragility curves for existing structures.
2. Develop retrofit and strengthening strategies.
3. Develop intelligent structures using high-tech and traditional sensors for on-line and real-time diagnoses of structural integrity under seismic excitation.
4. Improve and promote damage-control design for new structures.
5. Study critical code issues and assist code groups to upgrade seismic design code.
6. Investigate the integrity of nonstructural systems under seismic conditions.

This report presents an analytical method for generating damage probability matrix and fragility curves for structures subject to earthquakes. In the proposed method, synthetic ground motions are generated based on probability-based scenario earthquakes established from a probabilistic seismic hazard analysis. Second, the effect of local soil conditions on ground motions is included in the analysis. Third, a frame-wall model instead of a stick model is used to represent a reinforced concrete building. Fourth, all the uncertainties in seismic, site, and structural parameters are taken into consideration. Therefore, seismic hazards, local soil conditions, and nonlinear building behavior are systematically considered in the proposed method. The generated fragility curves can be used to estimate the expected damage cost of the structure in the event of an earthquake. For an illustration, the proposed method is used to generate damage probability matrix and fragility curves of Smith Hall on the main campus of Memphis State University, which is located close to the New Madrid seismic zone. The expected damage cost is also estimated based on the 1993 replacement value of the building.

ABSTRACT

This report presents an analytical method for generating fragility curves and corresponding damage probability matrix for structures subject to earthquakes. In the proposed method, seismic hazards, local soil conditions, and nonlinear building behavior are systematically considered, and all the uncertainties in seismic, site, and structural parameters are taken into account. For an illustration, the proposed method is used to generate fragility curves and damage probability matrix for Smith Hall on the main campus of the University of Memphis, which is located close to the New Madrid seismic zone. The expected damage cost is also estimated based on the 1993 replacement value of the building.

ACKNOWLEDGMENTS

This report is based on research supported by the National Center for Earthquake Engineering Research under contract numbers NCEER 914121 and 924001A (NSF Grant No. BCS-9025010). Any opinions, findings, and conclusions expressed in the report are those of the writers and do not necessarily reflect the views of the NCEER, or the NSF of the United States. CERI Contribution Number 185.

The IDARC computer program used in this study was provided by Prof. Andrei M. Reinhorn, State University of New York at Buffalo. His generosity is greatly appreciated.

The drawings of Smith Hall were made available by Physical Plant and Planning, The University of Memphis. The assistance by Mr. Tony Poteet, Manager of Facility Planning & Design, is greatly appreciated. Thanks are also due to Ms. Meta Laabs, Director of Space Planning and Utilization, for providing the replacement cost of the building.

PB95-181996

TABLE OF CONTENTS

LIST OF ILLUSTRATIONS

LIST OF TABLES

SECTION 1

INTRODUCTION

In the event of an earthquake, a building may sustain no damage at a low level of ground shaking, while it may collapse at an extremely high level of ground shaking. The likelihood of structural damage caused by various levels of ground shaking is usually expressed as a set of fragility curves or a damage probability matrix. The fragility data of a structure can be generated using earthquake experience data and analytical approaches. In the area where earthquake-induced damage data are too scarce to provide sufficient statistics, fragility data generated from analytical approaches may be the only alternative.

1.1 Review of Previous Work

Hwang and Jaw (1990) proposed an analytical approach to generate fragility data for multi-story reinforced concrete buildings. In their approach, a structure is represented by a multi-degree-of-freedom (MDOF) stick model fixed at the base. The hysteretic relationship between the restoring shear force and the inter-story displacement is described by the modified Takeda model, which has a bilinear skeleton curve and includes both stiffness degrading and pinching effect (Hwang et al. 1988). The synthetic earthquake accelerograms exciting the structure are generated from Kanai-Tajimi power spectra corresponding to various levels of the peak ground acceleration. Uncertainties in seismic and structural parameters that define the analytical model of the earthquake-structure system are quantified. Then, the Latin Hypercube sampling technique (Iman and Conover 1980) is utilized to establish samples of the earthquake-structure system. For each sample, a nonlinear seismic analysis is performed to estimate the system ductility ratio, that is defined as the largest value of the story ductility ratios. A statistical analysis is performed to determine the probabilistic characteristics of the system ductility ratio.

Hwang and Jaw (1990) considered five damage states: (1) nonstructural damage, (2) slight structural damage, (3) moderate structural damage, (4) severe structural damage, and (5) collapse of a structure. For each damage state, a corresponding capacity is established from experimental data. The structural capacity is modeled by a lognormal distribution. Given the distributions of the structural response and the structural capacity corresponding to varying PGA levels, the probabilities that the structural response exceeds the structural capacity are determined to construct fragility curves. Following the aforementioned procedure, Hwang and Jaw (1990) performed a fragility analysis of a five-story shear wall building designed according to the seismic provisions of ANSI Standard A58.1-1982 and ACI code 318-83. Figure 1-1 shows the resulting fragility curves.

1.2 Proposed Improvements of the Methodology

This report describes the improvements of the aforementioned methodology for generating fragility curves and corresponding damage probability matrix of structures. First, synthetic ground motions are generated using probability-based scenario earthquakes that are

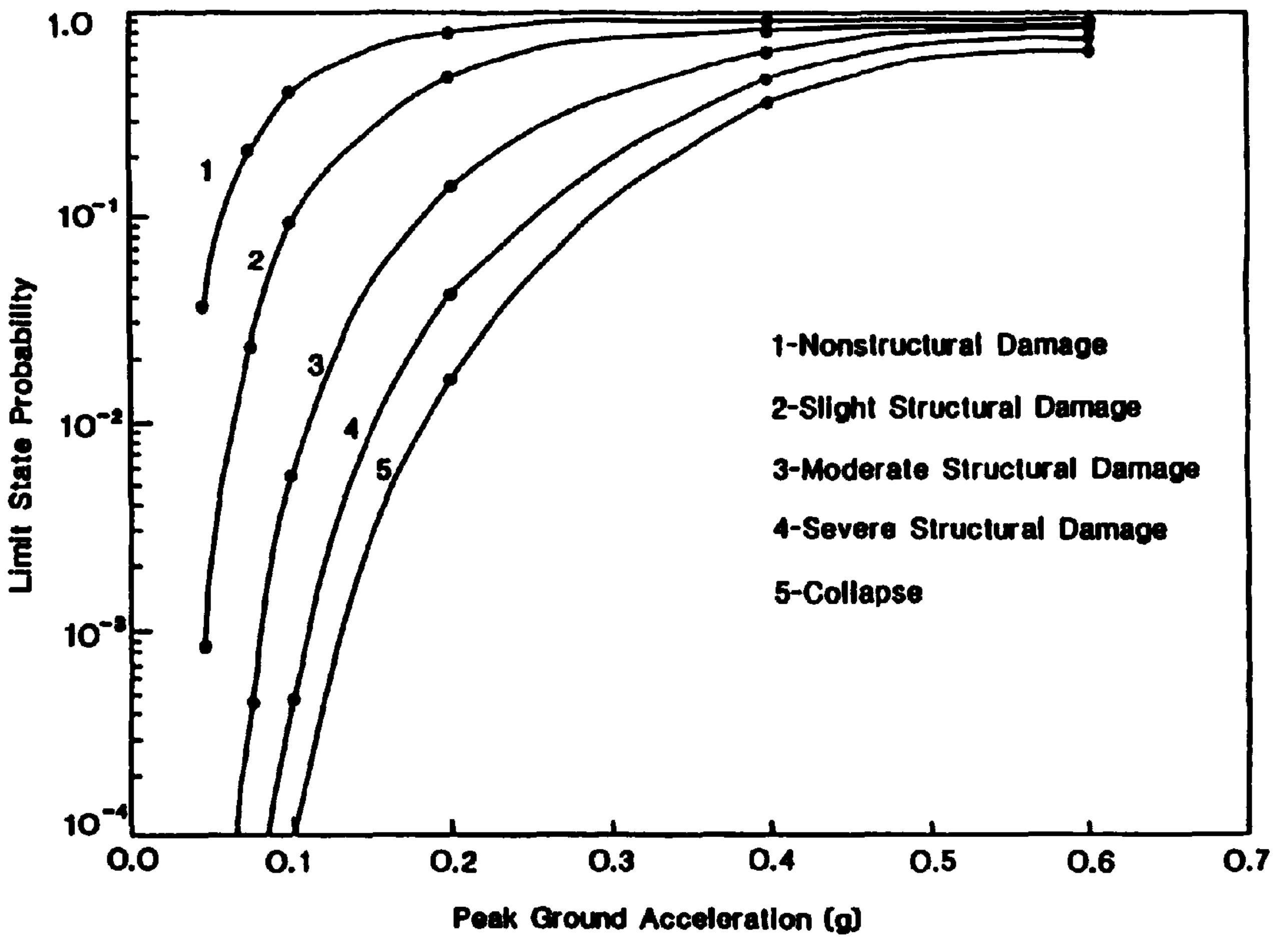

FIGURE 1-1 **Fragility Curves for a Five-Story Reinforced Concrete Building (after Hwang and Jaw 1990)**

established from a probabilistic seismic hazard analysis of the site where the analyzed structure is located. Second, the effect of local soil conditions on the ground motions is included in the analysis. Third, a frame-wall model instead of a stick model is used to represent a reinforced concrete building. Fourth, all the uncertainties in seismic, site, and structural parameters are taken into consideration in the reliability analysis. Figure 1-2 shows the major steps of the proposed methodology for generating fragility curves and estimating damage cost. In the following, an existing building on the main campus of the University of Memphis is used to illustrate the proposed methodology.

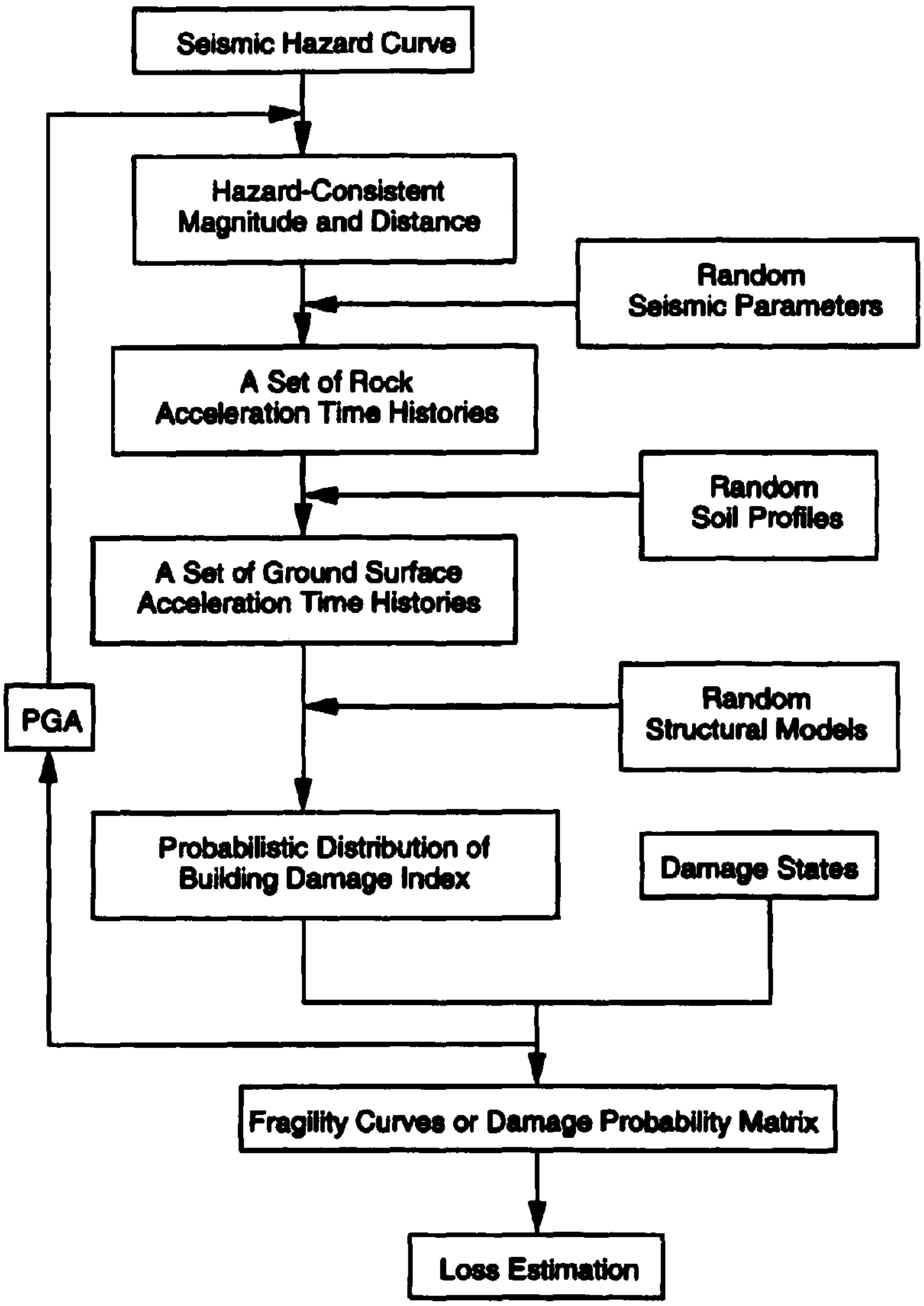

FIGURE 1-2 Proposed Procedure of Generating Seismic Fragility Curves of Structures

SECTION 2

PROBABILISTIC SEISMIC HAZARD ANALYSIS

The seismic hazard at a site is affected by the regional seismicity, source characteristics of earthquakes, attenuation of ground motion between the source and the site, and local soil conditions. By performing a probabilistic seismic hazard analysis, a seismic hazard curve is generated to display the annual probability of exceedance of a seismic intensity parameter, for example, the peak ground acceleration.

2.1 Seismic Source Zones

Figure 2-1 shows the seismicity of the New Madrid seismic zone (NMSZ) surrounding the site. The NMSZ is clearly delineated by the concentration of epicenters of earthquakes. Following Johnston and Nava (1990), the NMSZ is divided into two zones, Zone A and Zone B, as shown in Figure 2-1. Zone A is the same as that established by Johnston and Nava; while Zone B is taken as the upper half of a circular area within 200 km from the site. Zone B represents the background seismicity surrounding the site.

2.2 Frequency-Magnitude Relationship

A recurrence (frequency-magnitude) relationship indicates the chance of an earthquake occurring anywhere inside a source zone during a specified period of time, usually one year. In this study, the recurrence of earthquakes in a source zone is expressed using the frequency-magnitude relationship proposed by Gutenberg and Richter (1944).

$$\log N = a - b\, m_b \tag{2.1}$$

or

$$N(m_b) = e^{\alpha - \beta\, m_b} \tag{2.2}$$

where $\alpha = a \cdot \ln 10$, $\beta = b \cdot \ln 10$, m_b is the body-wave magnitude, and N is the cumulative number of earthquakes of magnitude m_b or greater. Hwang (1992) evaluated the coefficients a and b for Zone A from a combination of historical data (1804-1974) and instrumental data (1974-1990). The resulting frequency-magnitude relationship for Zone A is

$$\log N = 3.15 - 0.91\, m_b \tag{2.3}$$

For engineering applications, a lower-bound (minimum) magnitude m_{bo} and an upper-bound (maximum) magnitude m_{bu} need to be specified. The lower-bound and upper-bound magnitudes for Zone A are selected as body-wave magnitude of 5.0 and 7.5, respectively (Johnston 1988; Toro et al. 1992).

The frequency-magnitude relationship for Zone B is taken from Toro et al. (1992).

$$\log N = 2.51 - 0.88\, m_b \tag{2.4}$$

The lower-bound magnitude is also set as 5.0; however, the upper-bound magnitude is taken as 6.5 (Johnston and Nava 1990).

If the magnitude of an earthquake is limited by an upper bound and a lower bound, the frequency-magnitude relationship, equation (2.1), needs to be modified in order to satisfy the property of the probability distribution. The occurrence of an earthquake of magnitude equal to or greater than the lower-bound magnitude m_{bo} in a source zone is

$$N_o = N(m_{bo}) = e^{\alpha - \beta m_{bo}} \tag{2.5}$$

where N_o is the cumulative number of earthquakes of magnitude m_{bo} or greater. The probability distribution of m_b is

$$F(m_b) = 1 - \frac{N(m_b)}{N_o} = 1 - \frac{e^{\alpha - \beta m_b}}{e^{\alpha - \beta m_{bo}}} = 1 - e^{-\beta(m_b - m_{bo})} \tag{2.6}$$

To satisfy that $F(m_b)$ should be equal to one when m_b is equal to the upper-bound magnitude m_{bu}, a modified probability distribution $F^*(m_b)$ is defined as

$$F^*(m_b) = \frac{F(m_b)}{F(m_{bu})} = \frac{1 - e^{-\beta(m_b - m_{bo})}}{1 - e^{-\beta(m_{bu} - m_{bo})}} \tag{2.7}$$

Thus, the recurrence relationship bounded by a minimum magnitude and a maximum magnitude becomes as follows:

$$N(m_b) = N_o[1 - F^*(m_b)] = e^{\alpha - \beta m_b} \frac{1 - e^{-\beta(m_{bu} - m_b)}}{1 - e^{-\beta(m_{bu} - m_{bo})}} \tag{2.8}$$

Figure 2-2 shows the recurrence relationships for Zone A and Zone B.

2.3 Attenuation of Ground Motion

From the observation of past earthquakes, peak ground acceleration is usually attenuated as the epicentral distance increases, and the PGA values also exhibit a large dispersion. To include the dispersion of ground motion in the seismic hazard analysis, the horizontal peak ground acceleration A_H is assumed to be lognormally distributed. The coefficient of variation (COV) is taken as 0.5, and the mean value $\bar{A}_H$ is determined from the attenuation relationship for the NMSZ proposed by Nuttli and Herrmann (1984).

$$\log(\bar{A}_H) = 0.57 + 0.5\ m_b - 0.83\ \log(R^2 + h^2)^{1/2} - 0.00069\ R \tag{2.9}$$

where A_H is the horizontal peak ground acceleration averaged from two horizontal components recorded on unconsolidated soil sites, R is the epicentral distance, and h is the focal depth. On the basis of instrumental data in the NMSZ, the focal depth is taken as 10 km.

2.4 Seismic Hazard Curve

The occurrence of earthquakes in a seismic source zone is assumed to be a Poisson process. Thus, the probability that the horizontal peak ground acceleration A_H exceeds a specified value a^* is determined as

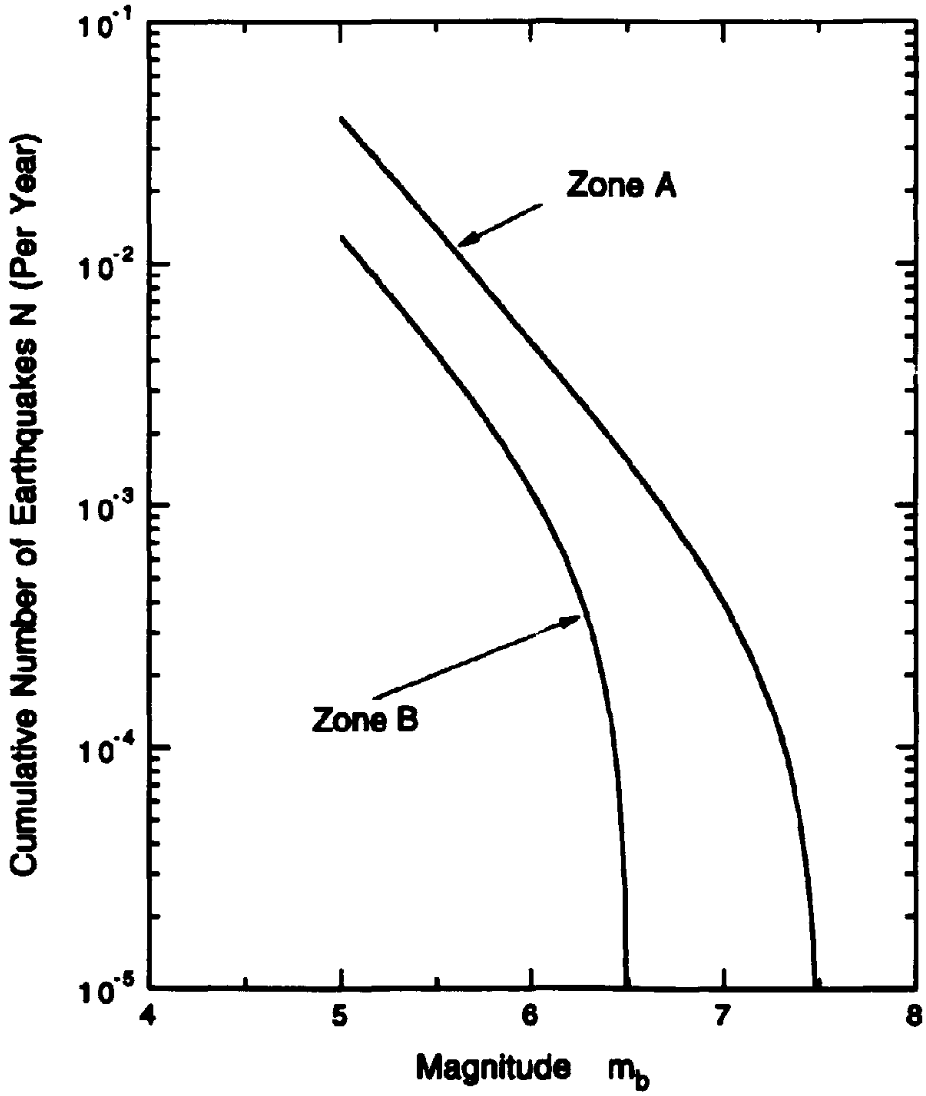

FIGURE 2-2 Recurrence Relationships for Zone A and Zone B

$$P(A_H > a^*) = 1 - \exp[-\nu_A(A_H > a^*)\,t] \qquad (2.10)$$

where t is the time period of interest (one year in this study); $\nu_A(A_H > a^*)$ is the annual occurrence of the events that A_H exceeds a^* and is calculated by summing contributions from all seismic source zones,

$$\nu_A(A_H > a^*) = \sum_k \nu_k(A_H > a^*) \qquad (2.11)$$

$$\nu_k(A_H > a^*) = N_{ko} \sum_i \sum_j P_k(A_H > a^* \mid m_{bi}, R_j)\, P_k(R_j)\, P_k(m_{bi}) \qquad (2.12)$$

where subscript "k" indicates the k-th seismic source zone. $P_k(A_H > a^* \mid m_{bi}, R_j)$ is the probability that A_H exceeds a^* given an earthquake of magnitude m_{bi} occurring at the distance R_j from the site. $P_k(m_{bi})$ is the probability that an earthquake of magnitude between m_{bi} and $m_{bi} + \Delta m_b$ occurs in the k-th source zone. $P_k(R_j)$ is the probability that an earthquake occurs at a distance between R_j and $R_j + \Delta R_j$ from the site.

By using the aforementioned procedure, a probabilistic seismic hazard analysis is performed for the site and the resulting seismic hazard curve is shown in Figure 2-3.

2.5 Probability-Based Scenario Earthquakes

The physical characteristics of earthquakes corresponding to a specified PGA level disappear in the process of performing a probabilistic seismic hazard analysis, because the resulting peak ground acceleration is

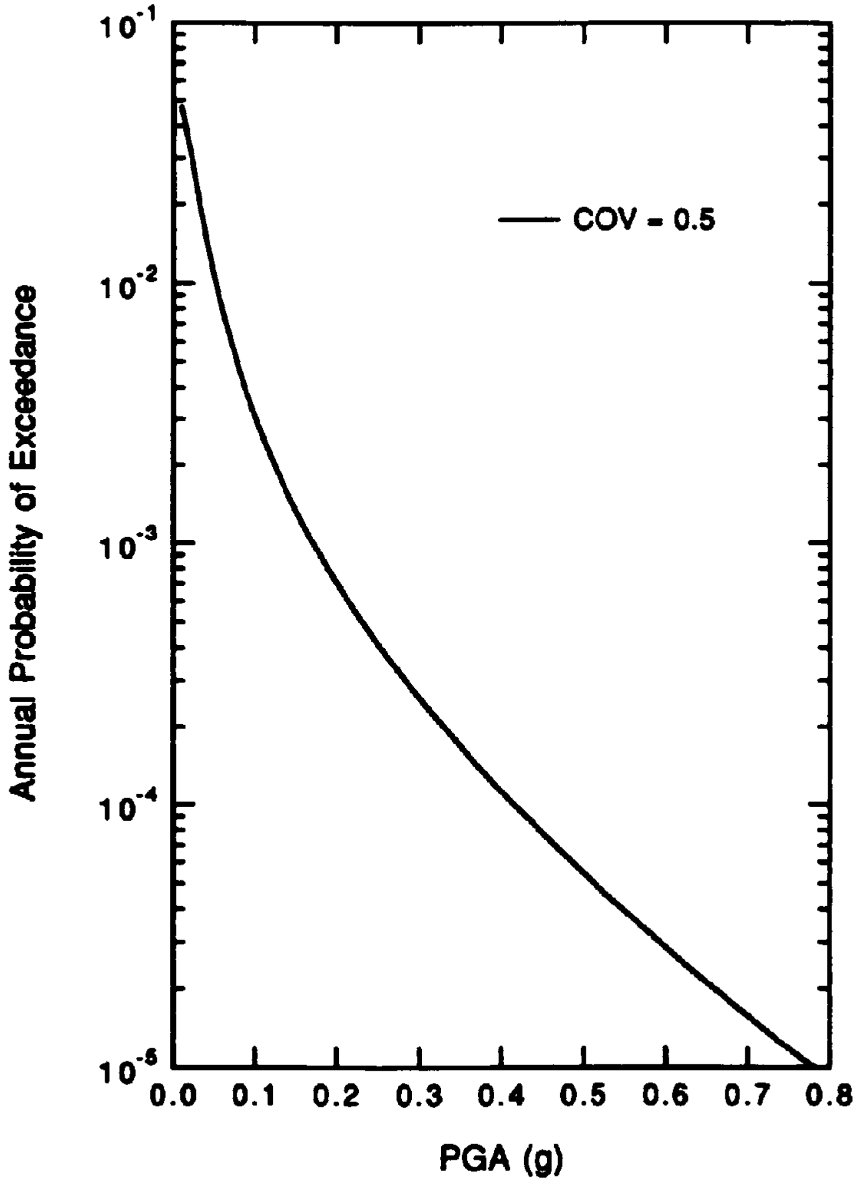

FIGURE 2-3 Seismic Hazard Curve for the Study Site

determined from the contribution of earthquakes of all magnitudes and distances within all seismic source zones. In order to establish the physical characteristics of an earthquake such as the acceleration time history, the probability-based scenario earthquake proposed by Ishikawa and Kameda (1991) is utilized. The probability-based scenario earthquake is defined by the contribution factor, hazard-consistent magnitude, and hazard-consistent distance for each seismic source zone.

For a specified PGA level, the contribution factor determines the contribution of a seismic source zone to the overall seismic hazard. The contribution factor C_k for the k-th seismic source zone is defined as

$$C_k(p_o) = \frac{\nu_k(p_o)}{\sum\limits_k \nu_k(p_o)} \tag{2.13}$$

The hazard-consistent magnitude $\bar{m}_{bk}$ and the hazard-consistent distance $\bar{R}_k$ for the k-th source zone are the conditional mean magnitude and the conditional mean distance, respectively, given that the A_H value exceeds a specified a^* value.

$$\bar{m}_{bk}(A_H > a^*(p_o))$$

$$= E(m_{bk} \mid A_H > a^*(p_o))$$

$$= \frac{\sum\limits_i \sum\limits_j m_{bi}\, P_k(A_H > a^*(p_o) \mid m_{bi}, R_j)\, P_k(R_j)\, P_k(m_{bi})}{\sum\limits_i \sum\limits_j P_k(A_H > a^*(p_o) \mid m_{bi}, R_j)\, P_k(R_j)\, P_k(m_{bi})} \tag{2.14}$$

and

$$\bar{R}_k(A_H > a^*(p_o))$$

$$= E(R_k \mid A_H > a^*(p_o))$$

$$= \frac{\sum_i \sum_j R_j P_k(A_H > a^*(p_o) \mid m_{bi}, R_j)\, P_k(R_j)\, P_k(m_{bi})}{\sum_i \sum_j P_k(A_H > a^*(p_o) \mid m_{bi}, R_j)\, P_k(R_j)\, P_k(m_{bi})} \tag{2.15}$$

Table 2-I summarizes the contribution factors, hazard-consistent magnitudes, and hazard-consistent distances for Zones A and B corresponding to the PGA values ranging from 0.05g to 0.5g. As shown in the table, the contribution factors of Zone A (about 75%) are much larger than those of Zone B (about 25%). It implies that the building will experience ground shaking mainly from earthquakes occurring in zone A. Thus, only the ground motions resulting from earthquakes occurring in Zone A are taken into consideration hereinafter.

In recent years, the moment magnitude **M** has been used for estimating ground motion. The moment magnitude **M** is defined as (Hanks and Kanamori 1979)

$$\mathbf{M} = \frac{2}{3}\log M_o - 10.7 \tag{2.16}$$

where M_o is the seismic moment. Using the relationship between the seismic moment M_o and the body-wave magnitude m_b proposed by Johnston (1989),

TABLE 2-I Hazard-Consistent Magnitudes and Distances

PGA (g)	Annual exceedance probability	Zone A			Zone B		
		C_A	$\bar{m}_{bA}$	$\bar{R}_A$ (km)	C_B	$\bar{m}_{bB}$	$\bar{R}_B$ (km)
0.05	0.1059×10^{-1}	0.77	5.9	104	0.23	5.7	86
0.10	0.3079×10^{-2}	0.76	6.4	100	0.24	5.8	57
0.15	0.1348×10^{-2}	0.76	6.6	98	0.24	5.8	42
0.20	0.7098×10^{-3}	0.76	6.8	95	0.24	5.9	33
0.25	0.4137×10^{-3}	0.76	6.9	93	0.24	5.9	28
0.30	0.2570×10^{-3}	0.76	7.0	90	0.24	6.0	25
0.40	0.1122×10^{-3}	0.76	7.1	86	0.24	6.0	20
0.50	0.5454×10^{-4}	0.75	7.2	82	0.25	6.1	17

$$\log M_o = 23.33 - 1.28\ m_b + 0.26\ m_b^2 \tag{2.17}$$

the moment magnitude **M** can be related to body-wave magnitude m_b as follows:

$$\mathbf{M} = 4.853 - 0.853\ m_b + 0.173\ m_b^2 \tag{2.18}$$

Using equation (2.18), the body-wave magnitudes in Table 2-I are converted into the moment magnitudes. The probability-based scenario earthquakes in terms of moment magnitude and epicentral distance are shown in Table 2-II.

TABLE 2-II Probability-Based Scenario Earthquakes

PGA (g)	m_b	M	R (km)
0.05	5.9	5.9	104
0.10	6.4	6.5	100
0.15	6.6	6.8	98
0.20	6.8	7.1	95
0.25	6.9	7.2	93
0.30	7.0	7.4	90
0.40	7.1	7.5	86
0.50	7.2	7.7	82

SECTION 3

GENERATION OF ACCELEROGRAMS AT THE BASE OF A SOIL PROFILE

3.1 Geological and Soil Conditions of the Study Site

Memphis and Shelby County are in the central part of the Mississippi embayment. The Paleozoic rock that forms the bedrock floor of the Mississippi embayment is located about 1 km (3000 ft) below the ground surface. This deep profile overlaying the bedrock is divided into soil layers and rock layers. The geological formation underlying the Memphis area is shown in Figure 3-1 (Whittenberg et al. 1977). The upper boundary of the Memphis sand, located about 100 m (300 ft) below the ground surface, has a shear wave velocity approximately 1000 m/sec. In engineering practice, soils with the shear wave velocity greater than 750 m/sec (2500 ft/sec) are regarded as rock (ICBO 1991; BSSC 1991). Thus, the interface of the Jackson formation and the Memphis sand (Figure 3-1) is taken as the base of the soil layers. Figure 3-2 shows the detailed strata of the soil layers of the study site. The soil profile is constructed based on the soil profiles established by Hwang and Lee (1990) for the Sheahan Pumping station, which is located close to the study site. Figure 3-3 shows the strata of rock layers established based on the studies by Hwang and Lee (1991) and Chiu et al. (1992). The effect of rock layers on the ground motion is included in the input motion at the base of the soil profile by using a frequency dependent amplification factor.

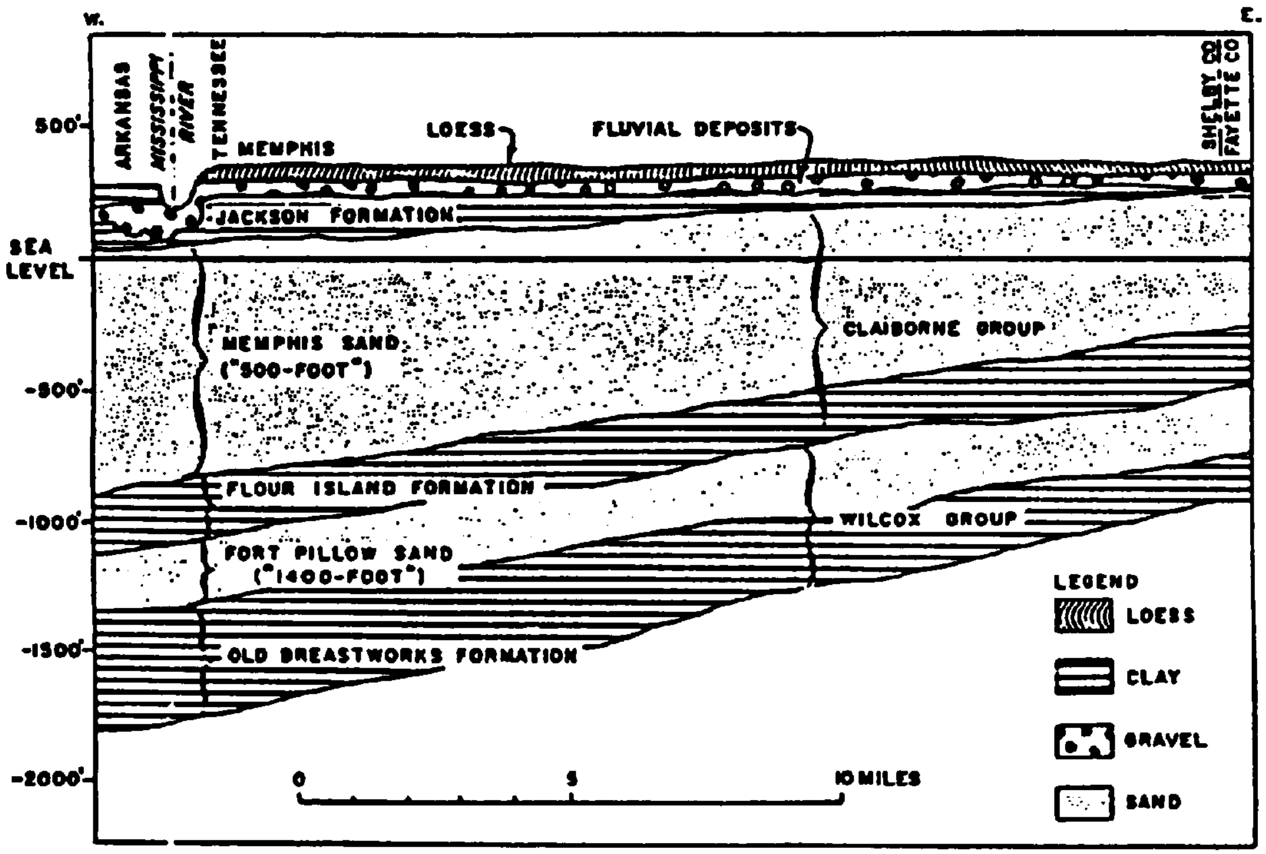

FIGURE 3-1 Geologic Formations Underlying Memphis and Shelby County (after Whittenberg et al. 1977)

Depth

0 m

STIFF CLAYEY SILT & SILTY CLAY (ML-CL)

$\gamma_S = 1.92$ g/cm^3 PI = 10-20 $S_u = 732$ g/cm^2 $V_S = 305.92$ m/s

3.66 m

VERY STIFF CLAYEY SILT & SILTY CLAY (ML-CL)

$\gamma_S = 2.00$ g/cm^3 PI = 10-20 $S_u = 1464$ g/cm^2 $V_S = 423.65$ m/s

10.37 m

DENSE CLAYEY SAND (SC)

$\gamma_S = 2.08$ g/cm^3 $K_o = 0.42$ $D_r = 0.75$ $\phi' = 35°$ $V_S = 255.59$ m/s

13.42 m

DENSE CLAYEY SAND TO SAND (SC-SP)

$\gamma_S = 2.08$ g/cm^3 $K_o = 0.41$ $D_r = 0.75$ $\phi' = 36°$ $V_S = 265.96$ m/s

15.86 m

DENSE SAND

$\gamma_S = 2.08$ g/cm^3 $K_o = 0.42$ $D_r = 0.75$ $\phi' = 36°$ $V_S = 274.5$ m/s

18.3 m

VERY DENSE SAND

$\gamma_S = 2.16$ g/cm^3 $K_o = 0.40$ $D_r = 0.93$ $\phi' = 38°$ $V_S = 313.85$ m/s

30.5 m

VERY STIFF CLAY

$\gamma_S = 1.98$ g/cm^3 PI = 40-80 $S_u = 1464$ g/cm^2 $V_S = 425.78$ m/s

42.7 m

HARD CLAY

$\gamma_S = 2.08$ g/cm^3 PI = 40-80 $S_u = 2928$ g/cm^2 $V_S = 588.65$ m/s

91.5 m

SOFT ROCK

$\gamma_S = 2.32$ g/cm^3 $V_S = 1000$ m/s

FIGURE 3-2 Soil Profile of the Study Site

0 m			Ground Surface
		Soil Layers	
91.5 m			
	Soft Rock	$\rho = 2.32\ g/cm^3$	$V_s = 1.0$ km/sec
200 m			
	Soft Rock	$\rho = 2.32\ g/cm^3$	$V_s = 1.1$ km/sec
500 m			
	Soft Rock	$\rho = 2.38\ g/cm^3$	$V_s = 1.4$ km/sec
700 m			
	Soft Rock	$\rho = 2.40\ g/cm^3$	$V_s = 1.7$ km/sec
900 m			
	Soft Rock	$\rho = 2.50\ g/cm^3$	$V_s = 2.0$ km/sec
1.0 km			
	Bedrock	$\rho = 2.70\ g/cm^3$	$V_s = 3.5$ km/sec
2.5 km			
	Bedrock	$\rho = 2.70\ g/cm^3$	$V_s = 3.2$ km/sec
5.0 km			
	Bedrock	$\rho = 2.70\ g/cm^3$	$V_s = 3.5$ km/sec
10.0 km			

FIGURE 3-3 Rock Layers Underlying the Study Site

3.2 Fourier Acceleration Amplitude Spectrum

An earthquake can be classified as a near-field, a far-field, or a long-distance earthquake, depending on the magnitude of the earthquake and its distance to the study site. The ground motion resulting from a near-field earthquake is dominated by both P- and S-waves, and the effects of source characteristics such as fault geometry and rupture direction must be considered in estimating ground motion. On the other hand, the ground motion from a far-field earthquake is mainly dominated by the direct S-wave, and the seismic source can be regarded as a point source in estimating ground motion. In the case of a long-distance earthquake, it is surface waves that contribute significantly to ground motion. The probability-based scenario earthquakes in Table 2-II are considered as far-field earthquakes, and a seismologically based model is utilized to establish the horizontal acceleration time history at the base of a soil profile.

Following Boore (1983), the Fourier acceleration amplitude spectrum at the base of a soil profile is expressed as follows:

$$A(f) = C \cdot S(f) \cdot D(f) \cdot AF(f) \tag{3.1}$$

where

C = scaling factor,
$S(f)$ = source spectral function,
$D(f)$ = diminution function, and
$AF(f)$ = amplification factor.

The source spectral function $S(f)$ used in this study is a ω^2 source acceleration spectrum proposed by Brune (Brune 1970, 1971). The source acceleration spectrum is expressed in terms of the corner frequency f_0 and seismic moment M_0:

$$S(f) = (2\pi f)^2 \frac{M_0}{1 + (f/f_0)^2} \tag{3.2}$$

The corner frequency f_0 is related to the seismic moment M_0 through the shear-wave velocity at the source region β and the stress parameter $\Delta\sigma$:

$$f_0 = 4.9 \times 10^6 \beta\left(\frac{\Delta\sigma}{M_0}\right)^{1/3} \tag{3.3}$$

The scaling factor C is given as

$$C = \frac{\langle R_{\theta\phi}\rangle \cdot F \cdot V}{4\pi\rho\beta^3} \cdot \frac{1}{r} \tag{3.4}$$

where

$\langle R_{\theta\phi}\rangle$ = radiation coefficient,
F = amplification factor due to the interface of the last soil layer and the first rock layer,
V = partition of a vector into horizontal components,
ρ = crustal density, and
r = hypocentral distance.

$<R_{\theta\phi}>$ is the radiation coefficient averaged over a range of azimuths θ and take-off angles ϕ. For ϕ and θ averaged over the whole focal sphere, the shear-wave radiation coefficient $<R_{\theta\phi}>$ is 0.55 (Boore and Boatwright 1984). V is the factor that accounts for the partition of a vector into horizontal components and is chosen as $1/\sqrt{2}$. The average focal depth in the NMSZ is taken as 10 km. The crustal density ρ of the continental crust at this focal depth is taken as 2.7 gm/cm^3 and the shear-wave velocity β is 3.5 km/sec.

F factor accounts for the amplification of the seismic wave as it is propagating through the interface of two layers with different properties. For the case of a vertical incident SH wave, F factor is the amplitude ratio of the incident wave and the refraction wave (Aki and Richards 1980).

$$F = \frac{2\rho_1\beta_1}{\rho_1\beta_1 + \rho_2\beta_2} \tag{3.5}$$

where subscripts "1" and "2" indicate the incident and refraction waves, respectively. By using the properties of the last soil layer and the first rock layer as shown in Figures 3-2 and 3-3, F factor is determined as 1.322.

The diminution function $D(f)$ represents the anelastic attenuation that accounts for the damping of the earth's crust and a sharp decrease of acceleration spectra above a cut-off frequency f_m.

$$D(f) = \exp\left[\frac{-\pi f r}{Q(f)\cdot\beta}\right] P(f, f_m) \tag{3.6}$$

where $Q(f)$ is the frequency-dependent quality factor for the study region,

$P(f, f_m)$ is the high-cut filter. The quality factor $Q(f)$ describes the attenuation of seismic waves and is frequency dependent. Dwyer et al. (1983) conducted an attenuation study in the central United States and suggested the quality factor of shear and L_g waves as follows:

$$Q(f) = 1500\, f^{0.40} \tag{3.7}$$

The high-cut filter $P(f, f_m)$ accounts for the observation that the acceleration spectra often show a sharp decrease above a cut-off frequency f_m, which cannot be attributed to path attenuation. In this study, a Butterworth filter is used as a high-cut filter.

The amplification factor $AF(f)$ is used to account for the effect of rock layers on earthquake motion because of the decrease of shear-wave velocities in the rock layers. Following Joyner et al. (1981), $AF(f)$ is calculated as

$$AF(f) = \sqrt{\frac{\rho\beta}{\rho_r\beta_r}} \tag{3.8}$$

where ρ_r and β_r are the effective density and the effective shear-wave velocity of the upper n layers. The cumulative travel time T_n of the upper n layers measured from the base of the soil profile is computed as

$$T_n = \sum_{i=1}^{n} \frac{H_i}{\beta_i} \tag{3.9}$$

where β_i and H_i are the shear-wave velocity and thickness of the i-th layer, respectively. The wave frequency f_n of the upper n layers is calculated as $f_n=1/(4T_n)$ based on the theory of repeated reflection waves. The effective shear-wave velocity β_r corresponding to the wave frequency f_n is

$$(\beta_r)_n = \frac{H_n}{T_n} = 4 f_n H_n \tag{3.10}$$

and the corresponding effective density $(\rho_r)_n$ is expressed as

$$(\rho_r)_n = \sum_{i=1}^{n} \frac{H_i \rho_i}{H_n} \tag{3.11}$$

where H_n is the total depth of the upper n layers. By using the properties of rock layers shown in Figure 3-3, the amplification factors for the study site are calculated and shown in Table 3-I.

3.3 Power Spectrum

An earthquake accelerogram generally shows a build-up segment followed by a strong-motion segment and then a decay segment. The frequency content of an earthquake accelerogram is found to be approximately constant during the strong-motion segment. Thus, the strong-motion segment of an acceleration time history is considered as a stationary random process, and the one-sided power spectrum $S_a(f)$ can be derived from the Fourier amplitude spectrum.

$$S_a(f) = \frac{1}{\pi T_e} |A(f)|^2 \tag{3.12}$$

TABLE 3-I Calculation of Amplification Factor

H_i (m)	$\sum H_i$ (m)	β_i (m/s)	ρ_i (t/m^3)	T_n (sec)	f_n (Hz)	β_r (m/s)	ρ_r (t/m^3)	AF
					>2.31			2.02
108	108	1000	2.32	0.11	2.31	1000.0	2.32	2.02
300	408	1100	2.32	0.38	0.66	1071.6	2.32	1.95
200	608	1400	2.38	0.52	0.48	1161.2	2.34	1.87
200	808	1700	2.40	0.64	0.39	1260.1	2.35	1.78
100	908	2000	2.50	0.69	0.36	1313.6	2.37	1.74
1500	2408	3500	2.70	1.12	0.22	2150.4	2.57	1.31
2500	4908	3200	2.70	1.90	0.13	2581.7	2.63	1.18
5000	9908	3500	2.70	3.33	0.07	2975.7	2.67	1.09

where T_e is the strong-motion duration. In this study, the strong-motion duration is determined by using the formula proposed by Huo et al. (1991).

$$Ln(T_e) = -5.222 + 0.751\ \mathbf{M} + 0.582\ Ln(R + 10) + \varepsilon \tag{3.13}$$

where ε is a normal random variable to account for the variability of the strong-motion duration. The mean value of ε is zero and the standard deviation is 0.37. For moment magnitude **M** of 7.1 and distance R of 95 km, the mean duration of the strong-motion is determined as 16.7 sec.

3.4 Synthetic Acceleration Time History

In this study, the synthetic acceleration time history is generated using the method proposed by Shinozuka (1974). Given the power spectrum, the stationary acceleration time history $a_s(t)$ is generated as follows:

$$a_s(t) = \sqrt{2} \sum_{k=1}^{N} \sqrt{S_a(\omega_k)\Delta\omega}\ \cos(\omega_k t + \phi_k) \tag{3.14}$$

where

$S_a(\omega_k)$ = one-sided earthquake power spectrum,

N = number of frequency intervals,

$\Delta\omega$ = frequency increment,

ω_k = $k\Delta\omega$, and

ϕ_k = random phase angles uniformly distributed between 0 and 2π.

The nonstationary acceleration time history a(t) is obtained by multiplying an envelope function w(t) to the stationary process $a_s(t)$.

$$a(t) = a_s(t) \cdot w(t) \tag{3.15}$$

The envelope function used in this study is modified from the one proposed by Cakmak et al. (1985).

$$w(t) = C_1 \cdot \left(\frac{t}{T_e}\right)^{\beta} \cdot \exp\left(-C_2 \cdot \frac{t}{T_e}\right) \tag{3.16}$$

where

$$C_1 = \left(\frac{C_2 \cdot e}{\beta}\right)^{\beta} \tag{3.17}$$

$$C_2 = 2\sqrt{3} \tag{3.18}$$

$$\beta = C_2 \cdot \frac{t_{max}}{T_e} \tag{3.19}$$

The parameter β controls the width of the envelope shape. t_{max} is the time at the peak of the envelope function and is determined as

$$t_{max} = (0.2 + 0.5\ C_3) \cdot T_e \tag{3.20}$$

where C_3 is a random variable uniformly distributed between zero and one. As an example, the envelope function with T_e = 16.7 sec and C_3 = 0.6 is shown in Figure 3-4. Using the aforementioned procedure and the seismic

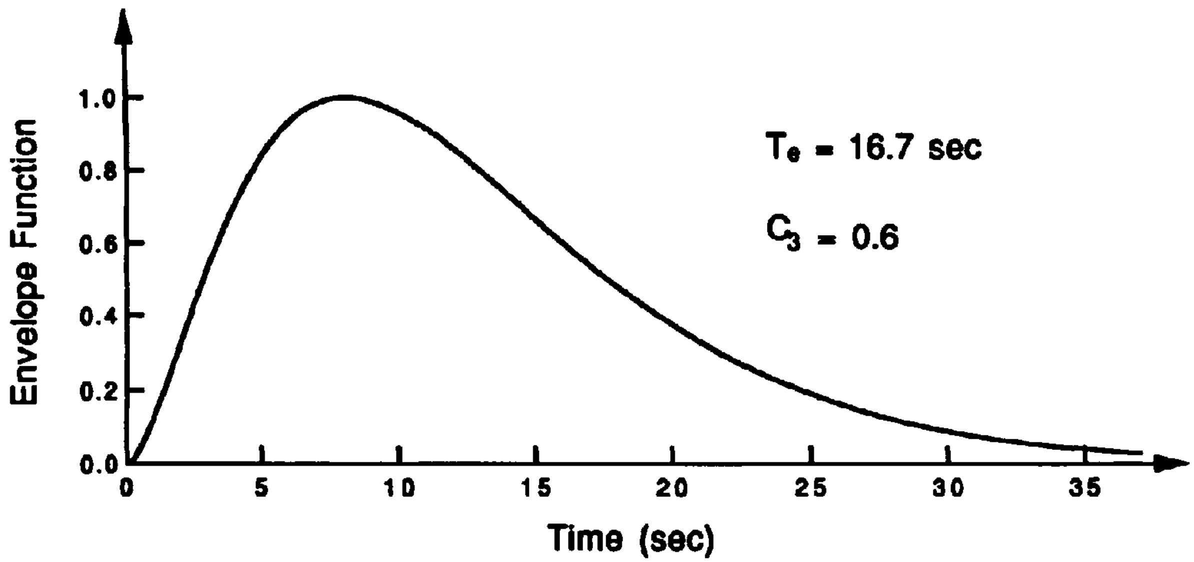

FIGURE 3-4 A Sample of Acceleration Envelope Function

parameters summarized in Table 3-II, a horizontal acceleration time history at the base of a soil profile is generated and shown in Figure 3-5.

3.5 Uncertainty in Seismic Parameters

For a specified moment magnitude and epicentral distance, some parameters such as the crustal density ρ and shear-wave velocity β appear to have less influence on the resulting horizontal accelerations. On the other hand, the stress parameter $\Delta\sigma$, strong-motion duration T_e, phase angle ϕ, and cut-off frequency f_m have significant effects on accelerations. In this study, the variation in the strong-motion duration is modeled with the lognormal distribution (equation 3.13), while the variation in the stress parameter and in the cut-off frequency is modeled with the uniform distribution. Following Hwang and Lee (1990), the range of the stress parameter is from 100 to 200 bars, and the range of the cut-off frequency is from 20 to 40 Hz. Table 3-III summarizes the random parameters ($\Delta\sigma$, T_e, ϕ, f_m, C_3) considered in this study. For each random parameter, 50 samples are generated according to the corresponding distribution. These samples are kept within two standard deviations around the mean value. The samples of these five random variables are then combined using the Latin Hypercube sampling technique to generate 50 earthquake time histories at the base of the soil profile for each scenario earthquake listed in Table 2-II.

TABLE 3-II Seismic Parameters Used in the Study

Item	Symbol	Value
Moment magnitude	$\mathbf{M}$	7.1
Epicentral distance	R	95 km
Focal depth	h	10 km
Radiation coefficient	$\langle R_{\theta\phi} \rangle$	0.55
Horizontal component	V	0.71
Source-rock shear-wave velocity	β	3.5 km/sec
Source-rock density	ρ	2.7 gm/cm^3
Quality factor	$Q(f)$	$1500f^{0.4}$
Stress parameter	$\Delta\sigma$	150 bars
Cut-off frequency	f_m	30 Hz
Strong-motion duration	T_e	16.7 sec

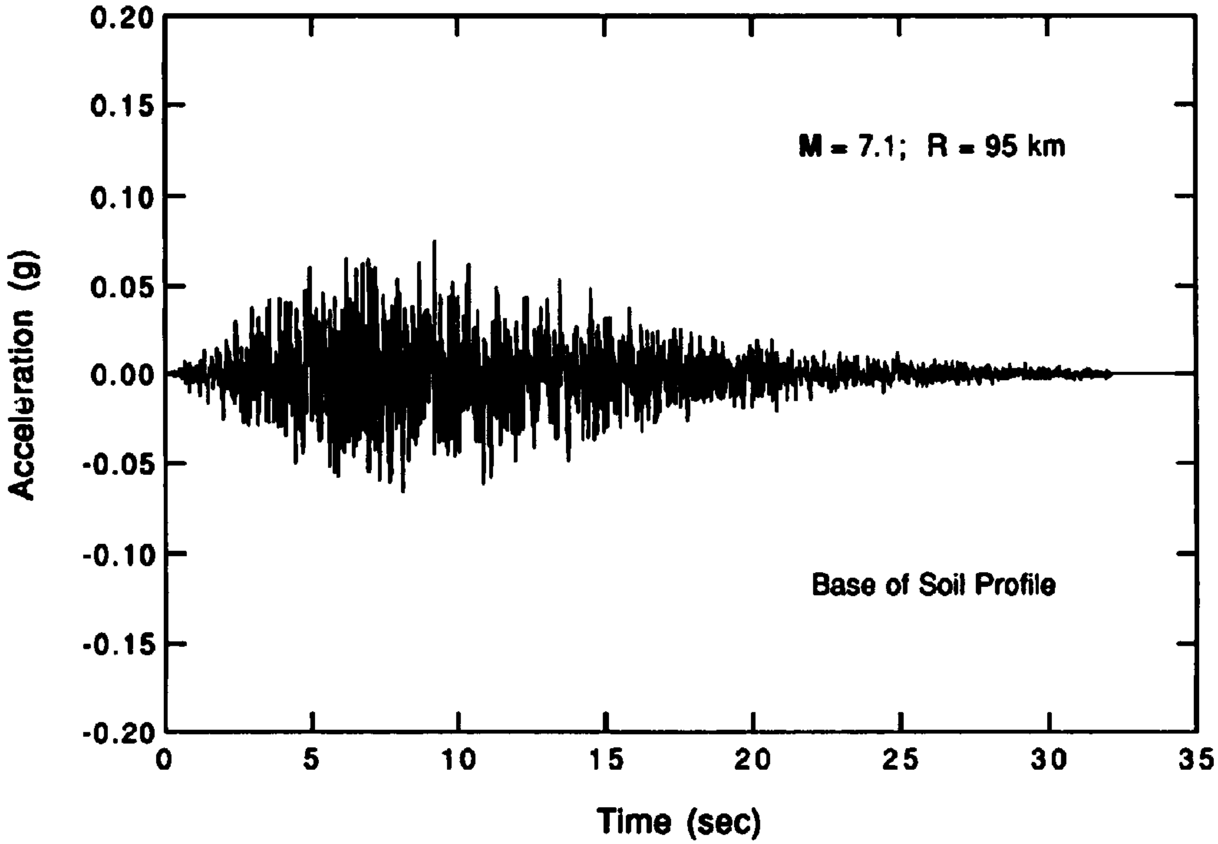

FIGURE 3-5 A Sample of Acceleration Time History at the Base of the Soil Profile (M = 7.1, R = 95 km)

TABLE 3-III Uncertainties in Seismic Parameters

Parameter	Distribution	Range
$\Delta\sigma$	Uniform	100 - 200 bars
f_m	Uniform	20 - 40 Hz
ϕ	Uniform	0 - 2π
C_3	Uniform	0 - 1
T_e	Lognormal	Equation (3.13)

SECTION 4

NONLINEAR SITE RESPONSE ANALYSIS

Soil exhibits significantly nonlinear behavior under strong ground shaking. In this study, the nonlinear site response analysis is performed using the SHAKE computer program (Schnabel et al. 1972). In the SHAKE program, the soil profile consists of horizontal soil layers, and the input earthquake ground motion is vertically incident from the base of the soil profile. For each soil layer, the soil parameters required by the SHAKE program include the thickness, unit weight γ_s, and shear wave velocity V_s or low-strain shear modulus G_0. Furthermore, the shear modulus ratio G/G_0 and damping ratio ζ, which are dependent of the shear strain γ, also need to be specified.

4.1 Probabilistic Soil Properties

The values of soil parameters determined from test data are greatly affected by testing conditions, calibration of testing equipment, and simulation of initial environmental conditions. The variability of soil parameters should be considered in the site response analysis to avoid the bias resulting from choosing a single value for the parameter.

Figure 3-2 shows the static soil properties and the shear wave velocity of each soil layer taken from Hwang and Lee (1990). In this study, the relative density of sand D_r and the undrained shear strength of clay S_u are considered as uniform random variables (see Table 4-I). The dynamic properties of soils in the Memphis area were investigated by Hwang et al.

(1990), Lee et al. (1991), and Chang et al. (1992). A review of these results is shown in Appendix A. On the basis of the review, the probabilistic dynamic characteristics of sands and clays in the Memphis area have been established. Figure 4-1 shows the shear modulus reduction curves and damping ratio curves for sands. The shear modulus reduction and damping ratio curves for clays with PI = 15 and 50 are shown in Figures 4-2 and 4-3, respectively.

4.2 Earthquake-Site Models

In this study, the relative density of sand, undrained shear strength of clay, shear modulus ratio and corresponding damping ratio for sands and clays are considered as random variables. For a sand layer, 50 random samples of D_r are generated according to the uniform distribution. Then, the low-strain shear modulus corresponding to each sample of D_r is determined. For a clay layer, the same procedure is used to construct 50 samples of S_u and corresponding low-strain shear moduli.

Fifty samples of the shear modulus ratio and the corresponding damping ratio at various levels of shear strain are generated according the normal distribution. These samples are within the probability between 2.275% and 97.725%. The sample values at various strain levels corresponding to the same probability are connected to form a sample of the shear modulus reduction curve or the damping ratio curve. A random number is then used to construct the shear modulus reduction curve and the corresponding damping ratio curve for each soil layer in the entire soil profile. Thus, 50 samples of the soil profile are constructed by considering uncertainties in

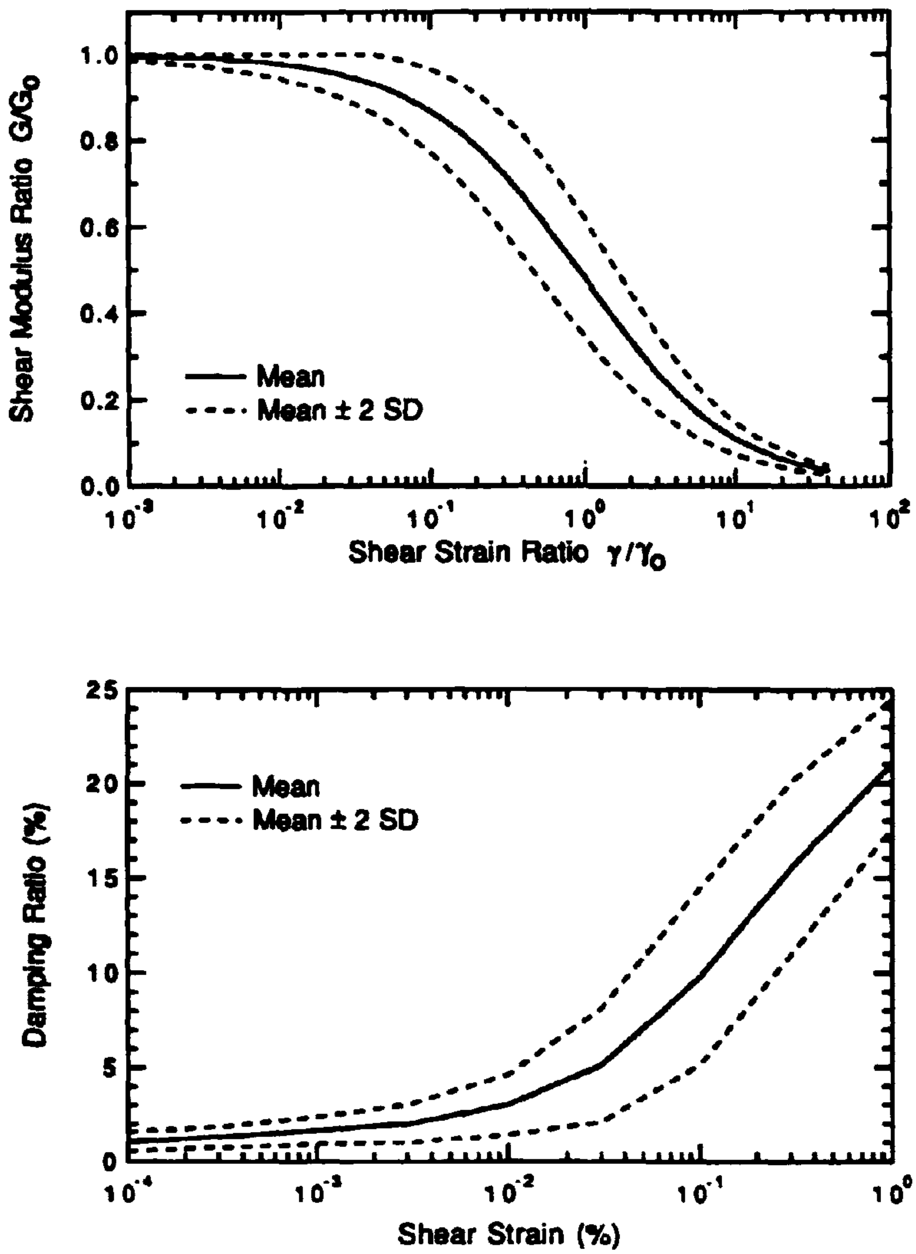

FIGURE 4-1 Shear Modulus Reduction and Damping Ratio Curves for Sands

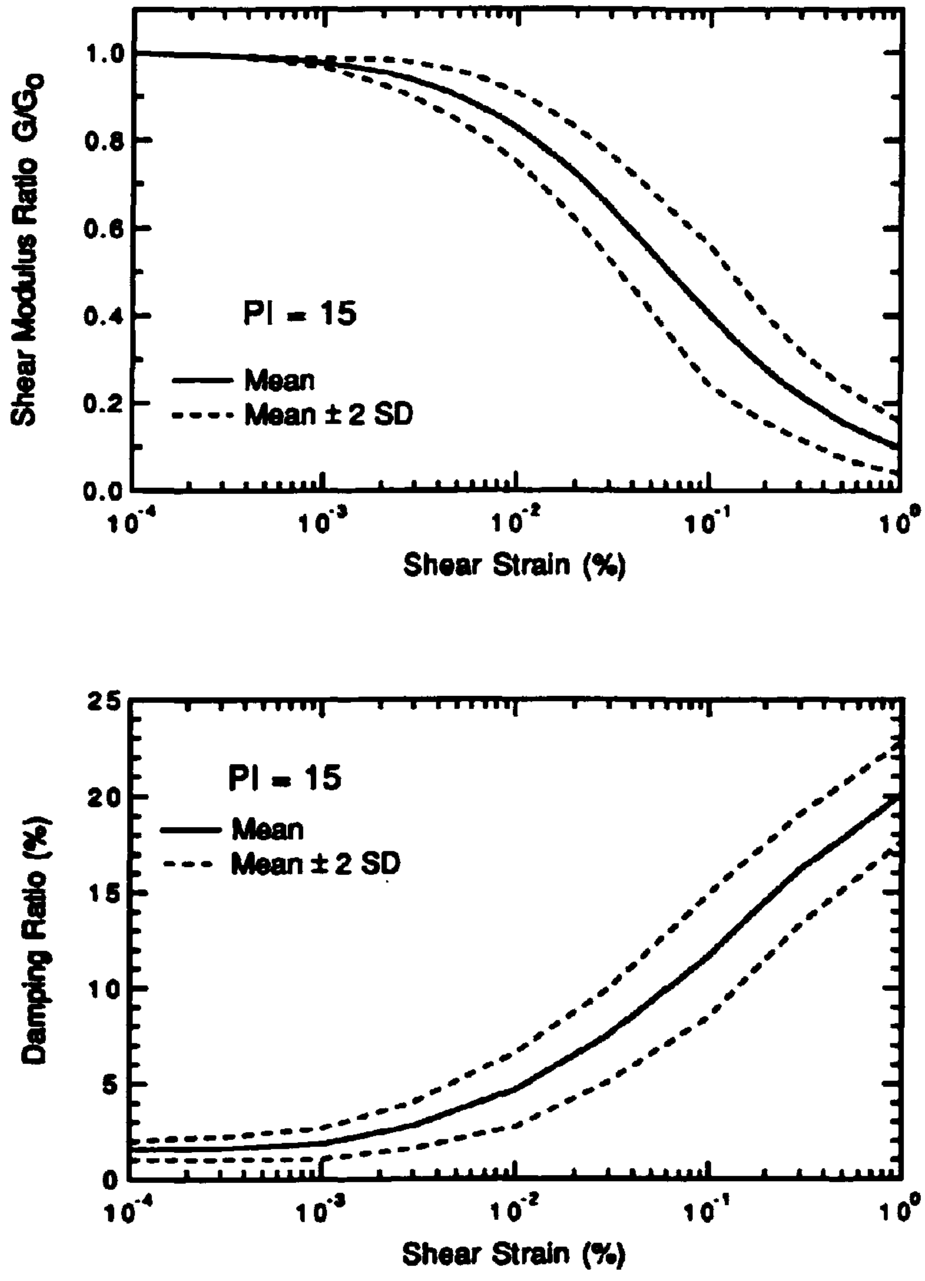

FIGURE 4-2 **Shear Modulus Reduction and Damping Ratio Curves for Clays with PI = 15**

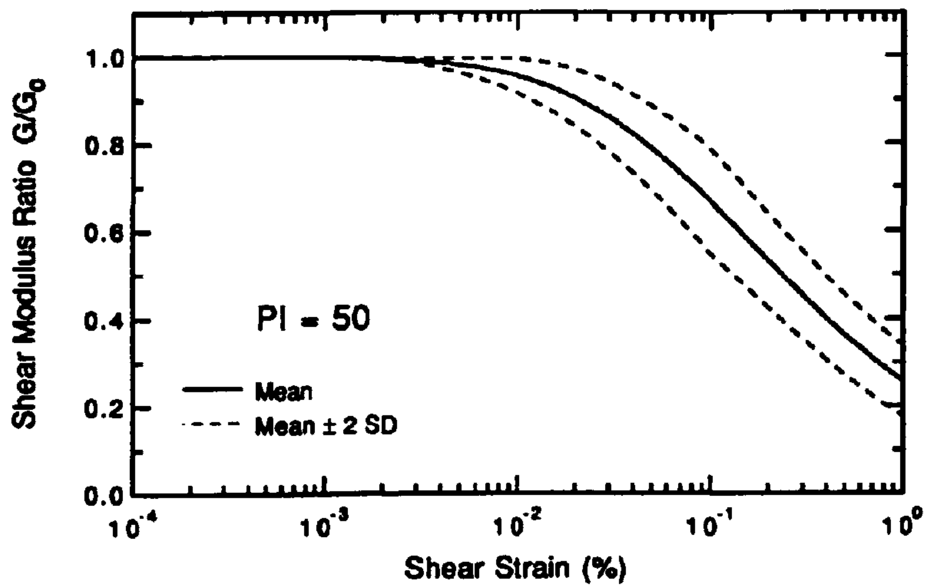

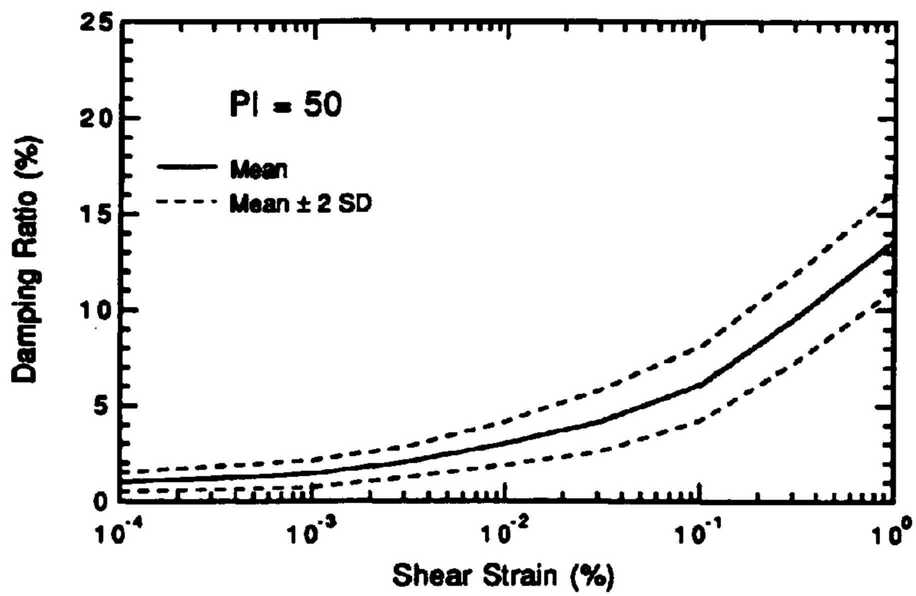

FIGURE 4-3 Shear Modulus Reduction and Damping Ratio curves for Clays with PI = 50

the relative density of sand, undrained shear strength of clay, shear modulus ratio and corresponding damping ratio for sands and clays. Fifty samples of the soil profile are then matched with 50 samples of earthquake base input accelerations using the Latin Hypercube sampling technique to establish 50 samples of the earthquake-site system for each probability-based scenario earthquake listed in Table 2-II.

4.3 Generation of Accelerograms at the Ground Surface

For each scenario earthquake, 50 runs are performed using the SHAKE program to generate the acceleration time histories at the ground surface. For fragility analysis, each acceleration time history at the ground surface is scaled by the PGA value associated with the scenario earthquake. For illustration, one sample of the acceleration time histories at the ground surface and at the base of the soil profile resulting from **M** = 7.1 and **R** = 95 km are shown in Figure 4-4. The acceleration time history is scaled to 0.2g (Figure 4-5). For comparison, the samples of the acceleration time histories with PGA equal to 0.05, 0.1, 0.2, and 0.3g are also shown in Figure 4-5.

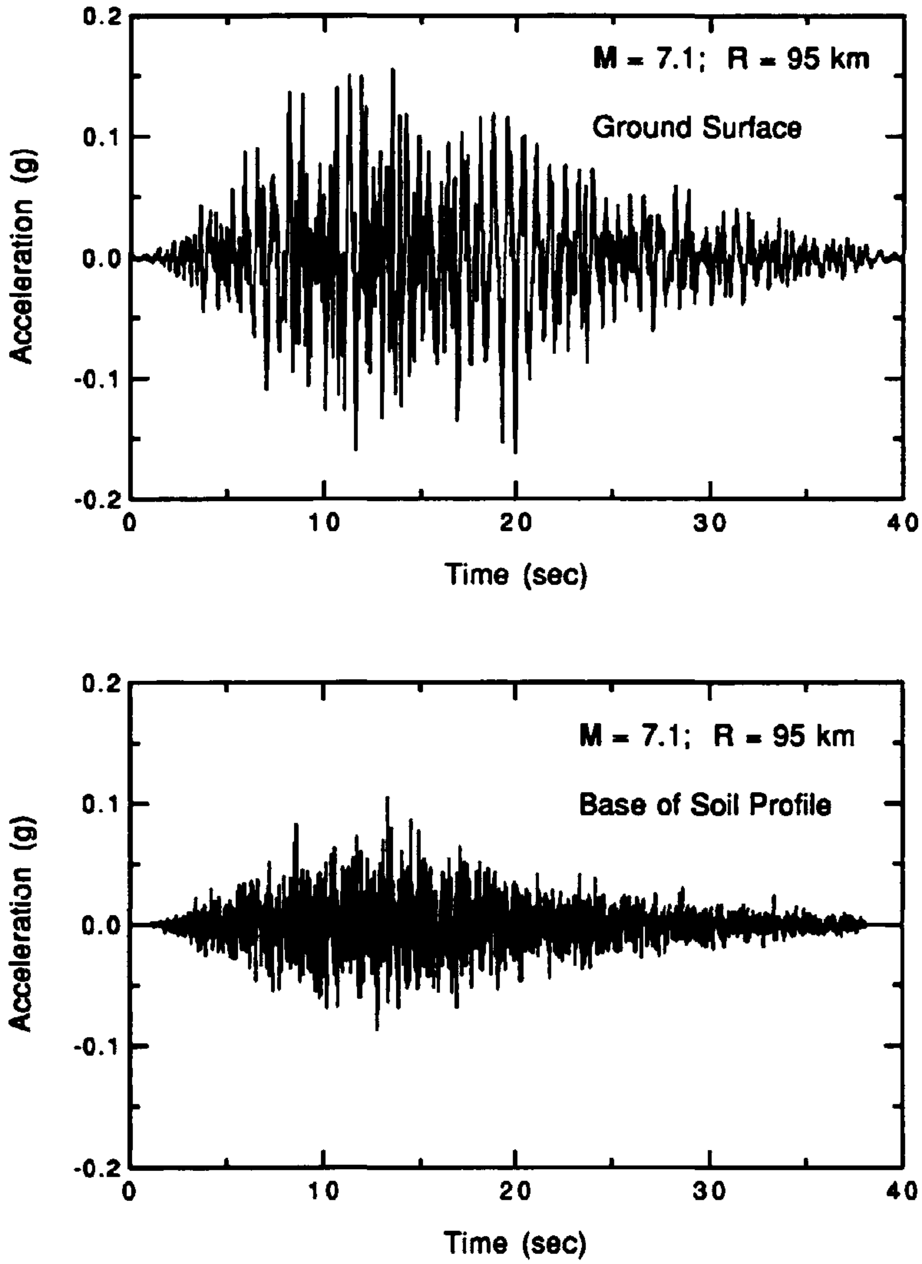

FIGURE 4-4 A Sample of Acceleration Time Histories (M = 7.1, R = 95 km)

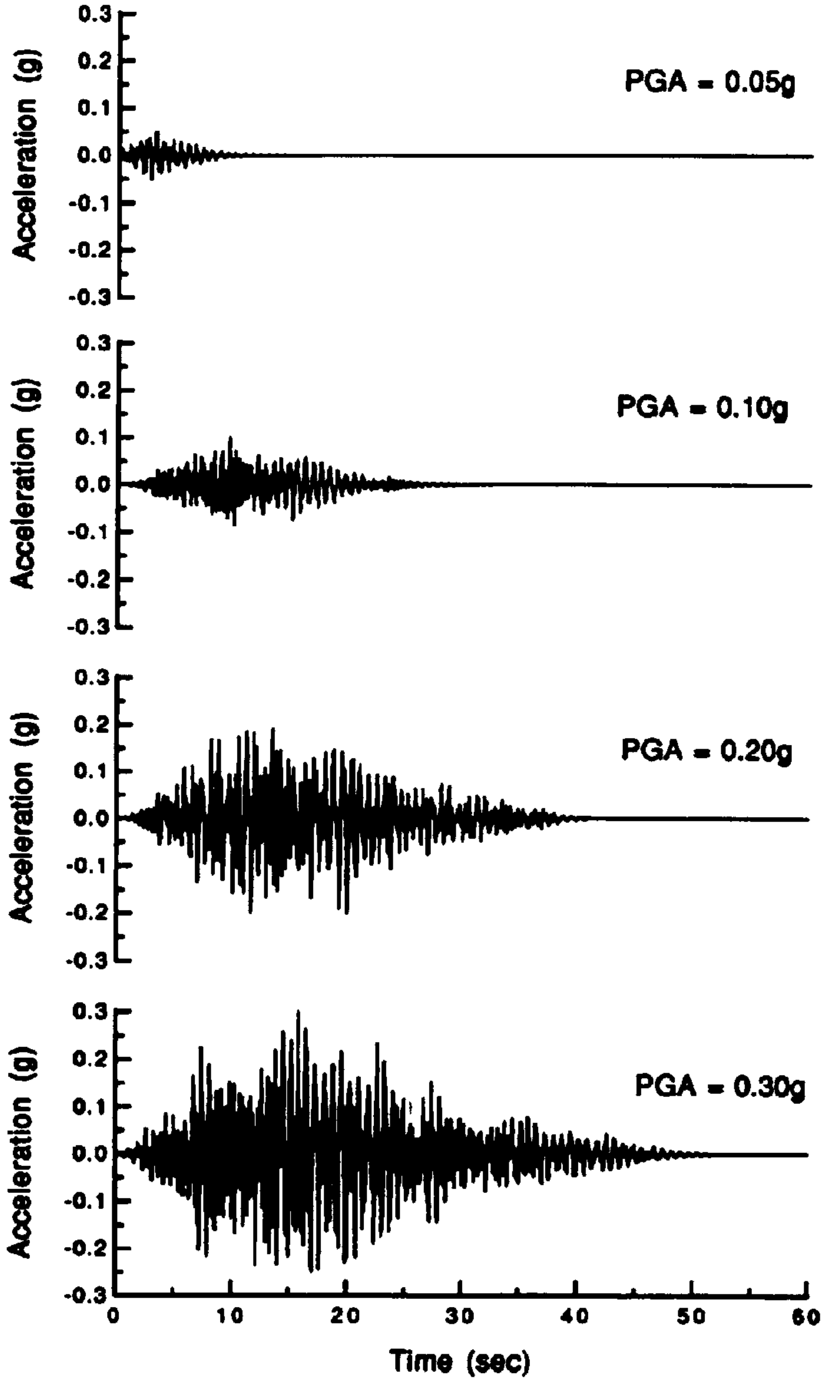

FIGURE 4-5 Acceleration Time Histories Caused by Various Scenario Earthquakes

SECTION 5

NONLINEAR BUILDING RESPONSE ANALYSIS

5.1 Description of Building

The building selected for this study is Smith Hall on the main campus of the University of Memphis. The building is a five-story reinforced concrete frame structure. A typical floor plan and two elevations are shown in Figures 5-1, 5-2 and 5-3, respectively. The plan is 60.96 m by 32.92 m (200 ft by 108 ft), and the story height is 3.81 m (12.5 ft). Figure 5-4 shows a typical floor framing plan of the building. The one-way slab with joists is supported by four frames (Frames A and B) in the N-S direction. Two exterior frames (Frame C) in the E-W direction are filled with unreinforced concrete blocks in the upper four stories, while they are filled with reinforced concrete walls in the first story because two-thirds of the first story is below the ground surface.

5.2 Modeling of Building

Smith Hall was built in 1966 without any consideration of seismic resistance. Nevertheless, the frame systems used to carry gravity loads have some capacity to resist earthquakes. Since there are four frames (Frames A and B) in the N-S direction, while only two frames in the E-W (Frame C) direction, the seismic capacity of the building is governed by the capacity of Frame C. In this study, the nonlinear seismic response analysis

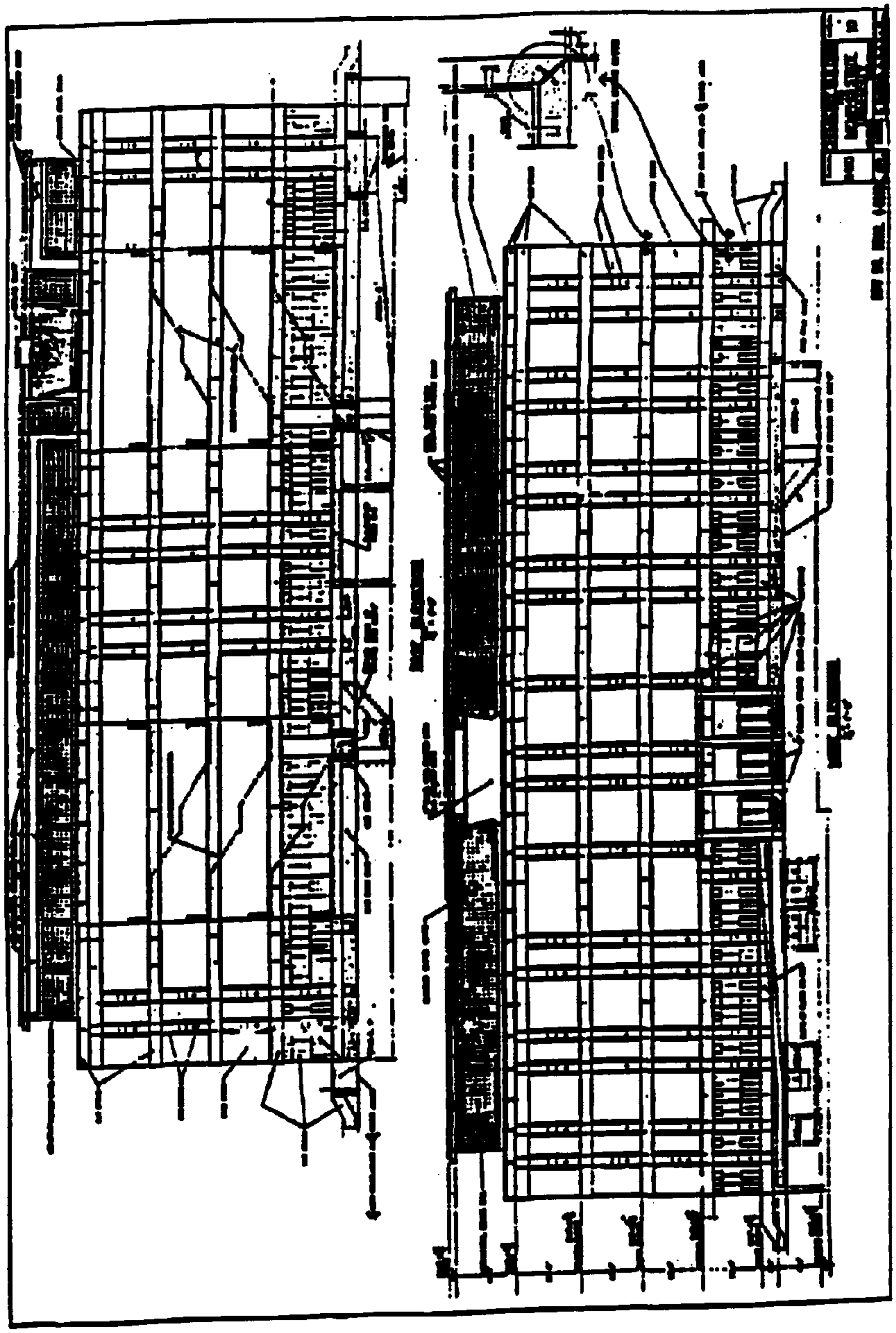

FIGURE 5-2 East and West Elevations of Smith Hall

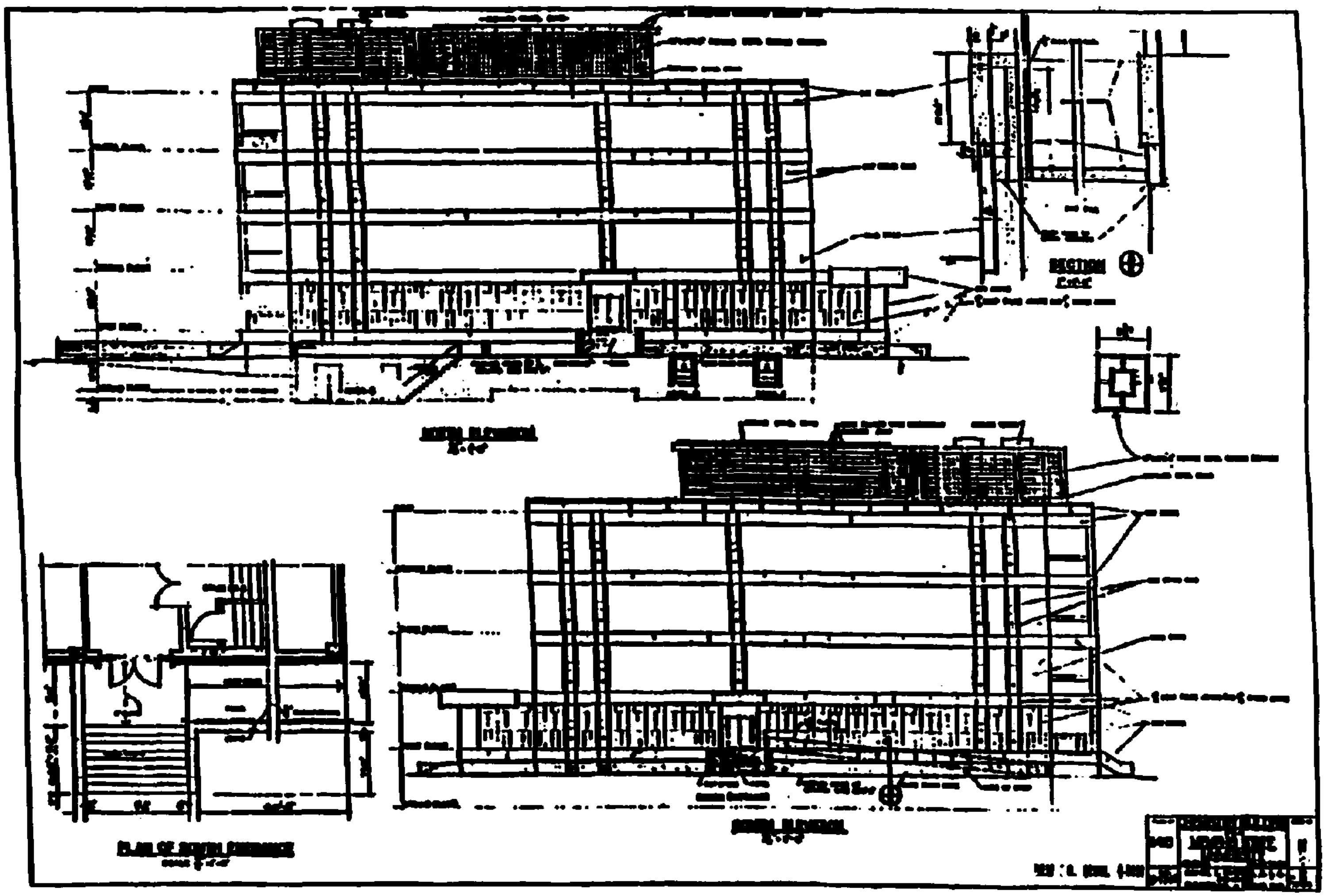

FIGURE 5-3 North and South Elevations of Smith Hall

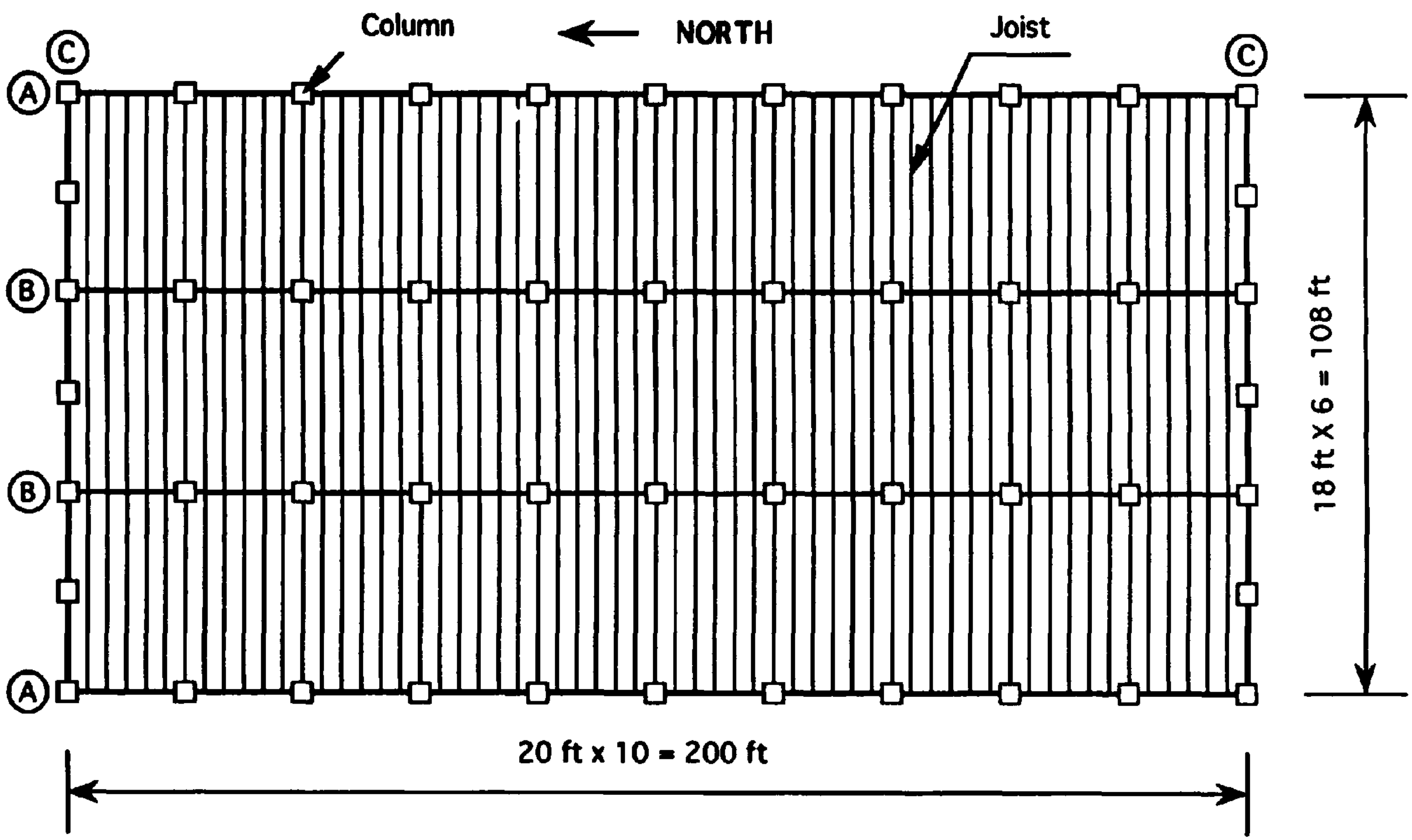

1 ft = 305 mm

FIGURE 5-4 Typical Structural Framing Plan of Smith Hall and damage evaluation of Frame C is performed using the IDARC computer program (Park et al. 1987; Kunnath et al. 1991). Frame C is modeled as a frame-wall system as shown in Figure 5-5. The dimensions and reinforcements of beams and columns are shown in Tables 5-I and 5-II, respectively. The reinforcing detail of a typical beam and column is shown in Figures 5-6 and 5-7, respectively. The unreinforced masonry walls in the upper four stories are made of eight-inch hollow concrete blocks. These walls are modeled as unreinforced solid concrete walls with equivalent thickness of 105 mm (4.12 in). The reinforced concrete walls in the first story are 203 mm (8 in) thick with #4 reinforcing bars spacing at 406 mm (16 in) in the center of the wall in both horizontal and vertical directions. These walls are modeled as shear walls without edge columns.

5.3 Inelastic Behavior of Reinforced Concrete Structure

The inelastic behavior of a reinforced concrete member (beam, column, or wall) may exhibit stiffness degrading, strength deterioration, and pinching. In the IDARC program, the inelastic behavior of a member is determined by using a trilinear skeleton curve and three model parameters α, β, γ. The trilinear skeleton curve is governed by the cracking point, yielding point, initial stiffness, and post-yielding stiffness. The initial stiffness, cracking and yielding points can be determined from the member properties such as dimensions and reinforcement. The post-yielding stiffness is taken as 0.01 of the initial stiffness for both flexural and shear hysteretic model. As shown in Figure 5-8, the parameter α is used for modeling stiffness degrading, β for strength deterioration, and γ for pinching. In the hysteretic model for beams and columns, only the flexural behavior is considered. All

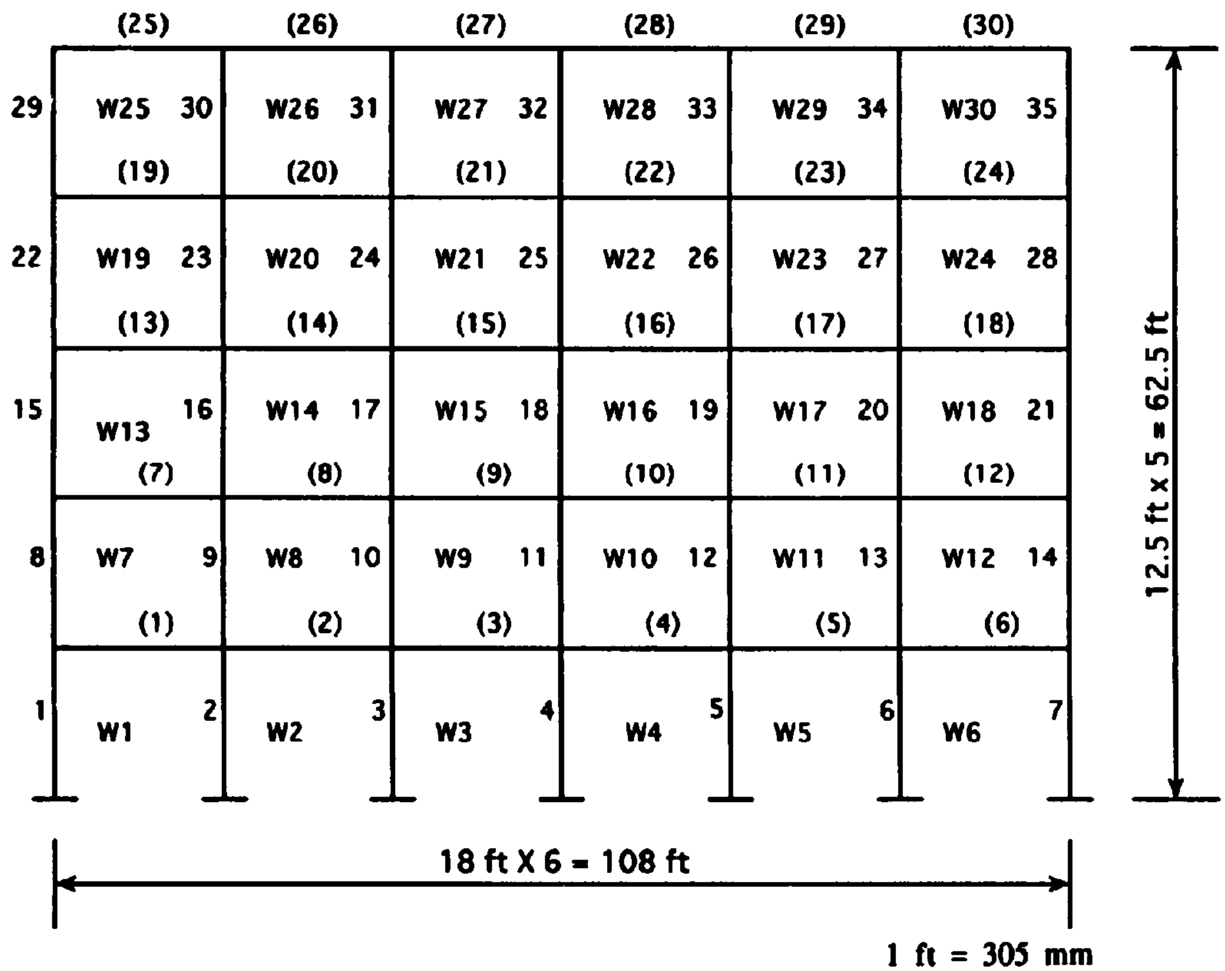

FIGURE 5-5 Modeling of Frame C

TABLE 5-I Beam Reinforcement

Beam number	Beam size (mm × mm)	Reinforcing bars			Stirrups (mm)
		Left end	Mid-span	Right end	
1	457 × 483	2#5+1#4 2#5+1#4	2#5+1#4 2#5+1#4	2#5+1#4 2#5+1#4	#3@305
2	457 × 483	2#5+1#4 2#5+1#4	2#5+1#4 2#5+1#4	2#5+1#4 2#5+1#4	#3@305
3	457 × 483	2#5+1#4 2#5+1#4	2#5+1#4 2#5+1#4	2#5+1#4 2#5+1#4	#3@305
4	457 × 483	2#5+1#4 2#5+1#4	2#5+1#4 2#5+1#4	2#5+1#4 2#5+1#4	#3@305
5	457 × 483	2#5+1#4 2#5+1#4	2#5+1#4 2#5+1#4	2#5+1#4 2#5+1#4	#3@305
6	457 × 483	2#5+1#4 2#5+1#4	2#5+1#4 2#5+1#4	2#5+1#4 2#5+1#4	#3@305
7	305 × 749	2#5 2#7	2#6 2#7	3#6 2#7	#3@305
8	305 × 749	3#6 2#7	2#6 2#7	3#6 2#7	#3@305
9	305 × 749	3#6 2#7	2#6 2#7	1#7+2#6 2#7	#3@305
10	305 × 749	1#7+2#6 2#7	2#6 2#7	3#6 2#7	#3@305
11	305 × 749	3#6 2#7	2#6 2#7	3#6 2#7	#3@305
12	305 × 749	3#6 2#7	2#6 2#7	2#5 2#7	#3@305
13	305 × 749	2#5 2#7	2#6 2#7	3#6 2#7	#3@305
14	305 × 749	3#6 2#7	2#6 2#7	3#6 2#7	#3@305
15	305 × 749	3#6 2#7	2#6 2#7	1#7+2#6 2#7	#3@305
16	305 × 749	1#7+2#6 2#7	2#6 2#7	3#6 2#7	#3@305

TABLE 5-I Beam Reinforcement (continued)

Beam number	Beam size (mm × mm)	Reinforcing bars			Stirrups (mm)
		Left end	Mid-span	Right end	
17	305 × 749	3#6 2#7	2#6 2#7	3#6 2#7	#3@305
18	305 × 749	3#6 2#7	2#6 2#7	2#5 2#7	#3@305
19	305 × 749	2#5 2#7	2#6 2#7	3#6 2#7	#3@305
20	305 × 749	3#6 2#7	2#6 2#7	3#6 2#7	#3@305
21	305 × 749	3#6 2#7	2#6 2#7	1#7+2#6 2#7	#3@305
22	305 × 749	1#7+2#6 2#7	2#6 2#7	3#6 2#7	#3@305
23	305 × 749	3#6 2#7	2#6 2#7	3#6 2#7	#3@305
24	305 × 749	3#6 2#7	2#6 2#7	2#5 2#7	#3@305
25	305 × 749	2#5 2#6	2#6 2#6	4#5 2#6	#3@305
26	305 × 749	3#5 2#6	2#6 2#6	3#5 2#6	#3@305
27	305 × 749	3#5 2#6	2#6 2#6	3#5 2#6	#3@305
28	305 × 749	3#5 2#6	2#6 2#6	3#5 2#6	#3@305
29	305 × 749	3#5 2#6	2#6 2#6	3#5 2#6	#3@305
30	305 × 749	4#5 2#6	2#6 2#6	2#5 2#6	#3@305

TABLE 5-II Column Reinforcement

Column number	Column size (mm × mm)	Reinforcing bars	Hoops (mm)
1	457 × 457	4#8	#3@406
2	305 × 457	4#8	#3@305
3	305 × 457	8#11	#3@305
4	305 × 457	4#7	#3@305
5	305 × 457	8#11	#3@305
6	305 × 457	4#8	#3@305
7	457 × 457	4#8	#3@406
8	457 × 457	4#8	#3@406
9	305 × 457	4#8	#3@305
10	305 × 457	8#11	#3@305
11	305 × 457	4#7	#3@305
12	305 × 457	8#11	#3@305
13	305 × 457	4#8	#3@305
14	457 × 457	4#8	#3@406
15	457 × 457	4#8	#3@406
16	305 × 457	4#7	#3@305
17	305 × 457	6#11	#3@305
18	305 × 457	4#7	#3@305
19	305 × 457	4#11	#3@305
20	305 × 457	4#7	#3@305
21	457 × 457	4#8	#3@406

TABLE 5-II Column Reinforcement (continued)

Column number	Column size (mm × mm)	Reinforcing bars	Hoops (mm)
22	457 × 457	4#8	#3@406
23	305 × 457	4#7	#3@305
24	305 ×457	4#9	#3@305
25	305 × 457	4#7	#3@305
26	305 × 457	4#8	#3@305
27	305 × 457	4#7	#3@305
28	457 ×457	4#8	#3@406
29	457 × 457	4#8	#3@406
30	305 × 457	4#7	#3@305
31	305 × 457	4#7	#3@305
32	305 ×457	4#7	#3@305
33	305 × 457	4#8	#3@305
34	305 × 457	4#7	#3@305
35	457 ×457	4#8	#3@406

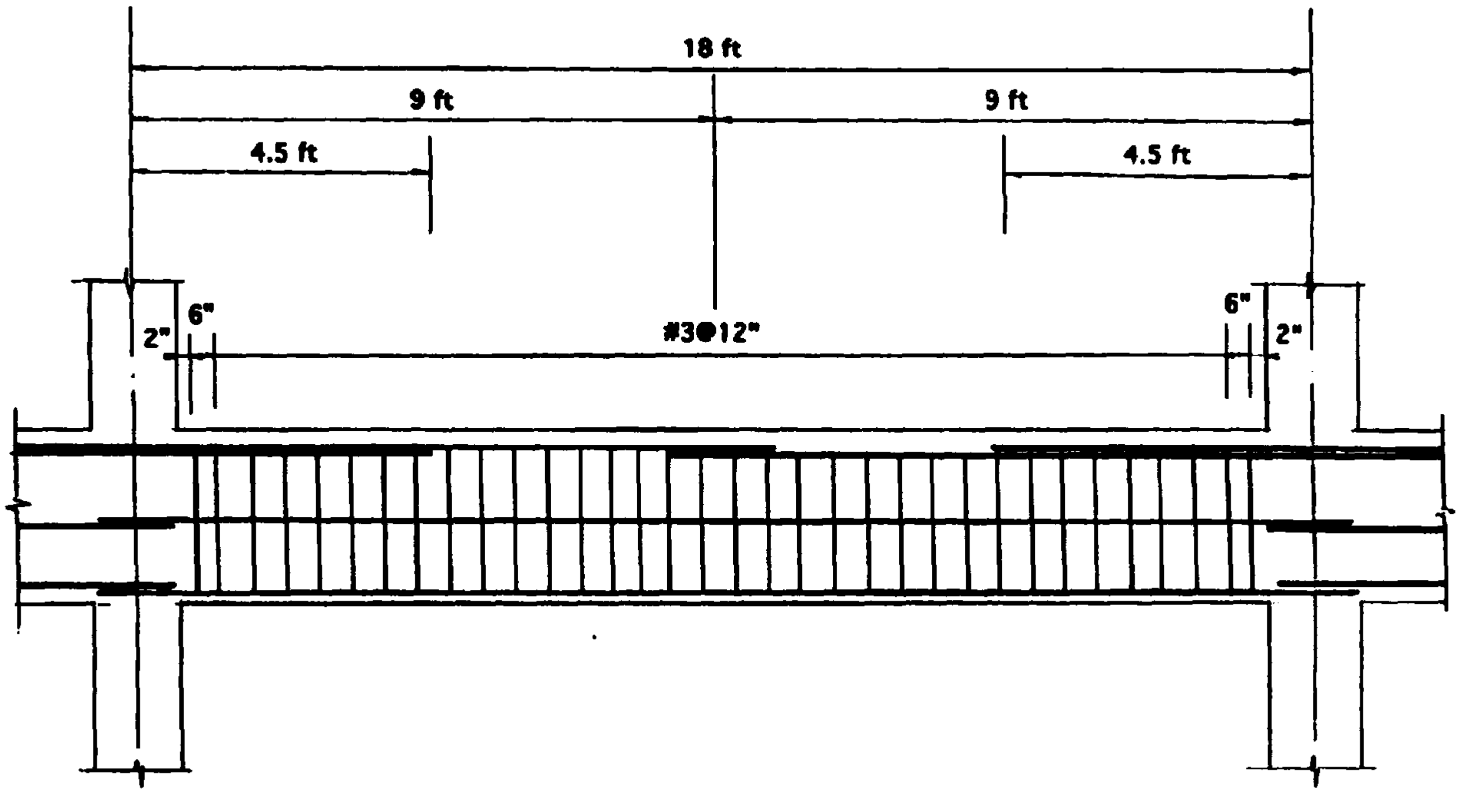

1 inch = 25.4 mm

FIGURE 5-6 Reinforcing Detail of Typical Beam

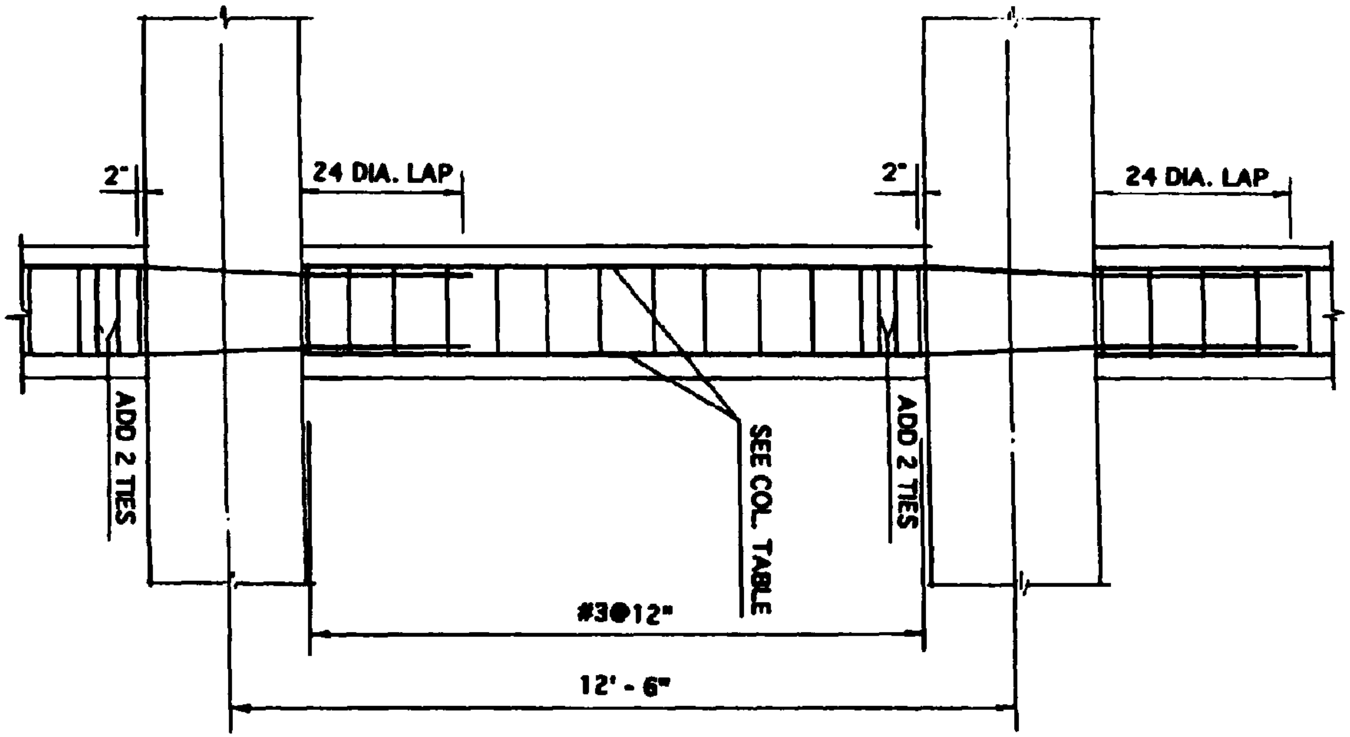

1 inch = 25.4 mm

FIGURE 5-7 Reinforcing Detail of Typical Column

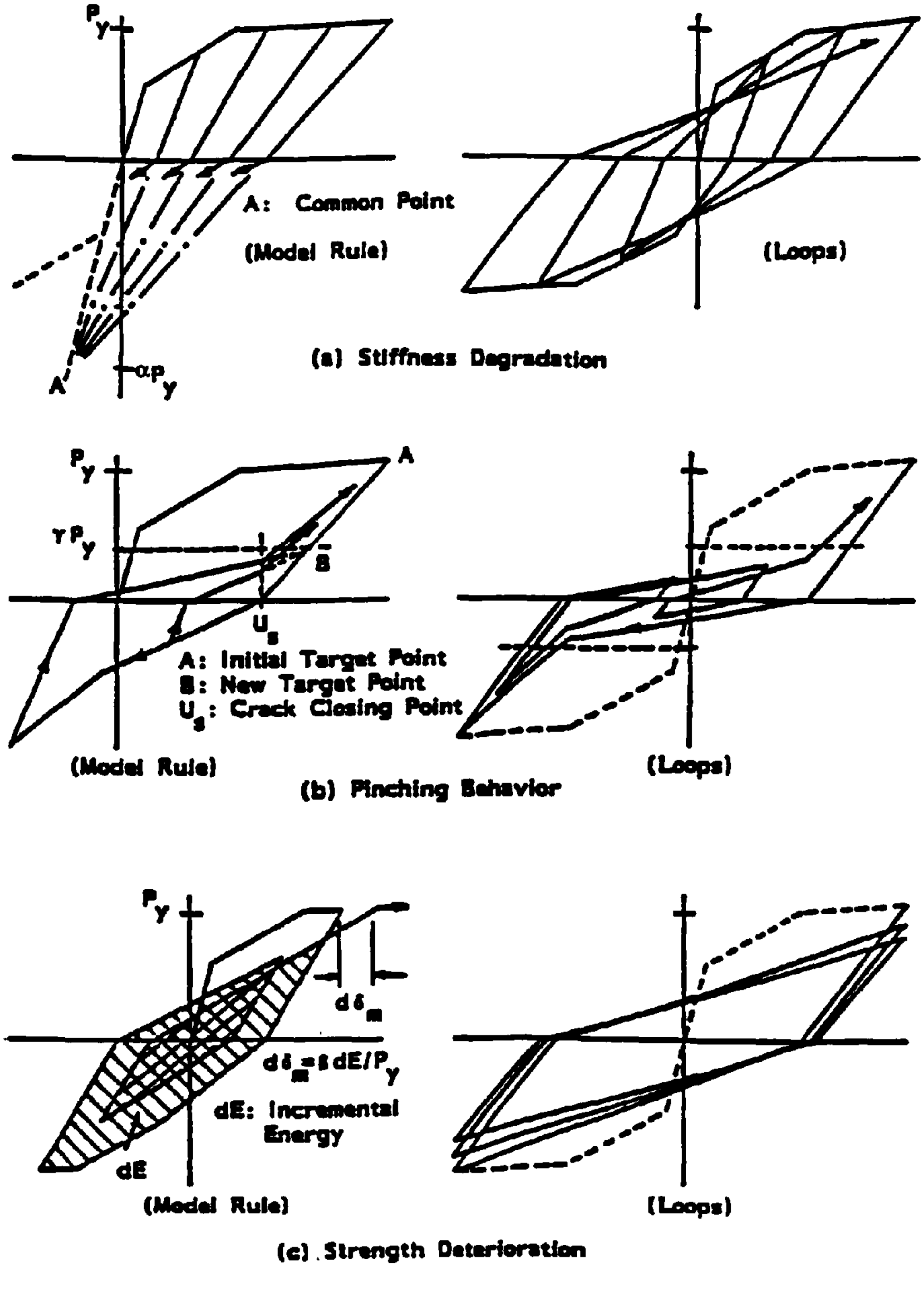

FIGURE 5-8 Effects of Three Parameters on Hysteretic Behavior (after Park et al. 1987)

the beams and columns of Frame C may have moderate degradation of stiffness in the event of an earthquake; thus, the stiffness degrading parameter α is taken as 2 (Reinhorn et al. 1988; Beres et al. 1991; El-Attar et al. 1991). On the other hand, no significant deterioration of strength is expected to occur in beams and columns, the strength deterioration parameter β is taken as 0.01. The pinching parameter γ is taken as ∞ to reflect that the pinching behavior in beams and columns is negligible, because the flexure controls the behavior of beams and columns. For shear and unreinforced concrete walls, both shear behavior and flexural behavior are considered in the analysis. The flexural model of the wall is the same as that for beams and columns. For the shear behavior, the values of α, β, and γ are taken as 0.0, 0.0, and ∞, respectively, so the resulting three-parameter hysteretic model is equivalent to the origin-oriented hysteretic model (Park et al. 1987).

5.4 Uncertainties in Structural Parameters

The structural parameters with uncertainties taken into consideration are the viscous damping ratio, strength and stiffness of construction materials. The viscous damping ratio is assumed to be uniformly distributed between 0.02 and 0.04. The concrete used to construct Frame C has a specified compressive strength of 20.70 MPa (3000 psi). The actual concrete compressive strength is modeled by a normal distribution. The mean strength is determined as 29.53 MPa (4279 psi), while the coefficient of variation (COV) is taken as 0.15 (Ellingwood and Hwang 1985). Young's modulus of concrete is determined using the formula specified in ACI code. Young's modulus is also modeled by a normal distribution. The mean value is determined as 25727 MPa (3729 ksi) and its COV is taken as 0.15.

The property of masonry is controlled by several components such as masonry unit, mortar, and grout. In this study, the specified compressive strength of masonry is taken as 13.80 MPa (2000 psi), assuming the specified compressive strength of concrete masonry unit is 19.32 MPa (2800 psi) and the mortar is S type (Amrhein 1992). According to the UBC code, the specified strength is about 75% of the average value determined from the in-situ test data (Amrhein 1992). Thus, the mean compressive strength of masonry is taken as 18.40 MPa (2667 psi) and the COV is assumed as 0.15. In this study, the mean value of Young's modulus is taken as 20700 MPa (3000 ksi) and the COV is set as 0.15. Both compressive strength and Young's modulus of masonry are assumed to be normally distributed.

The reinforcement used in all elements is grade 40 steel bar. Mill tests of Grade 40 reinforcement of all sizes show that the distribution of yielding strength can be modeled by a lognormal distribution with a mean yielding strength of 336.72 MPa (48.8 ksi) and a COV about 0.11 (Mirza and MacGregor 1979). The statistical data show that the variability of Young's modulus of reinforcement is very small (3.3%) with an average of 200100 MPa (29000 ksi) (Mirza and MacGregor 1979). Thus, Young's modulus of reinforcement is taken as deterministic and an average value of 200100 MPa is used in the analysis.

Table 5-III summarizes the variability of structural parameters. Noted that the parameters α, β, γ in the hysteretic model are taken as constant. It

TABLE 5-III Uncertainties in Structural Parameters

Parameter	Distribution	Mean	Notes
Concrete compressive strength	Normal	29.53 MPa	COV = 0.15
Concrete Young's modulus	Normal	25727.35 MPa	COV = 0.15
Masonry compressive strength	Normal	18.40 MPa	COV = 0.15
Masonry Young's modulus	Normal	20700.00 MPa	COV = 0.15
Steel yielding strength	Lognormal	336.72 MPa	COV = 0.11
Viscous damping ratio	Uniform	0.03	Range: 0.02 - 0.04

means that the moving track of the hysteretic loops will follow the same rule. However, the shape of the hysteretic loops will be changed with the variation in the skeleton curve, which is affected by variations in initial stiffness, cracking point, and yielding point.

5.5 Probabilistic Seismic Response

For each structural parameter considered as a random variable, 50 samples are selected randomly within two standard deviations around the mean value. The samples are combined using the Latin Hypercube sampling technique to generate 50 samples of the structural model. For each PGA level, these structural samples are combined with 50 samples of the acceleration time histories to establish 50 samples of the earthquake-site-structure system. For each sample, the IDARC computer program is used to determine the nonlinear seismic response of structure. To perform a seismic response analysis, a static (dead load) analysis of Frame C is first carried out and the results are used as the initial conditions for the seismic analysis. The seismic analysis is performed in the time domain using the Newmark-β algorithm to estimate the structural responses such as the floor displacement, floor acceleration, and member forces. As an example, using the earthquake time history with PGA equal to 0.2g as shown in Figure 4-5, the time histories of displacement and acceleration are shown in Figures 5-9 and 5-10, respectively. The final damage state of Frame C is shown in Figure 5-11. It is observed that yield occurs in beams and/or columns of all the joints and most of the walls in the second through fourth stories.

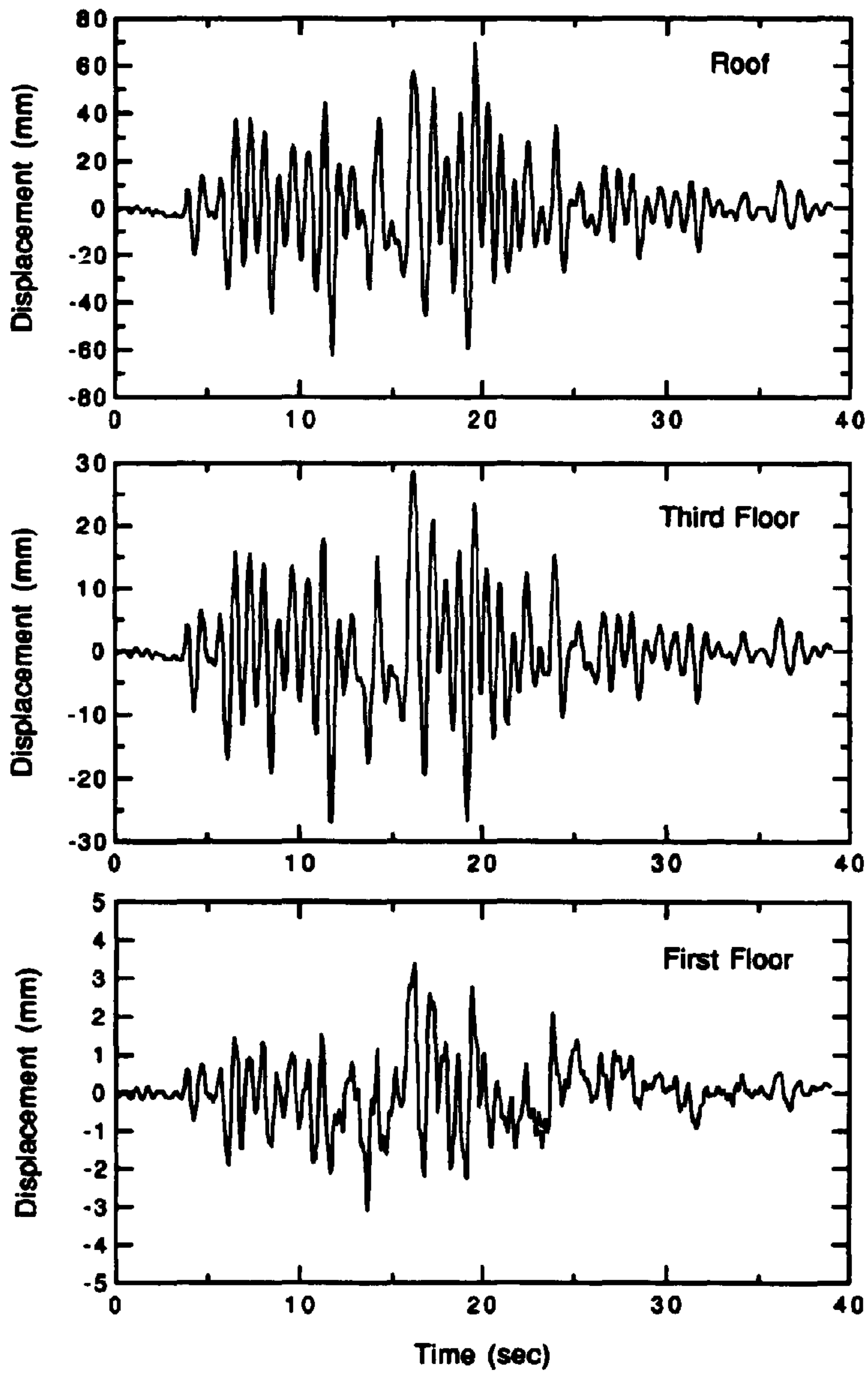

FIGURE 5-9 Floor Displacement Time Histories

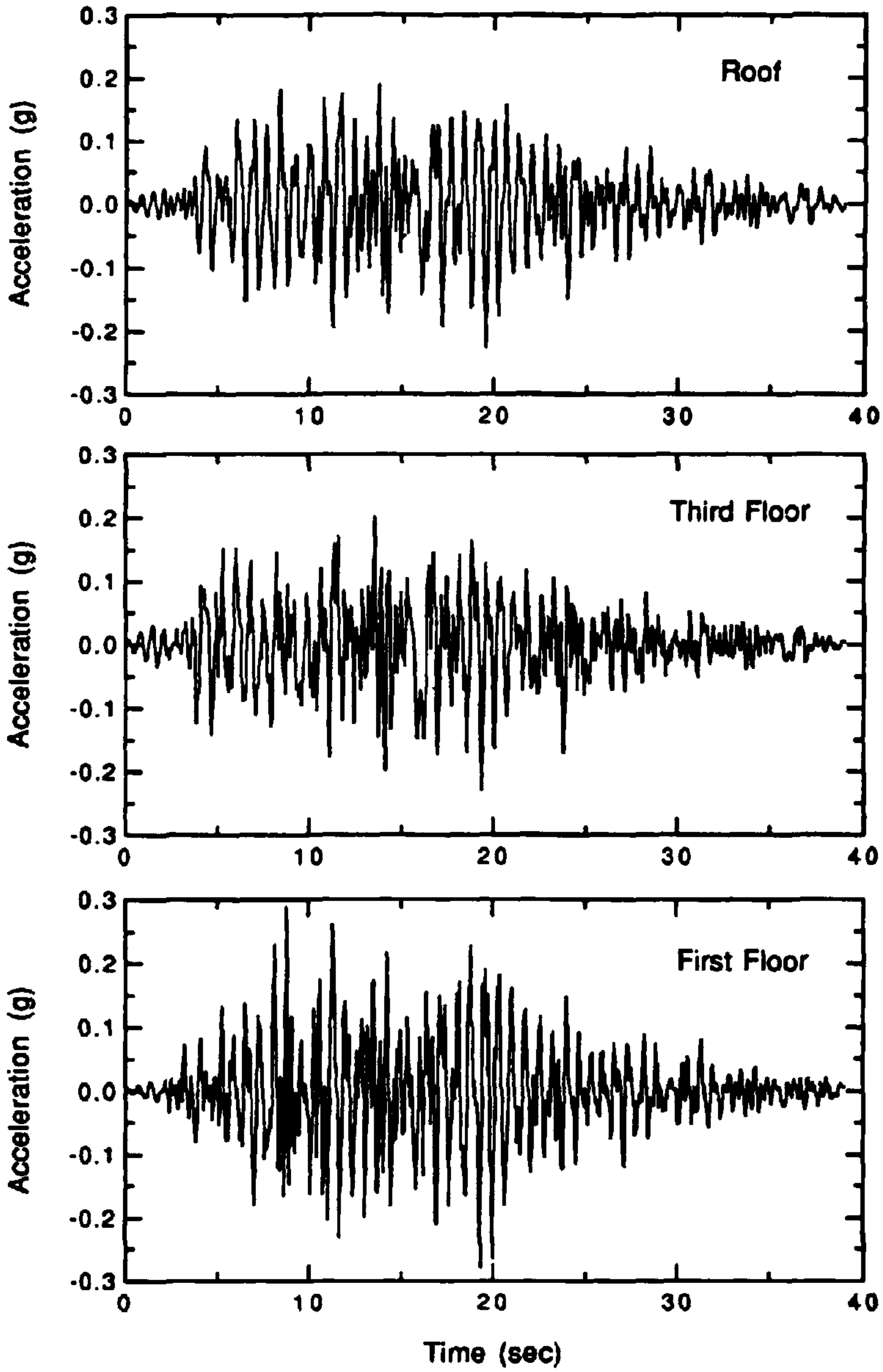

FIGURE 5-10 Floor Acceleration Time Histories

NOTATION: - = BEAM, I = COLUMN, W = SHEAR WALL; E = ELASTIC, C = CRACK, Y = YIELD.

```
+Y-----------------C+C-----------------Y+C-----------------Y+C-----------------Y+C-----------------C+C-----------------Y+
C        E         Y         E         Y         E         Y         E         Y         E         Y         E         C
!        W         !         W         !         W         !         W         !         W         !         W         !
!        E         !         C         !         C         !         C         !         C         !         C         !
!        W         !         W         !         W         !         W         !         W         !         W         !
C        C         Y         C         C         C         Y         Y         Y         C         Y         C         Y
+Y-----------------Y+C-----------------Y+Y-----------------Y+C-----------------Y+Y-----------------Y+C-----------------Y+
C        C         Y         Y         C         C         Y         Y         C         C         Y         C         C
!        W         !         W         !         W         !         W         !         W         !         W         !
!        C         !         C         !         C         !         C         !         C         !         C         !
!        W         !         W         !         W         !         W         !         W         !         W         !
C        Y         Y         Y         C         Y         Y         Y         C         Y         Y         Y         C
+Y-----------------C+Y-----------------Y+Y-----------------C+C-----------------Y+Y-----------------C+C-----------------Y+
C        Y         Y         Y         C         Y         Y         Y         C         Y         Y         Y         C
!        W         !         W         !         W         !         W         !         W         !         W         !
!        C         !         C         !         C         !         C         !         C         !         C         !
!        W         !         W         !         W         !         W         !         W         !         W         !
C        Y         Y         Y         C         Y         Y         Y         C         Y         Y         Y         C
+Y-----------------C+C-----------------Y+Y-----------------C+C-----------------Y+Y-----------------C+C-----------------Y+
C        Y         C         Y         C         Y         Y         Y         C         Y         Y         Y         C
!        W         !         W         !         W         !         W         !         W         !         W         !
!        Y         !         Y         !         Y         !         C         !         C         !         Y         !
!        W         !         W         !         W         !         W         !         W         !         W         !
C        Y         C         Y         C         Y         Y         Y         C         Y         C         Y         C
+Y-----------------Y+Y-----------------Y+Y-----------------Y+Y-----------------Y+Y-----------------Y+C-----------------Y+
C        C         C         Y         E         C         C         Y         E         C         C         E         E
!        W         !         W         !         W         !         W         !         W         !         W         !
!        E         !         C         !         E         !         E         !         C         !         C         !
!        W         !         W         !         W         !         W         !         W         !         W         !
C        Y         C         Y         E         Y         C         Y         E         Y         C         Y         E
```

FIGURE 5-11 Final Damage State of Frame C (PGA = 0.2g)

SECTION 6

DEVELOPMENT OF FRAGILITY CURVES AND ESTIMATION OF DAMAGE COST

6.1 Damage States and Damage Index

When buildings are subjected to an earthquake, varying degrees of damage from no damage to collapse have been observed. In this study, five damage states are considered: (1) nonstructural damage, (2) slight structural damage, (3) moderate structural damage, (4) severe structural damage, and (5) collapse. These damage states are defined using the damage index proposed by Park and Ang (1985).

According to Park and Ang, the damage index D for a structural element is defined as

$$D = \frac{\delta_m}{\delta_u} + \frac{\beta}{\delta_u Q_y} \int dE \qquad (6.1)$$

where

δ_m = maximum deformation caused by an earthquake,

δ_u = ultimate deformation under monotonic loading,

$\int dE$ = cumulative dissipated energy,

Q_y = yield strength, and

β = coefficient related to structural types.

TABLE 6-I Damage States

Damage state		DT	
		Range	Best estimate
1	Nonstructural damage	0.01 - 0.10	0.05
2	Slight structural damage	0.10 - 0.20	0.15
3	Moderate structural damage	0.20 - 0.50	0.35
4	Severe structural damage	0.50 - 0.85	0.67
5	Collapse	0.85 - 1.15	1.00

PGA equal to a_j can be determined as

$$\begin{aligned} PF_{ij} &= Prob(DT \geq DT_i \mid PGA = a_j) \\ &= F_{DT}(DT_i \mid PGA = a_j) \end{aligned} \qquad (6.3)$$

where

DT_i = building damage index corresponding to the i-th damage state, and

$F_{DT}(\cdot)$ = probability distribution function of DT.

The fragility curve with respect to the i-th damage state can be constructed using the PF_{ij} values at various PGA levels.

The damage probability matrix describes the probability of damage in various damage states caused by an earthquake. The probability PDS_{ij} that the damage to a structure caused by an earthquake with PGA equal to a_j is in the i-th damage state can be derived from the fragility data,

$$PDS_{ij} = \begin{cases} PF_{ij} - PF_{i+1j} & (i \leq 4) \\ PF_{ij} & (i = 5) \end{cases} \qquad (6.4)$$

6.3 Seismic Damage Cost

In this study the damage cost resulting from an earthquake is referred to the direct cost of repairing a building. The cost resulting from damage to building content and the indirect cost due to loss of building function are not included. To estimate damage cost, the central damage cost ratio CDR_i

corresponding to the i-th damage state is defined as the ratio of the average repair cost of a structure in the i-th damage state to the replacement cost of the structure. Table 6-II through Table 6-V show the central damage cost ratios suggested in several studies (Whitman 1973; ATC 1985; FEMA 1985; Pappin 1991). The central damage cost ratios adopted for this study are shown in Table 6-VI.

The mean damage cost ratio $\overline{DR}_j$ induced by an earthquake with PGA equal to a_j can be determined as follows:

$$\overline{DR}_j = \sum_{i=1}^{5} PDS_{ij} \times CDR_i \tag{6.5}$$

The damage cost DC_j given the occurrence of an earthquake with PGA level equal to a_j can then be calculated as

$$DC_j = \overline{DR}_j \times RPC \tag{6.6}$$

where RPC is the replacement cost of a structure. Considering the occurrence of an earthquake, the expected annual earthquake loss AEL of a structure is determined as follows:

$$AEL = \sum_{j=1}^{N_a} DC_j \cdot \{F_A(a_j + \frac{\Delta a}{2}) - F_A(a_j - \frac{\Delta a}{2})\} \tag{6.7}$$

where $F_A(\cdot)$ is the probability distribution function of peak ground acceleration in one year.

TABLE 6-II Damage Cost Ratios Corresponding to Various Damage States (Whitman 1973)

Damage state		Damage cost ratio	
		Range (%)	Central value (%)
0	No damage	0 - 0.05	0
1	Minor nonstructural damage — a few walls and partitions cracked, incidental mechanical and electrical damage	0.05 - 0.3	0.1
2	Localized nonstructural damage — more extensive cracking (but still not widespread); possibly damage to elevators and/or other mechanical/electrical components	0.3 - 1.25	0.5
3	Widespread nonstructural damage — possibly a few beams and columns cracked, although not noticeable	1.25 - 3.5	2
4	Minor structural damage — obvious cracking or yielding in a few structural members; substantial nonstructural damage with widespread cracking	3.5 - 7.5	5
5	Substantial structural damage requiring repair or replacement of some structural members; associated extensive nonstructural damage	7.5 - 20	10
6	Major structural damage requiring repair or replacement of many structural members; associated non-structural damage requiring repairs to major portion of interior; building vacated during repairs	20 - 65	30
7	Building condemned	65 - 100	100
8	Collapse	100	100

TABLE 6-III Damage Cost Ratios Corresponding to Various Damage States (ATC 1985)

Damage state		Damage cost ratio range (%)	Central damage cost ratio (%)
1	None	0	0
2	Slight	0 - 1	0.5
3	Light	1 - 10	5
4	Moderate	10 - 30	20
5	Heavy	30 - 60	45
6	Major	60 - 100	80
7	Destroyed	100	100

Note: Definitions

1 - None: No damage

2 - Slight: Limited localized minor damage not requiring repair.

3 - Light: Significant localized damage of some components generally not requiring repair.

4 - Moderate: Significant localized damage of many components warranting repair.

5 - Heavy: Extensive damage requiring major repairs.

6 - Major: Major widespread damage that may result in the facility being razed, demolished, or repaired.

7 - Destroyed: Total destruction of the majority of the facility.

TABLE 6-IV Damage Cost Ratios Corresponding to Various Damage States (FEMA 1985)

Damage state		Damage cost ratio range (%)	Central damage cost ratio (%)
0	No damage	0 - 0.05	0
1	Minor nonstructural	0.05 - 1.25	0.3
2	Slight	1.25 - 7.50	3.5
3	Moderate	7.5 - 20	10
4	Severe	20 - 90	65
5	Collapse	90 - 100	95

TABLE 6-V Damage Cost Ratios Corresponding to Various Damage States (Pappin 1991)

Damage state		Definition for loadbearing masonry	Definition for R.C. framed buildings	Damage cost ratio (%)
0	Undamaged	No visible damage	No visible damage	0
1	Slight damage	Hairline cracks	Infill panels damaged	0.05
2	Moderate damage	Cracks 5-20 mm	Cracks 10 mm in structure	0.20
3	Heavy damage	Cracks 20 mm or wall material dislodged	Heavy damage to structural members, loss of concrete	0.50
4	Partial destruction	Complete collapse of individual wall or individual roof support	Complete collapse of structural member or major deflection to frame	0.80
5	Collapse	More than one wall collapsed or more than half of roof	Failure of structure members to allow fall of roof or slab	1.0

TABLE 6-VI Recommended Damage Cost Ratios Corresponding to Various Damage States

Damage state		Damage cost ratio range (%)	Central damage cost ratio (%)
1	Nonstructural damage	0.05 - 2	1
2	Slight structural damage	2 - 10	6
3	Moderate structural damage	10 - 30	20
4	Severe structural damage	30 - 100	65
5	Collapse	100	100

6.4 Seismic Performance of Smith Hall

To evaluate the seismic performance of Smith Hall, eight PGA levels ranging from 0.05g to 0.5g are used in the analysis. For each PGA level, 50 values of the building damage index DT are obtained from nonlinear seismic response analyses using the IDARC program. The building damage index is considered to follow a lognormal distribution. Using these 50 values, the statistics of DT are determined and shown in Table 6-VII.

Using the best-estimate values listed in Table 6-I to define the damage states, the best-estimate fragility data for five damage states are calculated according to equation (6.3) and shown in Table 6-VIII. The lower- and upper-bound fragility data can be computed using the limit values that define the ranges of the building damage indexes for the damage states listed in Table 6-I. Using these fragility data, the lower-bound, best-estimate, and upper-bound fragility curves are plotted in Figure 6-1. The damage probability matrix can be determined from the fragility data by using equation (6.4). For example, using the best-estimate fragility data (Table 6-VIII), the corresponding damage probability matrix is calculated and shown in Table 6-IX. As shown in the table, Smith Hall is expected to sustain slight damage in the event of a moderate earthquake, and to sustain moderate damage in the event of a large earthquake. The chance of complete collapse of the building is very small, even a large earthquake occurs in the New Madrid seismic zone.

To estimate the damage cost in the event of an earthquake, the best-

TABLE 6-VII Statistics of Building Damage Index

PGA (g)	DT			
	Mean	COV	Median	β_D
0.05	0.05	0.51	0.04	0.48
0.10	0.15	0.44	0.14	0.42
0.15	0.26	0.50	0.23	0.47
0.20	0.41	0.46	0.37	0.44
0.25	0.54	0.46	0.59	0.44
0.30	0.78	0.51	0.69	0.48
0.40	1.13	0.47	1.02	0.45
0.50	1.77	0.54	1.55	0.51

TABLE 6-VIII Fagility Data (best estimate)

PGA (g)	Non-structural damage	Slight structural damage	Moderate structural damage	Severe structural damage	Collapse
0.05	0.60	0.02	0.00	0.00	0.00
0.10	0.98	0.50	0.02	0.00	0.00
0.15	1.00	0.89	0.22	0.01	0.00
0.20	1.00	0.98	0.57	0.10	0.02
0.25	1.00	1.00	0.82	0.31	0.09
0.30	1.00	1.00	0.93	0.55	0.22
0.40	1.00	1.00	0.99	0.87	0.57
0.50	1.00	1.00	1.00	0.97	0.82

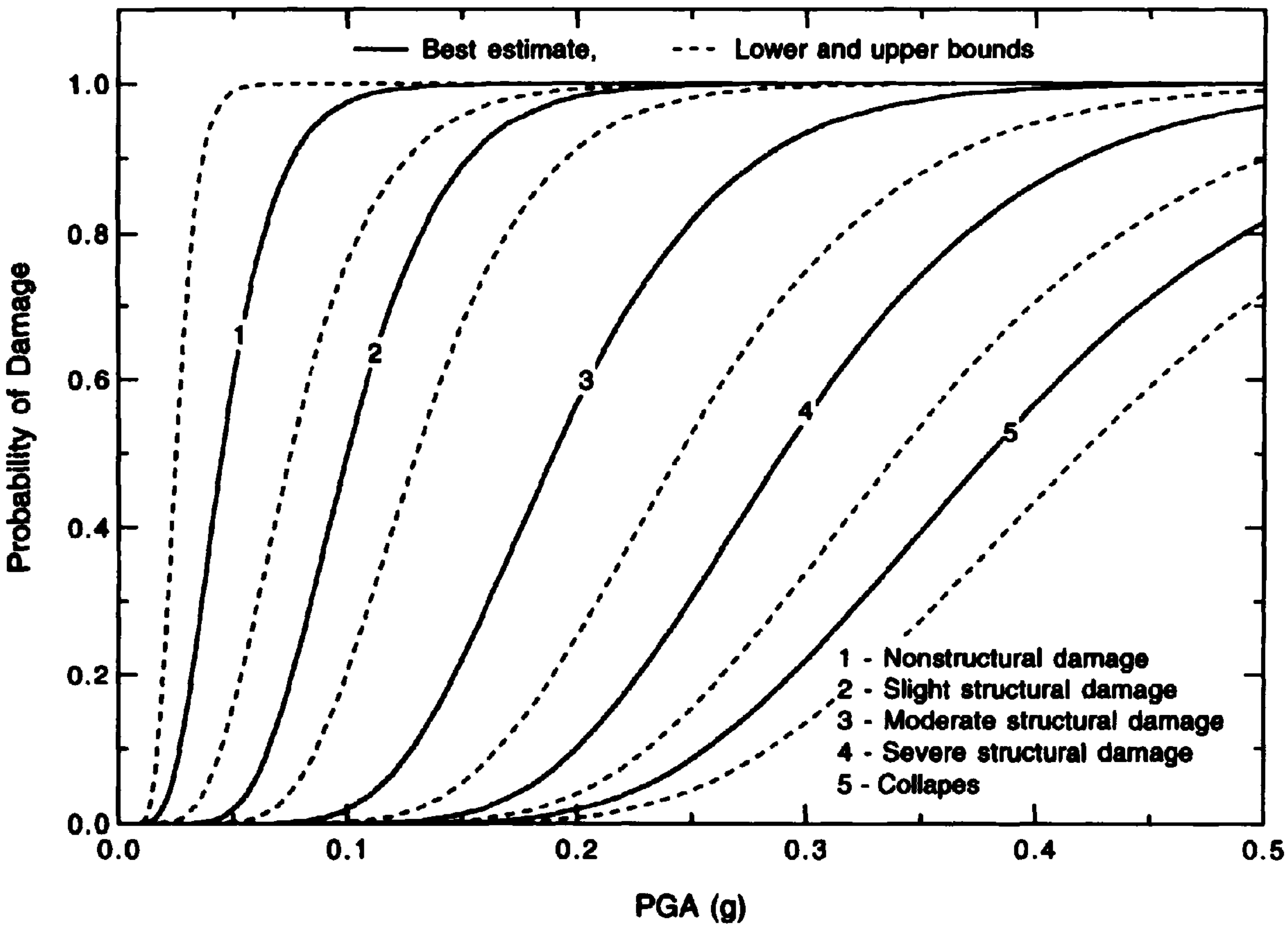

FIGURE 6-1 Fragility Curves of Smith Hall

TABLE 6-IX Damage Probability Matrix (best estimate)

PGA (g)	Non-structural damage	Slight structural damage	Moderate structural damage	Severe structural damage	Collapse
0.05	0.58	0.02	0.00	0.00	0.00
0.10	0.48	0.48	0.02	0.00	0.00
0.15	0.11	0.67	0.21	0.01	0.00
0.20	0.02	0.41	0.47	0.08	0.02
0.25	0.00	0.18	0.51	0.22	0.09
0.30	0.00	0.07	0.38	0.33	0.22
0.40	0.00	0.01	0.12	0.30	0.57
0.50	0.00	0.00	0.03	0.15	0.82

estimate mean damage cost ratios for various PGA levels are calculated according to equation (6.5) and shown in Table 6-X. The corresponding mean damage cost ratio curve is plotted in Figure 6-2. The 1993 replacement cost for Smith Hall was estimated as $14,070,560 by the Office of Space Planning and Utilization, the University of Memphis. Using this replacement cost value, the damage cost resulting from earthquakes with various PGA levels are also listed in Table 6-X. As shown in the table, the damage cost is estimated as $565,637, if a 0.1g earthquake occurs. The damage cost will be increase to $3,013,914 if Smith Hall is subject to a 0.2g earthquake. As previously noted, the damage cost estimated in this study is only the direct cost of repairing the building. The cost resulting from damage to building content and the indirect cost due to the loss of use of the building are not included.

By considering all possible earthquakes that might occur within a year as displayed by the seismic hazard curve in Figure 2-3, the expected annual earthquake loss is estimated as $8,442 per year. This annual loss seems small because the probability that a large earthquake occurs in the New Madrid seismic zone is low. The expected annual earthquake loss may be used to determine the premium for earthquake insurance.

TABLE 6-X Cost of Earthquake Damage to Smith Hall (best-estimate)

PGA (g)	Mean damage cost ratio (%)	Damage cost ($)
0.05	0.87	122,414
0.10	4.02	565,637
0.15	10.22	1,438,011
0.20	21.43	3,013,914
0.25	33.54	4,719,266
0.30	54.74	7,702,225
0.40	78.75	11,080,566
0.50	92.25	12,980,092

TABLE 6-X Cost of Earthquake Damage to Smith Hall (best-estimate)

PGA (g)	Mean damage cost ratio (%)	Damage cost ($)
0.05	0.87	122,414
0.10	4.02	565,637
0.15	10.22	1,438,011
0.20	21.43	3,013,914
0.25	33.54	4,719,266
0.30	54.74	7,702,225
0.40	78.75	11,080,566
0.50	92.25	12,980,092

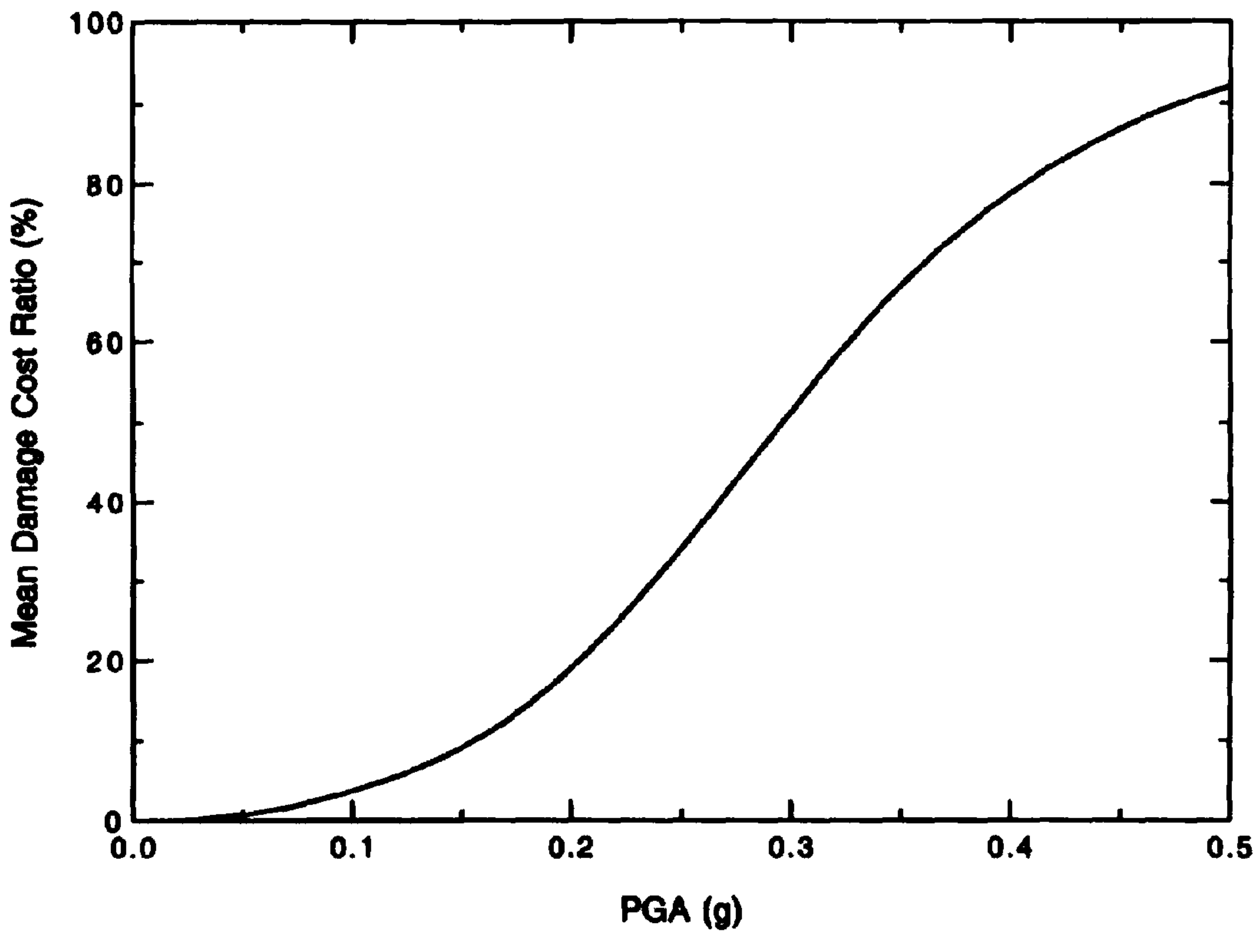

FIGURE 6-2 Damage Cost Ratio Curve of Smith Hall

SECTION 7

CONCLUSIONS

This report presents an analytical method for generating fragility curves and corresponding damage probability matrix for structures. The proposed method includes the following features:

(1) The earthquake acceleration time histories are generated based on the scenario earthquakes that are established from a probabilistic seismic hazard analysis. Thus, the resulting ground motion is consistent with the expected seismic hazard.

(2) The nonlinear site response analysis is utilized to take the effect of local soil conditions on ground motions into consideration.

(3) The reinforced concrete building is modeled using a frame-wall model instead of a stick model. In addition, the nonlinear behavior of the building is incorporated in the analysis.

(4) Uncertainties are quantified by evaluating uncertainties in the seismic, soil, and structural parameters that define an analytical model of the earthquake-site-structure system. Thus, uncertainties in the entire system can be easily assessed and verified.

In summary, seismic hazards, local soil condition, and nonlinear building behavior are considered systematically in the proposed method for generating fragility curves and corresponding damage probability matrix. The fragility curves (damage probability matrix) can be used to estimate expected loss of life and damage of properties caused by an earthquake, and to develop earthquake preparedness and emergency response plan.

SECTION 8

REFERENCES

Aki, K., and Richards, P.G. (1980). *Quantitative Seismology: Theory and Method*. W. H. Freeman and Company, New York, New York.

American Concrete Institute (1983). *Building Code Requirement for Reinforced Concrete* (ACI 318-83). Detroit, Michigan.

American National Standards Institute (1982). *Minimum Design Loads for Buildings and Other Structures* (ANSI A58.1-1982). New York, New York.

Amrhein, J.E. (1992). *Reinforced Masonry Engineering Handbook — Clay and Concrete Masonry* (Fifth edition). Masonry Institute of America, Los Angeles, California.

Applied Technology Council (1985). "Earthquake Damage Evaluation Data for California." ATC-13, Redwood City, California.

Beres, A., Pessiki, S.P., White, R.N., and Gergely, P. (1991). "Behavior of Existing Reinforced Concrete Frames Designed Primarily for Gravity Loads." *International Meeting on Earthquake Protection of Buildings*, Ancona, B75-B86.

Boore, D.M. (1983). "Stochastic Simulation of High-Frequency Ground Motion Based on Seismological Models of the Radiated Spectra." *Bulletin of the Seismological Society of America*, Vol. 73, 1865-1894.

Boore, D.M., and Boatwright, J. (1984). "Average Body-Wave Radiation Coefficients." *Bulletin of the Seismological Society of America*, Vol. 74, 1615-1621.

Brune, J.N. (1970). "Tectonic Stress and Spectra of Seismic Shear Waves from Earthquakes." *Journal of Geophysical Research*, Vol. 75, 4997-5009.

Brune, J.N. (1971). "Correction." *Journal of Geophysical Research*, Vol. 76, 5002.

Building Seismic Safety Council (1991). *NEHRP Recommended Provisions for the Development of Seismic Regulations for New Buildings* (1991 Edition). FEMA 222, Federal Emergency Management Agency, Washington, D.C.

Cakmak, A.S., Sherif, I., and Ellis, G.W. (1985). "Modelling Earthquake Ground Motion in California Using Parametric Time Series Methods." *International Journal of Soil Dynamics and Earthquake Engineering*, Vol. 4, No. 3, 124-131.

Chang, T.-S., Teh, L.K., and Zhang, Y. (1992). "Seismic Characteristics of Sediments in the New Madrid Seismic Zone." Technical Report, Center for Earthquake Research and Information, The University of Memphis, Memphis, Tennessee.

Chiu, J.M., Johnston, A.C., and Yang, Y.T. (1992). "Imaging the Active Faults of the Central New Madrid Seismic Zone Using PANDA Array Data." *Seismological Research Letters*, Vol. 63, No. 3, 375-394.

Dwyer, J.J., Herrmann, R.B., and Nuttli, O.W. (1983). "Spatial Attenuation of the Lg Wave in the Central United States." *Bulletin of the Seismological Society of America*, Vol. 73, 781-796.

El-Attar, A.G., White, R.N., and Gergely, P. (1991). "Shake Table Test of a 1/8 Scale Three-Story Lightly Reinforced Concrete Building." Technical Resort NCEER-91-0018, National Center for Earthquake Engineering Research, State University of New York at Buffalo, Buffalo, New York.

Ellingwood, B.R., and Hwang, H. (1985). "Probabilistic Descriptions of Resistance of Safety-Related Structures in Nuclear Power Plant." *Nuclear Engineering and Design*, Vol. 88, 167-178.

Federal Emergency Management Agency (1985). "An Assessment of Damage and Casualties for Six Cities in the Central United States Resulting from Earthquakes in the New Madrid Seismic Zone." Report for Central United States Earthquake Preparedness Project, Washington, D.C.

Gutenberg, B., and Richter, C.F. (1944). "Frequency of Earthquakes in California." *Bulletin of the Seismological Society of America*, Vol. 34, 185-188.

Hanks, T.C., and Kanamori, H. (1979). "A Moment Magnitude Scale." *Journal of Geophysics Research*, Vol. 84, 2348-2350.

Huo, J.-R., Hu, Y., and Feng, Q. (1991). "Study on the Envelop Function of the Ground Motion Acceleration Time History." *Earthquake Engineering and Engineering Vibration*, Vol. 11, No. 1, 1-12 (in Chinese).

Hwang, H. (1992). "Seismic Hazard Along a Central U.S. Oil Pipeline." *Lifeline Earthquake Engineering in the Central and Eastern U.S.*, D.B. Ballantyne (ed.), Monograph No. 5, ASCE Technical Council on Lifeline Earthquake Engineering, American Society of Civil Engineers, New York, 110-124.

Hwang, H., and Jaw, J.-W. (1990). "Probabilistic Damage Analysis of Structures." *Journal of Structural Engineering*, ASCE, Vol. 116, No. 7, 1992-2007.

Hwang, H., Jaw, J.-W., and Shau, H.-J. (1988). "Seismic Performance Assessment of Code-Designed Structures." Technical Report NCEER-88-0007, National Center for Earthquake Engineering Research, State

University of New York at Buffalo, Buffalo, New York.

Hwang, H., and Lee, C.S. (1990). "Site-Specific Response Spectra for Memphis Sheahan Pumping Station." Technical Resort NCEER-90-0007, National Center for Earthquake Engineering Research, State University of New York at Buffalo, Buffalo, New York.

Hwang, H., and Lee, C.S. (1991). "Probabilistic Evaluation of Liquefaction Potential." Technical Resort NCEER-91-0025, National Center for Earthquake Engineering Research, State University of New York at Buffalo, Buffalo, New York.

Hwang, H., Lee, C.S., and Ng, K.W. (1990). "Soil Effects on Earthquake Ground Motions in the Memphis Area." Technical Resort NCEER-90-0029, National Center for Earthquake Engineering Research, State University of New York at Buffalo, Buffalo, New York.

Iman, R.L., and Conover, W.J. (1980). "Small Sample Sensitivity Analysis Techniques for Computer Models, With an Application to Risk Assessment." *Communications in Statistics*, Vol. A9, No. 17, 1749-1842.

International Conference of Building Officials (1991). *Uniform Building Code*. Whittier, California.

Ishikawa, Y., and Kameda, H. (1991). "Probability-Based Determination of Specific Scenario Earthquakes." *Proceedings of the Fourth International Conference on Seismic Zonation*, Earthquake Engineering Research Institute, Oakland, California, Vol. II, 3-10.

Johnston, A.C. (1988). "Seismic Ground Motions in Shelby County." Technical Report 88-1, Center for Earthquake Research and Information, The University of Memphis, Memphis, Tennessee.

Johnston, A.C. (1989). "Moment Magnitude Estimation for Stable

Continental Earthquakes." *Seismological Research Letters*, Vol. 60, No. 1, 13.

Johnston, A.C., and Nava, S.J. (1990). "Seismic-Hazard Assessment in the Central United States." *Neotectonics in Earthquake Evaluation*, E.L. Krinitzsky and D.B. Slemmons (eds.), Geological Society of America, Vol. VIII, 47-57.

Joyner, W.B., Warrick, R.E., and Fumal, T.E. (1981). "The Effects of Quaternary Alluvium on Strong Ground Motion in the Coyote Lake, California, Earthquake of 1979." *Bulletin of Seismological Society of America*, Vol. 71, 1333-1349.

Kunnath, S.K., Reinhorn, A.M., and Lobo, R.F. (1991). "IDARC — Inelastic Damage Analysis of Reinforced Concrete Frame-Wall Structures (Version 2.1)." Technical Report (draft), National Center for Earthquake Engineering Research, State University of New York at Buffalo, Buffalo, New York.

Lee, C.S., Hwang, H., and Chang, T.-S. (1991). "Subsurface Exploration at Pipeline Crossing near the Wolf River." Technical Report, Center for Earthquake Research and Information, The University of Memphis, Memphis, Tennessee.

Leon, D.D., and Ang, A.H-S. (1993). "A Damage Model for Reinforced Concrete Buildings — Further Study with the 1985 Mexico City Earthquake." *Proceedings of the Sixth International Conference on Structural Safety and Reliability*, Innsbruck, Austria, Vol. III, 2081-2088.

Mirza, S.A., and MacGregor, J.G. (1979). "Variability of Mechanical Properties of Reinforcing Bars." *Journal of Structural Engineering*, ASCE, Vol. 105, No. 5, 921-937.

Nuttli, O.W., and Herrmann, R.B. (1984). "Ground Motion of Mississippi Valley Earthquakes." *Journal of Technical Topics in Civil Engineering*, Vol. 110, No. 1, 54-69.

Pappin, J.W. (1991). "Earthquake Engineering in Regions of Low Seismicity." *Proceedings of Pacific Conference on Earthquake Engineering*, Auckland, New Zealand, Vol. II, 1-20.

Park, Y.J., and Ang, A.H-S. (1985). "Mechanistic Seismic Damage Model for Reinforced Concrete." *Journal of Structural Engineering*, ASCE, Vol. 111, No. 4, 722-739.

Park, Y.J., Ang, A.H-S., and Wen, Y.K. (1985). "Seismic Damage Analysis of Reinforced Concrete Building." *Journal of Structural Engineering*, ASCE, Vol. 111, No. 4, 740-757.

Park, Y.J., Reinhorn, A.M., and Kunnath, S.K. (1987). "IDARC: Inelastic Dynamic Analysis of Reinforced Concrete Frame-Shear-Wall Structures." Technical Report NCEER-87-0008, National Center for Earthquake Engineering Research, State University of New York at Buffalo, Buffalo, New York.

Reinhorn, A.M., Seidel, M.J., Kunnath, S.K., and Park, Y.J. (1988). "Damage Assessment of Reinforced Concrete Structures in Eastern United States." Technical Report NCEER-88-0016, National Center for Earthquake Engineering Research, State University of New York at Buffalo, Buffalo, New York.

Schnabel, P.B., Lysmer, J., and Seed, H.B. (1972). "SHAKE, A Computer Program for Earthquake Response Analysis of Horizontally Layered Sites." Report No. EERC 72-12, Earthquake Engineering Research Center, University of California, Berkeley, California.

Shinozuka, M. (1974). "Digital Simulation of Random Processes in Engineering Mechanics with the Aid of FFT Technique." *Stochastic Problems in Mechanics*, Ariaratnam, S.T. and Leipholz, H.H.E. (eds.), University of Waterloo Press, Waterloo, 277-286.

Toro, G.R., Silva, W.J., McGuire, R.K., and Herrmann, R.B. (1992). "Probabilistic Seismic Hazard Mapping of the Mississippi Embayment." *Seismological Research Letters*, Vol. 63, No. 3, 449-475.

Whitman, R.V. (1973). "Damage Probability Matrices for Prototype Buildings." Research Report No. R73-57, Department of Civil Engineering, Massachusetts Institute of Technology, Cambridge, Massachusetts.

Whitterberg, P.L., et al. (1977). "Natural and Physical Characteristics of Memphis and Shelby County." Office of Planning and Development, Memphis and Shelby County, Tennessee.

APPENDIX A

PROBABILISTIC DYNAMIC CHARACTERISTICS OF SOILS IN THE MEMPHIS AREA

In this appendix, the dynamic characteristics of soils in the Memphis area are reviewed based on the test results available in the literature. The main dynamic parameters required in the SHAKE program (Schnabel et al. 1972) are the shear modulus ratio and damping ratio. Thus, the review concentrates on these two parameters. Since data from soil dynamic testing usually exhibit large scattering, the probabilistic characteristics such as the mean value and coefficient of variation will be determined for each soil parameter.

A.1 Shear Modulus Reduction Curve for Sands

The results of dynamic testing of sands in the Memphis area have been documented in Hwang et al. (1990), Lee et al. (1991), and Chang et al. (1992). Figure A-1 shows the shear modulus reduction curve for Collierville sand tested with the relative density D_r of 0.7 and the confining pressure $\bar{\sigma}$ of 0.28 MPa (40 psi) (Hwang et al. 1990). Three sets of the shear modulus reduction curve from Lee et al. (1991) are shown in Figures A-2(a), A-2(b), and A-2(c). These curves are for three sand layers at a site near Wolf River in Fayette County, Tennessee. Chang et al. (1992) conducted laboratory tests for three types of sand: alluvial sand (SP-SM), Terrace sand and gravel, and Jackson fine sand (SP). For each type of sand, several samples were tested with various void ratios and confining

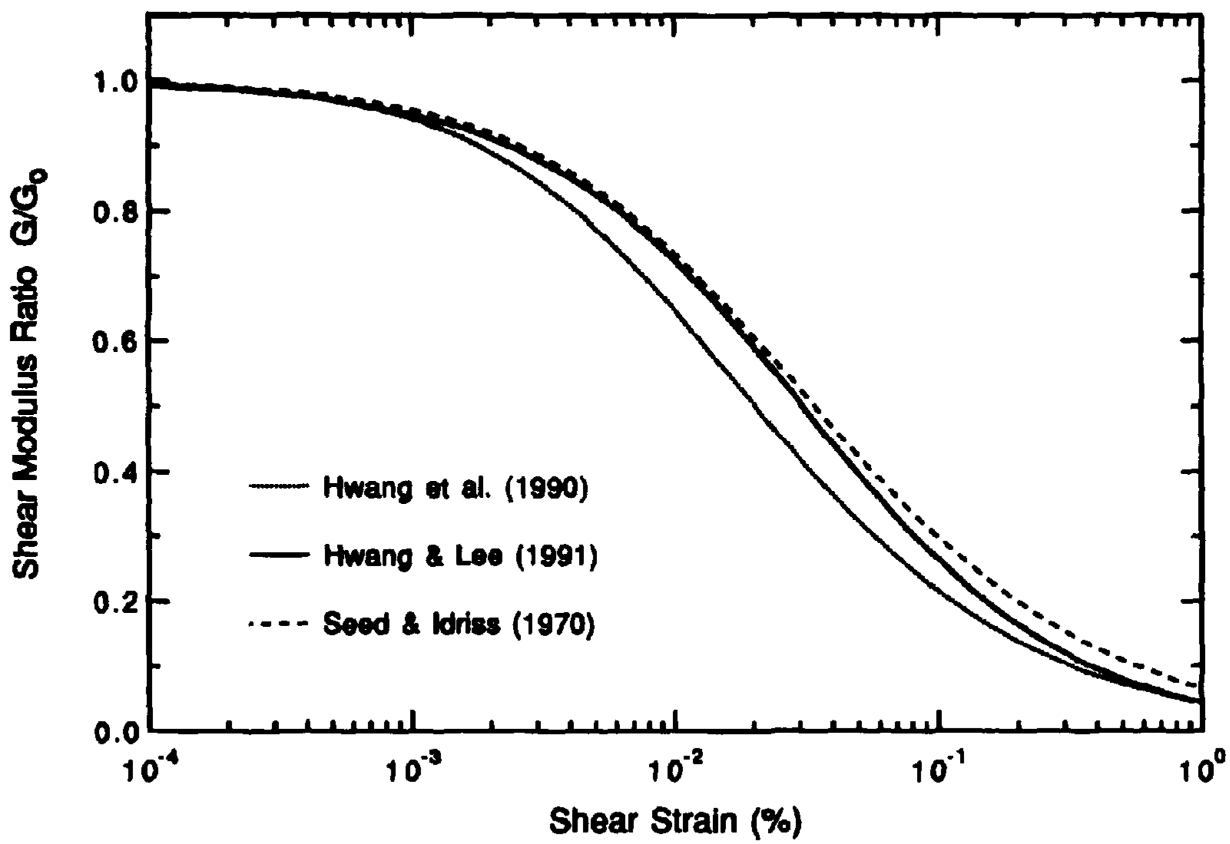

FIGURE A-1 Shear Modulus Reduction Curve for Collierville Sand (after Hwang et al. 1990)

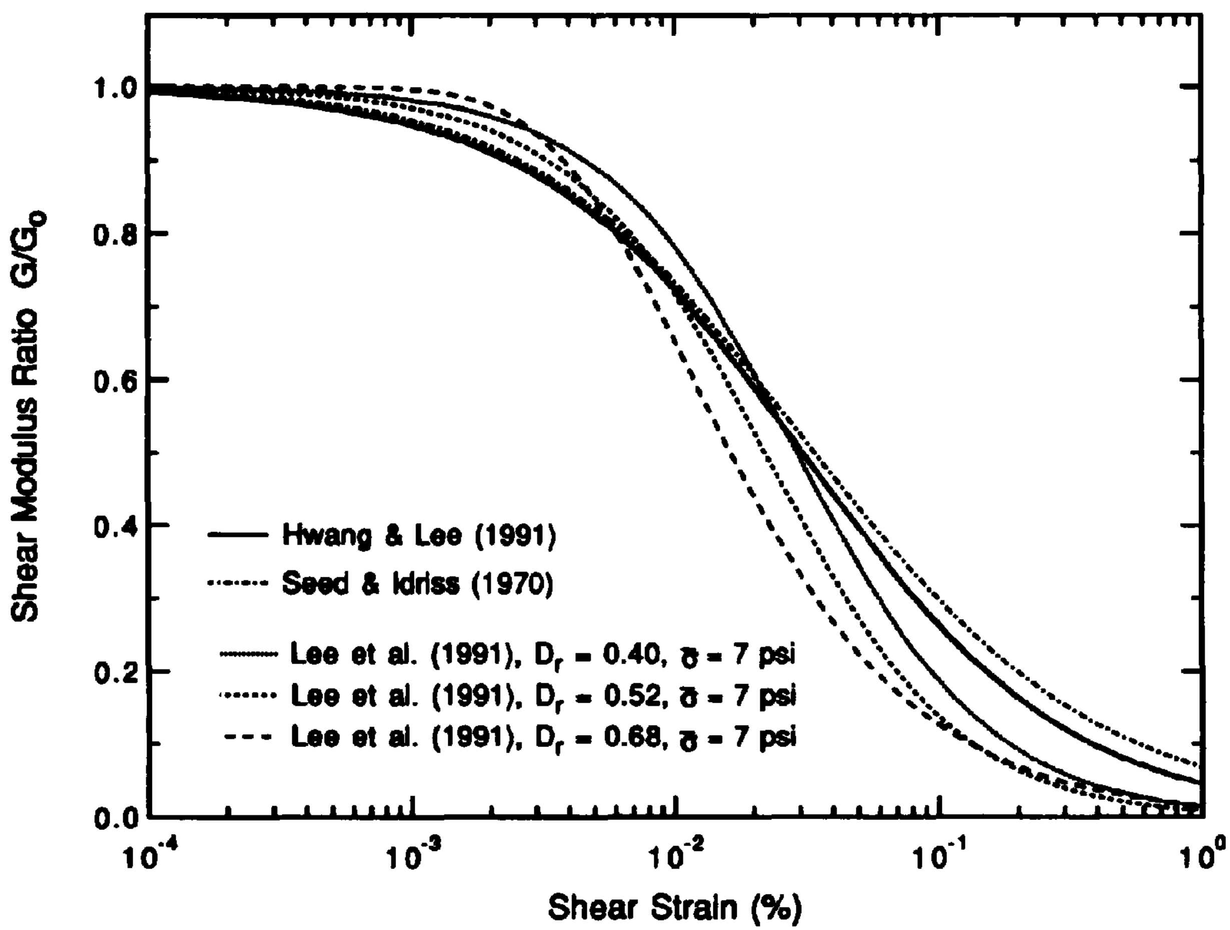

FIGURE A-2(a) **Shear Modulus Reduction Curves for Sand (Sample 3, after Lee et al. 1991)**

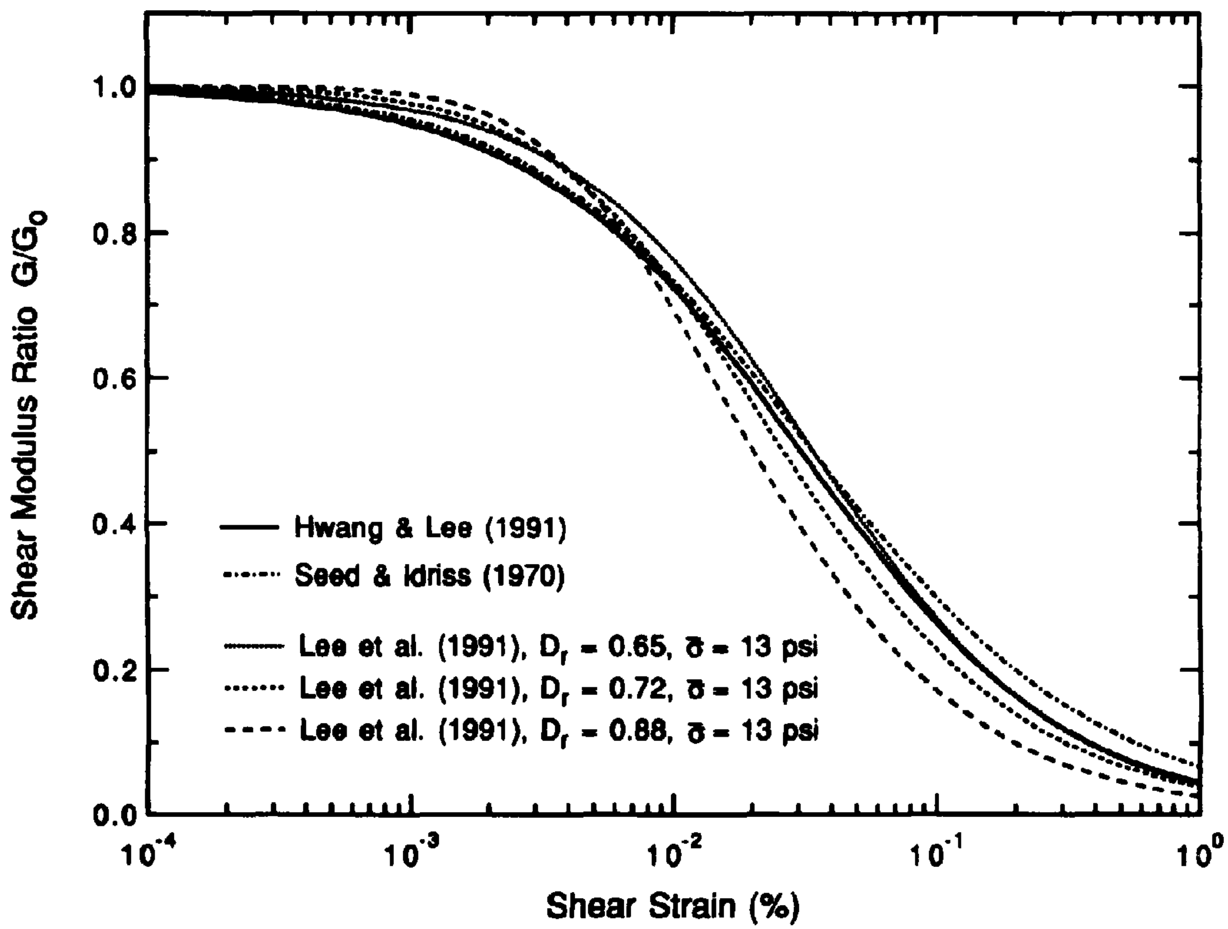

FIGURE A-2(b) Shear Modulus Reduction Curves for Sand (Sample 4, after Lee et al. 1991)

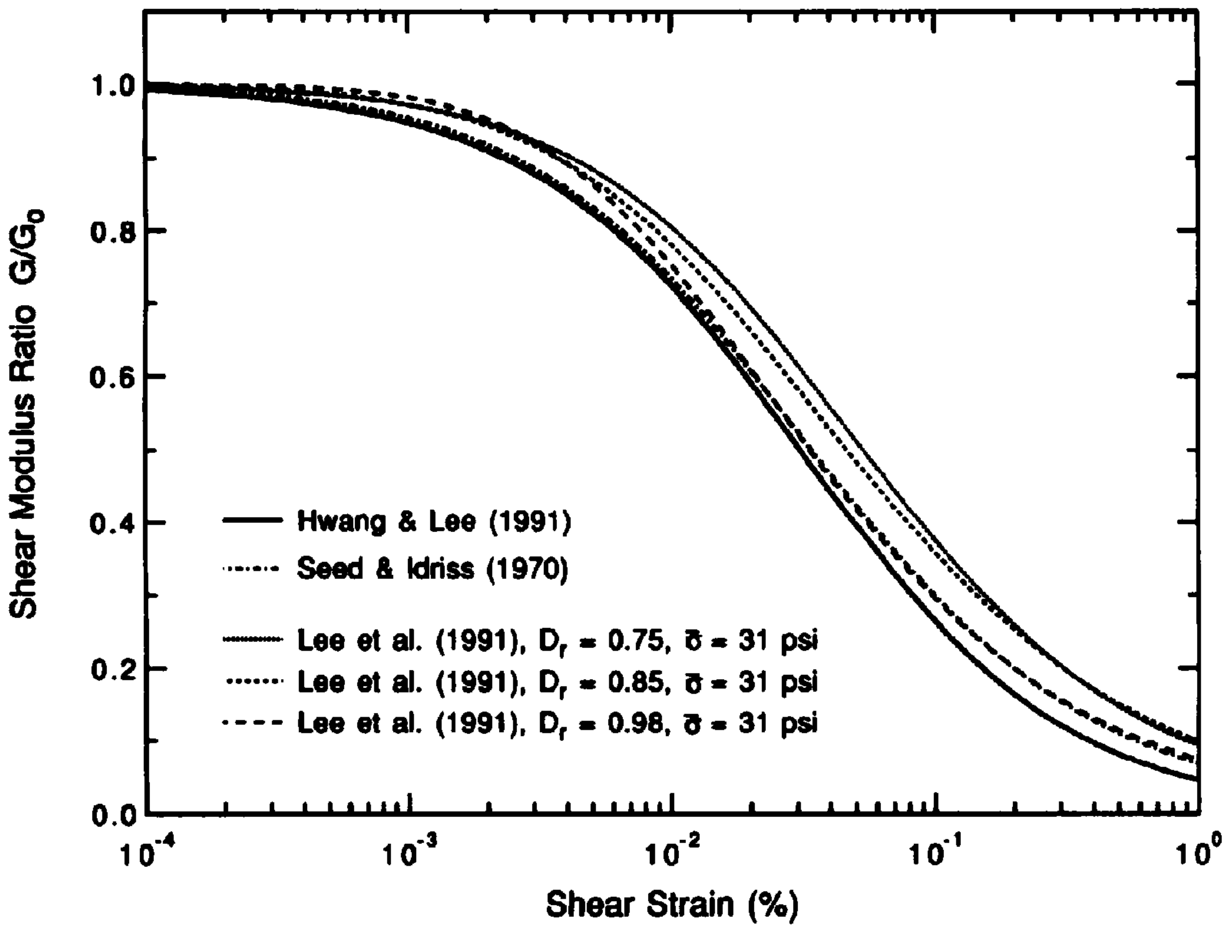

FIGURE A-2(c) Shear Modulus Reduction Curves for Sand (Sample 5, after Lee et al. 1991) pressures. The mean shear modulus reduction curves for these three types of sand are shown in Figures A-3(a), A-3(b), and A-3(c), respectively. Figure A-4 shows the comparison of the shear modulus reduction curves for sands in the Memphis area under similar testing conditions. The curves from Chang et al. (1992) are significantly higher than those from Hwang et al. (1990), and Lee et al. (1991).

Seed and Idriss (1970), Hwang and Lee (1991), and others, have investigated the shear modulus reduction curve for typical sand based on the test data available in the literature. The mean shear modulus reduction curves proposed by Seed and Idriss (1970), and Hwang and Lee (1991) are also displayed in Figures A-1 through A-3. The curve from Hwang and Lee (1991) is close to the one by Seed and Idriss (1970). In this study, we use the curve proposed by Hwang and Lee (1991) to represent the shear modulus of typical sand. As shown in Figures A-1 and A-2, even though the results vary under various testing conditions, the shear modulus reduction curves from Hwang et al. (1990), and Lee et al. (1991) agree well with the mean curves for typical sand (Hwang and Lee 1991). However, at the range of moderate to high strain, the shear modulus reduction curves from Chang et al. (1992) are much higher than the curve for typical sand (see Figures A-3(a), A-3(b), and A-3(c)). Furthermore, in Figure A-3(c), it is noted that the shear moduli with the confining pressure of 0.14 MPa (20 psi) are larger than those with the confining pressure of 0.38 MPa (55 psi) at the high strain range. This is not consistent with the dynamic characteristics of sand, that is, the shear modulus of sand is higher as the confining pressure increases. On the basis of the aforementioned discussions, it is concluded that the shear modulus reduction curves from

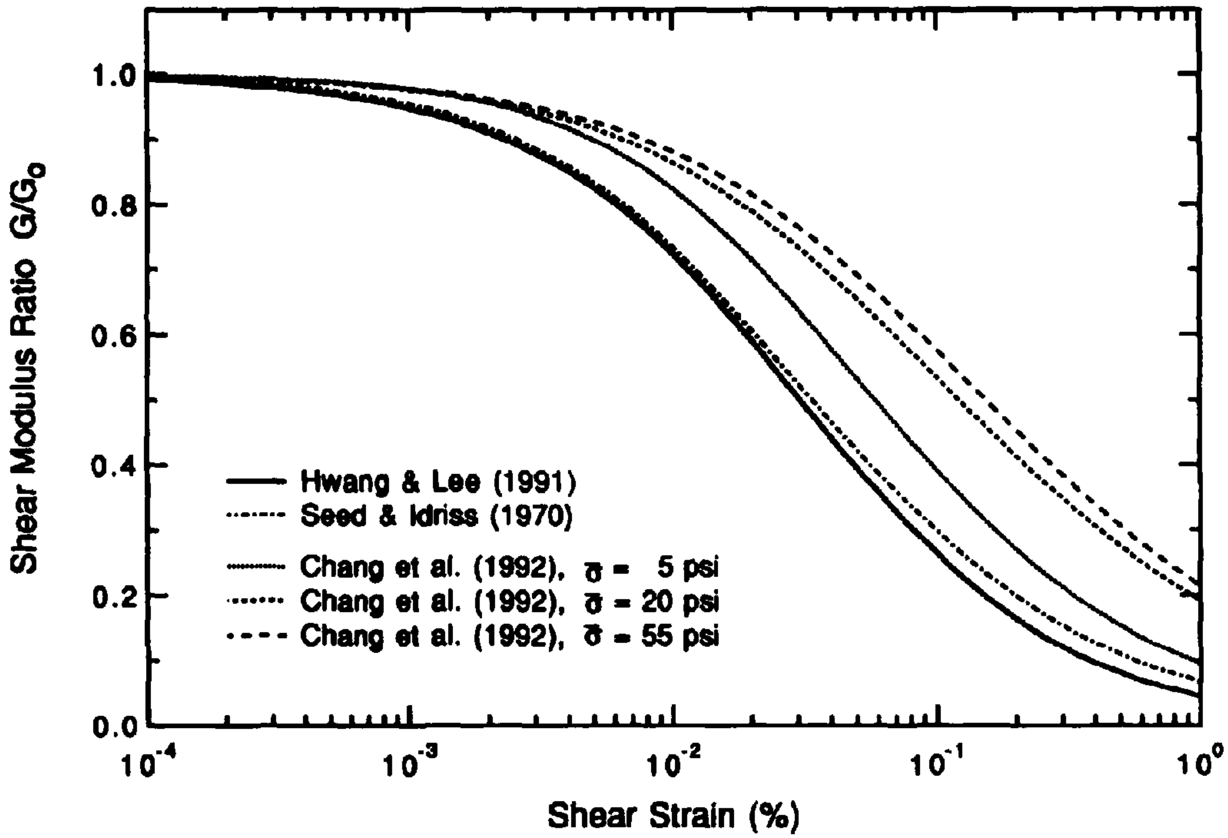

FIGURE A-3(a) Mean Shear Modulus Reduction Curves for Alluvial Sand (after Chang et al. 1992)

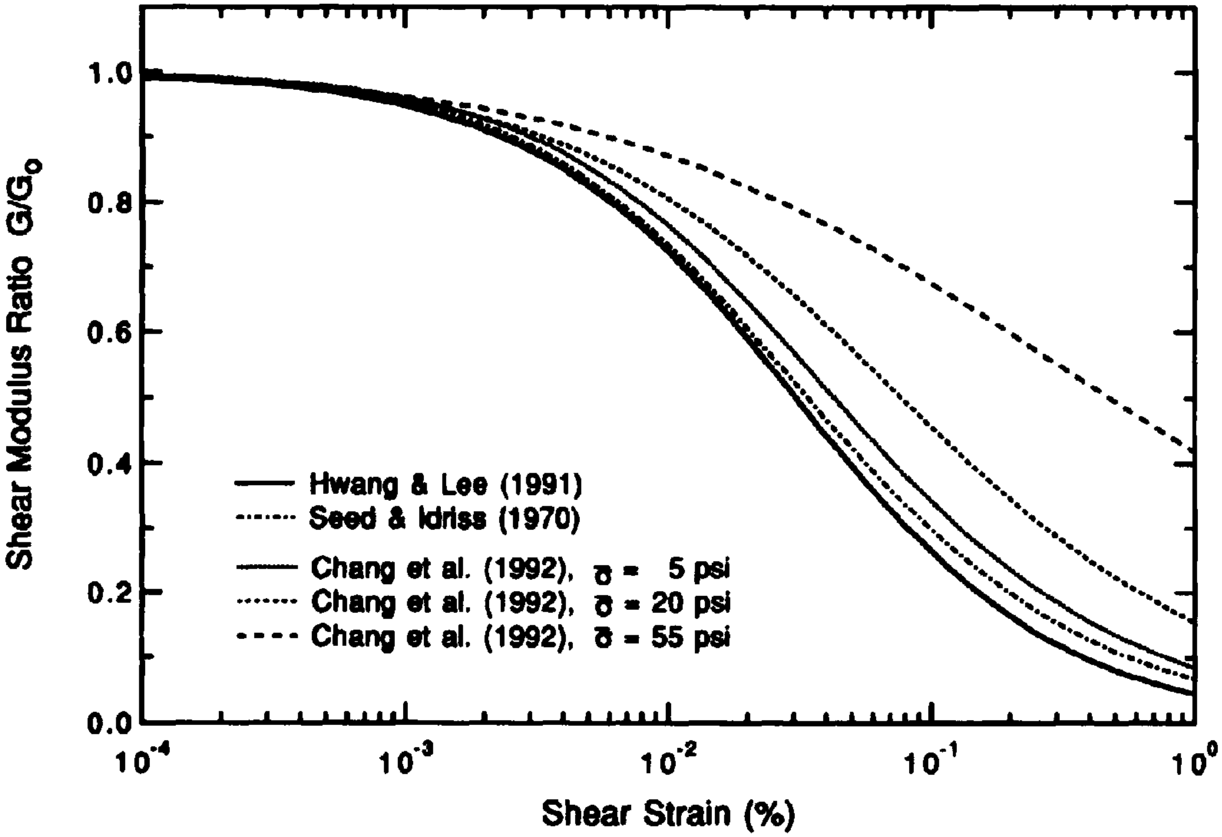

FIGURE A-3(b) Mean Shear Modulus Reduction Curves for Terrace Sand and Gravel (after Chang et al. 1992)

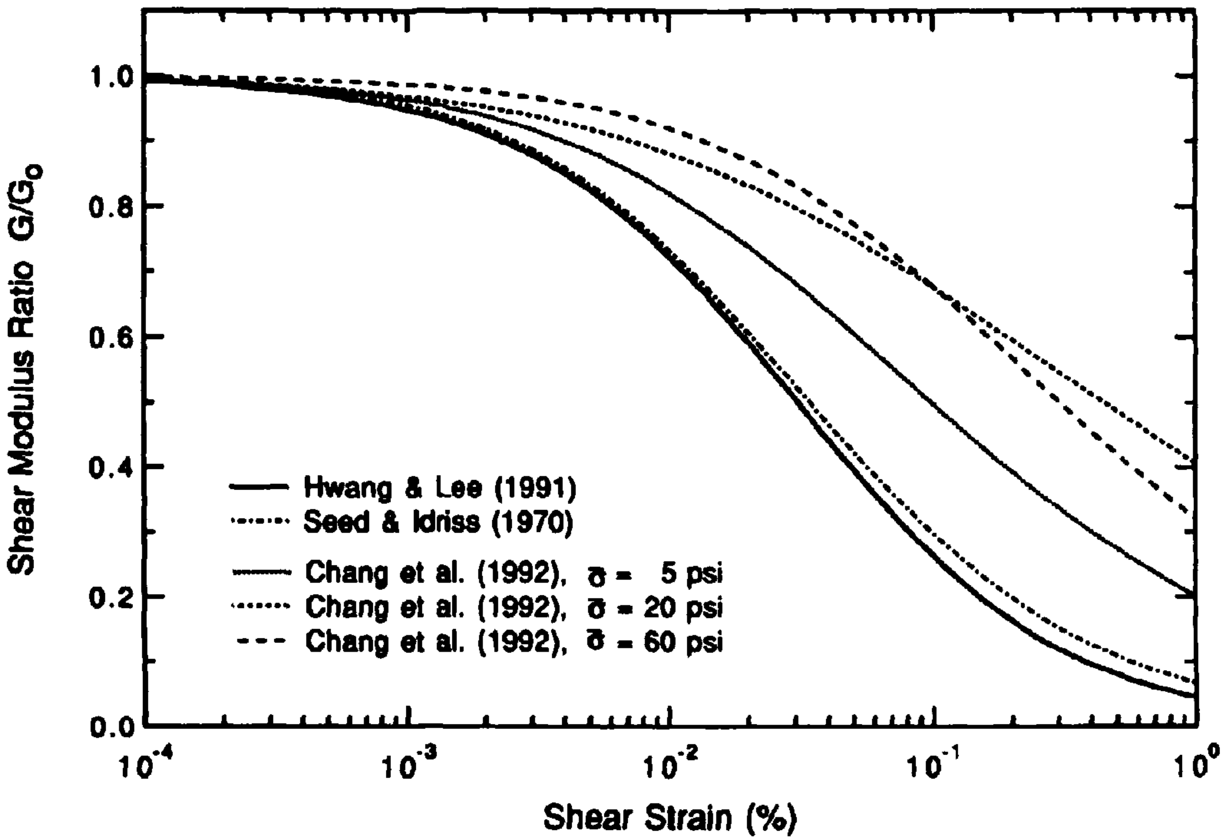

FIGURE A-3(c) Mean Shear Modulus Reduction Curves for Jackson Fine Sand (after Chang et al. 1992)

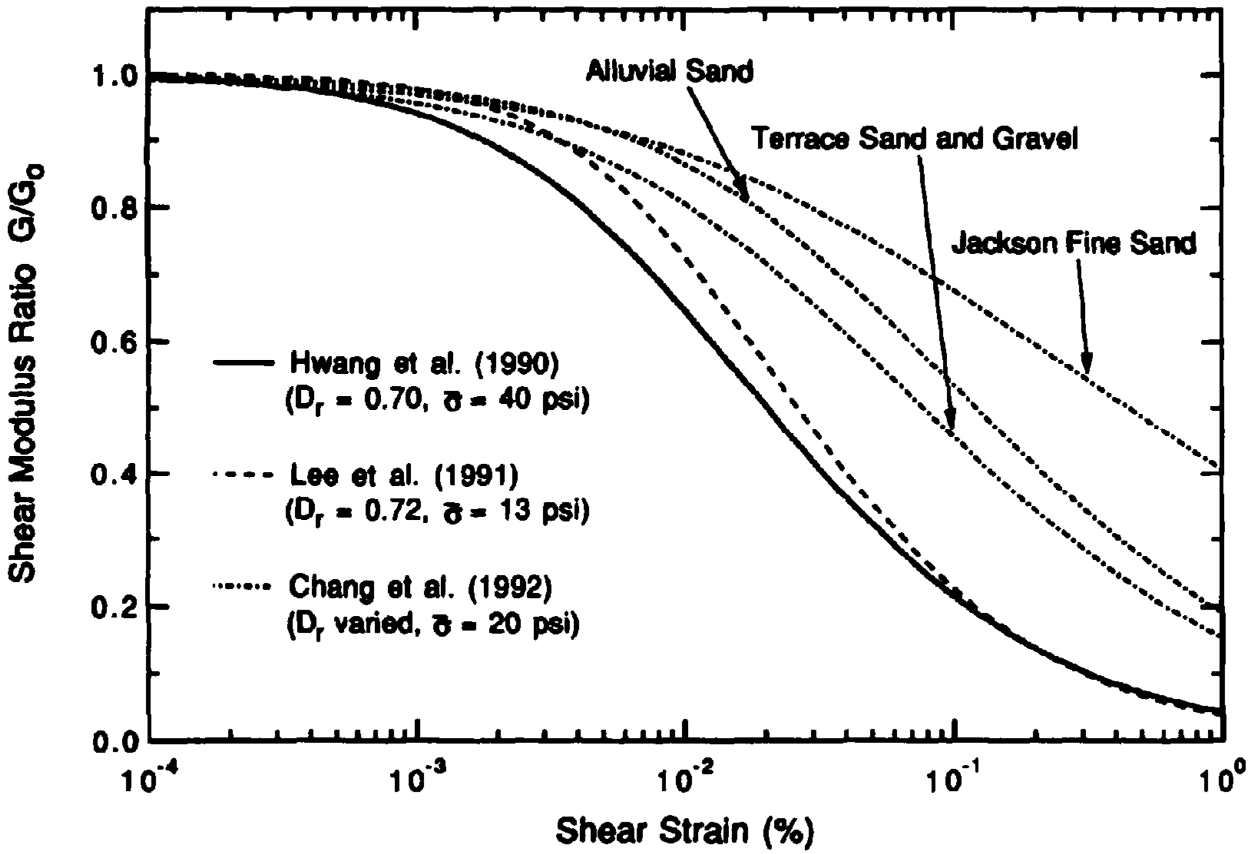

FIGURE A-4 Comparison of the Shear Modulus Reduction Curves for Sands in the Memphis Area

Hwang and Lee (1991) are appropriate to represent the dynamic characteristics of sands in the Memphis area.

The shear modulus reduction curves from Hwang and Lee (1991) are expressed in the form of the Martin-Davidenkov model (Martin 1976),

$$\frac{G}{G_0} = 1 - \left[\frac{(\gamma/\gamma_0)^{2B}}{1 + (\gamma/\gamma_0)^{2B}}\right]^A \tag{A.1}$$

where G/G_0 is the shear modulus ratio and G_0, γ_0, A, and B are four parameters defining the shear modulus reduction curve. G_0 is the low-strain shear modulus and is usually taken as the shear modulus corresponding to shear strain of 10^{-4} % or less. In this study, G_0 is estimated from the following empirical equation:

$$G_0 = 61000\ [1 + (D_r - 75)\ 0.01]\ (\bar{\sigma})^{1/2} \tag{A.2}$$

where $\bar{\sigma}$ is the average effective confining pressure in psf and D_r is the relative density in percentage. γ_0 is the reference strain and is determined as

$$\gamma_0 = \frac{\tau_{max}}{G_0} \tag{A.3}$$

where τ_{max} is the maximum shear stress of soils under dynamic loading and is computed using the following equation (Hardin and Drnevich 1972):

$$\tau_{max} = \left\{ \left[\left(\frac{1 + K_0}{2}\right) \sigma_v' \sin \phi' + c' \cos \phi' \right]^2 - \left[\left(\frac{1 - K_0}{2}\right) \sigma_v' \right]^2 \right\}^{1/2} \tag{A.4}$$

in which c' is the apparent cohesion and is negligible for sand; ϕ' is the effective angle of internal friction; σ_V' is the effective vertical stress in psf; and K_0 is the coefficient of earth pressure at rest. The parameters A and B define the shape of the shear modulus reduction curve. Table A-I lists the values of A and B for the mean, lower- and upper-bound shear modulus reduction curves of sand from Hwang and Lee (1991) as shown in Figure A-5.

The soil testing results vary greatly, since the soil dynamic testing is affected by many factors such as testing technique, calibration of testing equipment, and simulation of in-situ condition. Consequently, the soil parameters cannot be determined precisely. Because the test data of sands in the Memphis area are limited, these data cannot be used to determine the variation of the soil parameter. The upper- and lower-bound shear modulus reduction curves for sand from Hwang and Lee (1991) were determined based on the wide range of test data available in the literature. Thus, these curves are used to determine the variation of the shear moduli at various levels of shear strain.

In this study, the shear modulus ratio G/G_0 is assumed as a normal random variable. The mean value at each level of shear strain is taken from the mean shear modulus reduction curve proposed by Hwang and Lee (1991). The standard deviation (SD) is determined from the upper- and lower-bound values by considering these values as the mean plus or minus three standard deviations, respectively. The probabilistic characteristics of the shear modulus ratio of sand in the Memphis area are summarized in Table

TABLE A-I Parameter Values of A and B for Sand

Cases	A	B
Upper	1.775	0.489
Mean	0.941	0.441
Lower	0.509	0.480

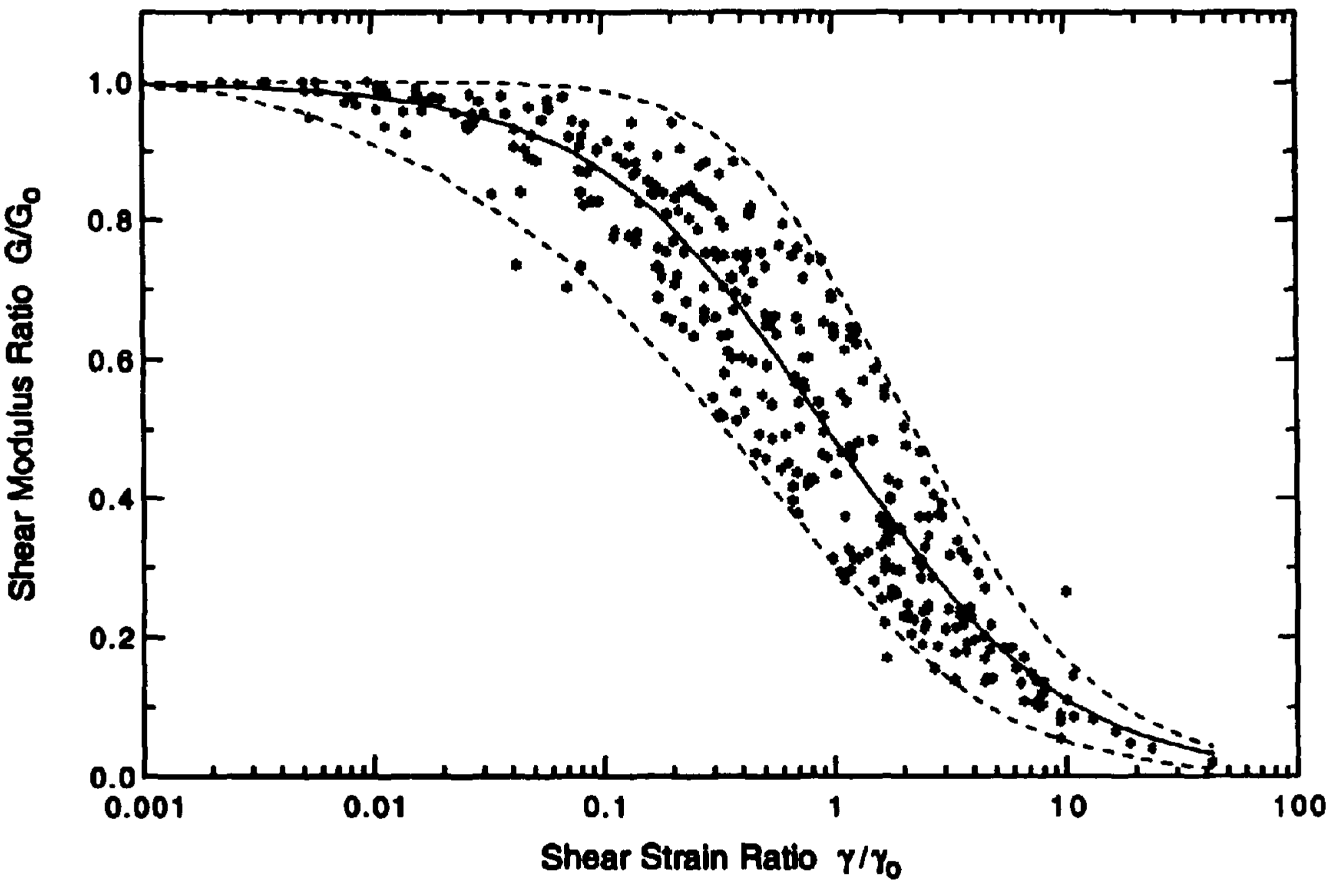

FIGURE A-5 Shear Modulus Reduction Curves for Typical Sand (after Hwang and Lee 1991)

A-II. In addition, the mean and mean ± 2SD shear modulus reduction curves are also plotted in Figure A-6.

A.2 Damping Ratio for Sands

The testing of sands reported in Hwang et al. (1990) and Lee et al. (1991) is mainly to establish the shear modulus reduction curve, and thus the damping of the soil was not measured. Chang et al. (1992) measured the damping for three types of sand in the range of shear strain from 0.001% to 0.1%. Their results are shown in Figures A-7(a), A-7(b) and A-7(c), respectively. The damping for sands has been investigated by many researchers, for example, Seed and Idriss (1970), Idriss (1990), and Geomatrix (1991). The results obtained by these researchers are also displayed in Figure A-7. The test results from Chang et al. (1992) are compatible with others in the range of shear strain from 0.001% to 0.05%. However, the results from Chang et al. are higher than others at the shear strain around 0.1%. Furthermore, Chang et al. did not measure the damping at the shear strain higher than 0.1% or less than 0.0005%. From the comparison shown in Figures A-7, the damping ratio curve proposed by Idriss (1990) seems to be appropriate for representing the damping ratio of sands in the Memphis area, except for the damping at the very low level of shear strain. The damping ratio for shear strain less than 10^{-3} % is modified from about 0.5% to 1.0 - 1.5% based on the data shown in Figure A-7 and the damping values determined from shear-wave propagating at low levels of ground motion reported by Joyner et al. (1976, 1981) and Johnson and Silva (1981).

TABLE A-II Probabilistic Characteristics of Shear Modulus Ratio for Sands

Strain ratio (γ/γ_0)	Mean	SD	COV
1×10^{-3}	1.00	0.01	0.01
3×10^{-3}	0.99	0.01	0.01
1×10^{-2}	0.98	0.02	0.02
3×10^{-2}	0.95	0.03	0.03
1×10^{-1}	0.87	0.05	0.06
3×10^{-1}	0.72	0.07	0.09
1×10^{0}	0.48	0.07	0.14
3×10^{0}	0.26	0.04	0.17
1×10^{1}	0.11	0.02	0.17
3×10^{1}	0.05	0.01	0.20

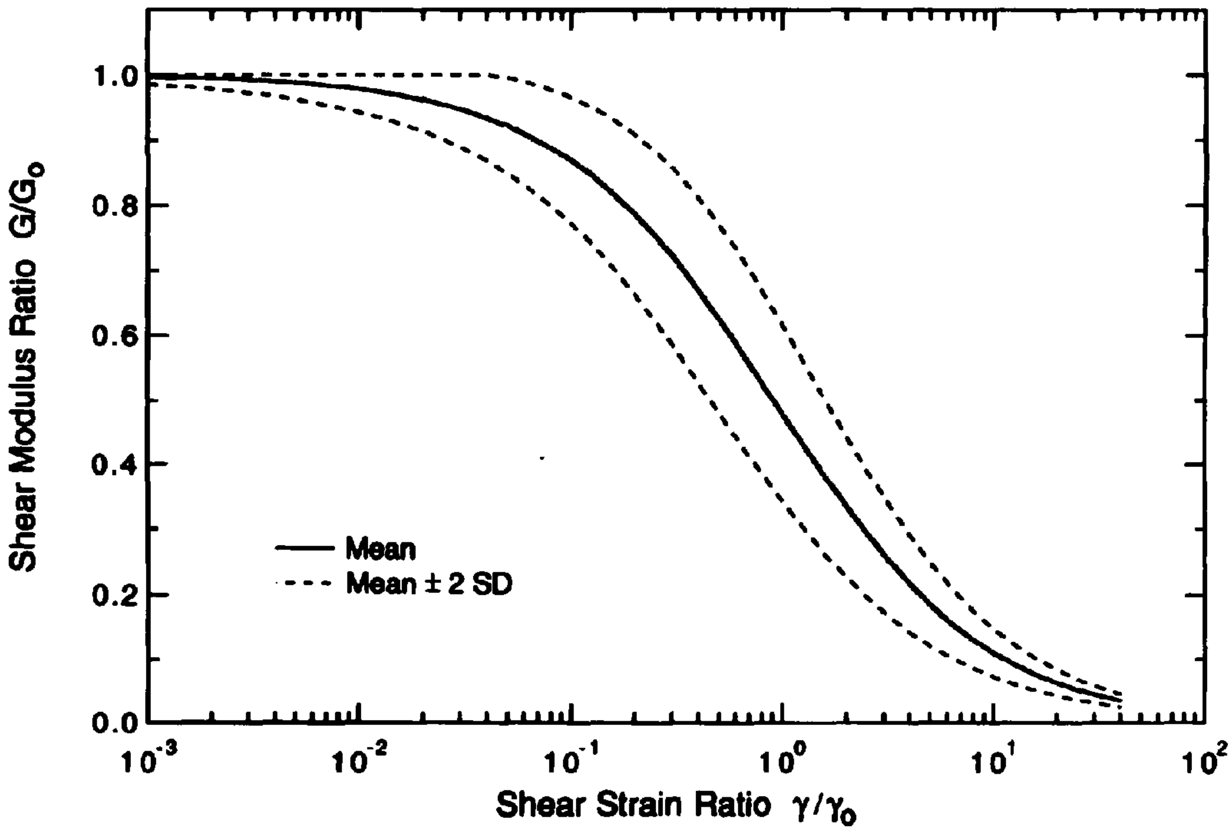

FIGURE A-6 **Recommended Shear Modulus Reduction Curves for Sand in the Memphis Area**

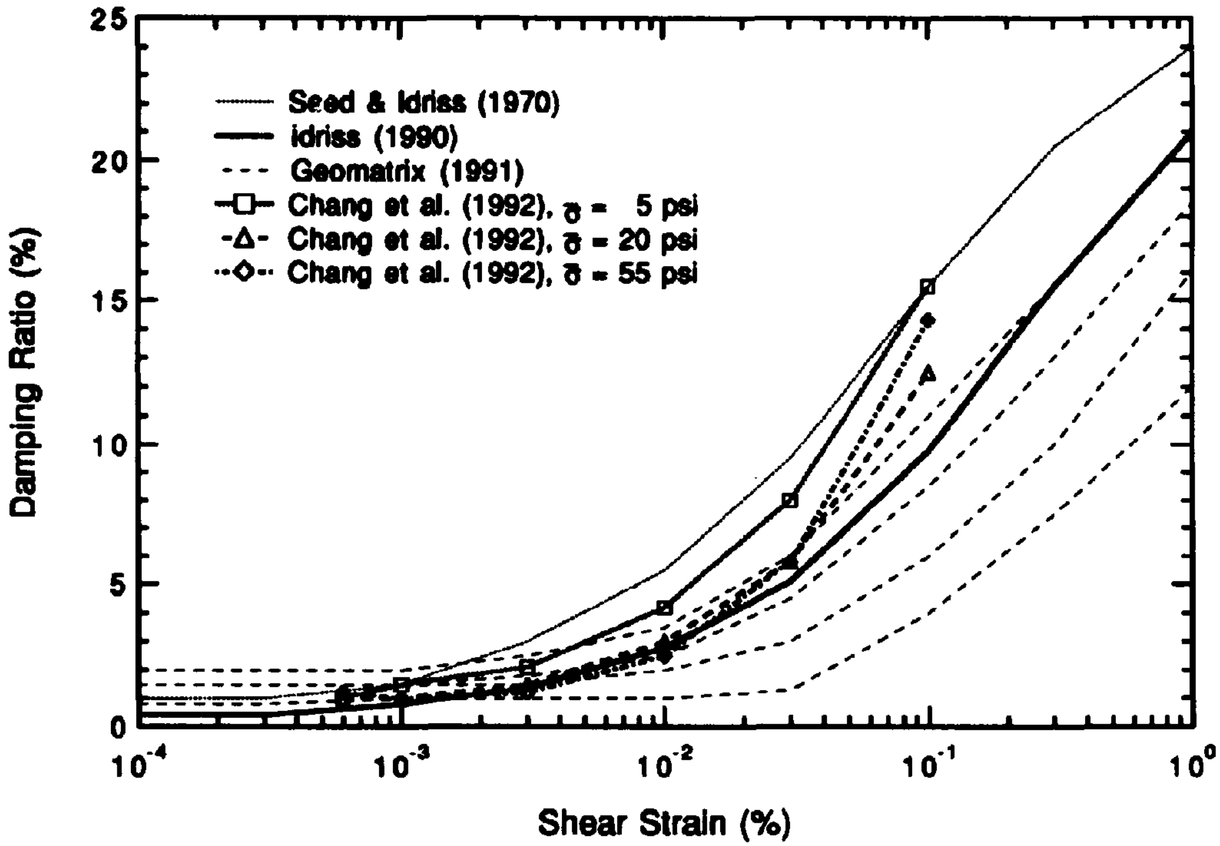

FIGURE A-7(a) Comparison of the Damping Ratio Curves for Alluvial Sand from Chang et al. (1992) and Other Experimental Results

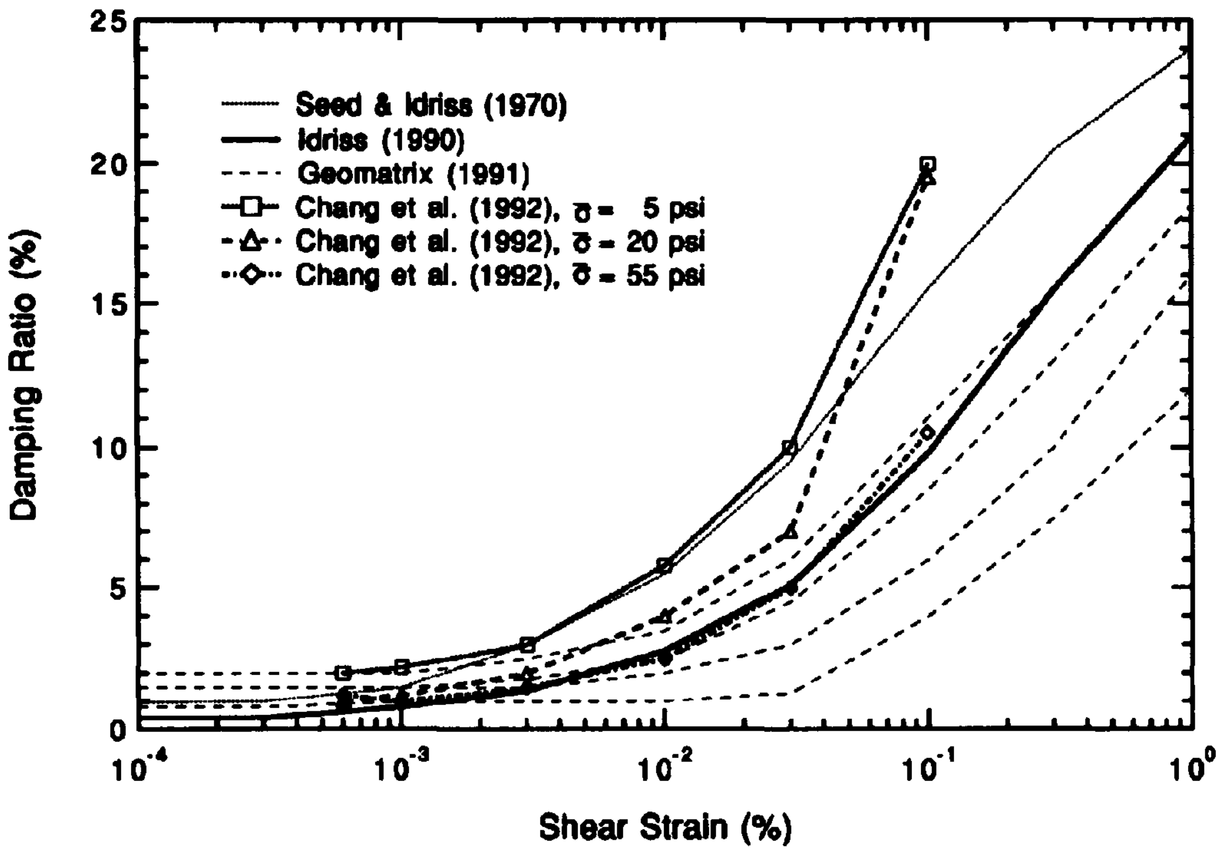

FIGURE A-7(b) Comparison of the Damping Ratio Curves for Terrace Sand and Gravel from Chang et al. (1992) and Other Experimental Results

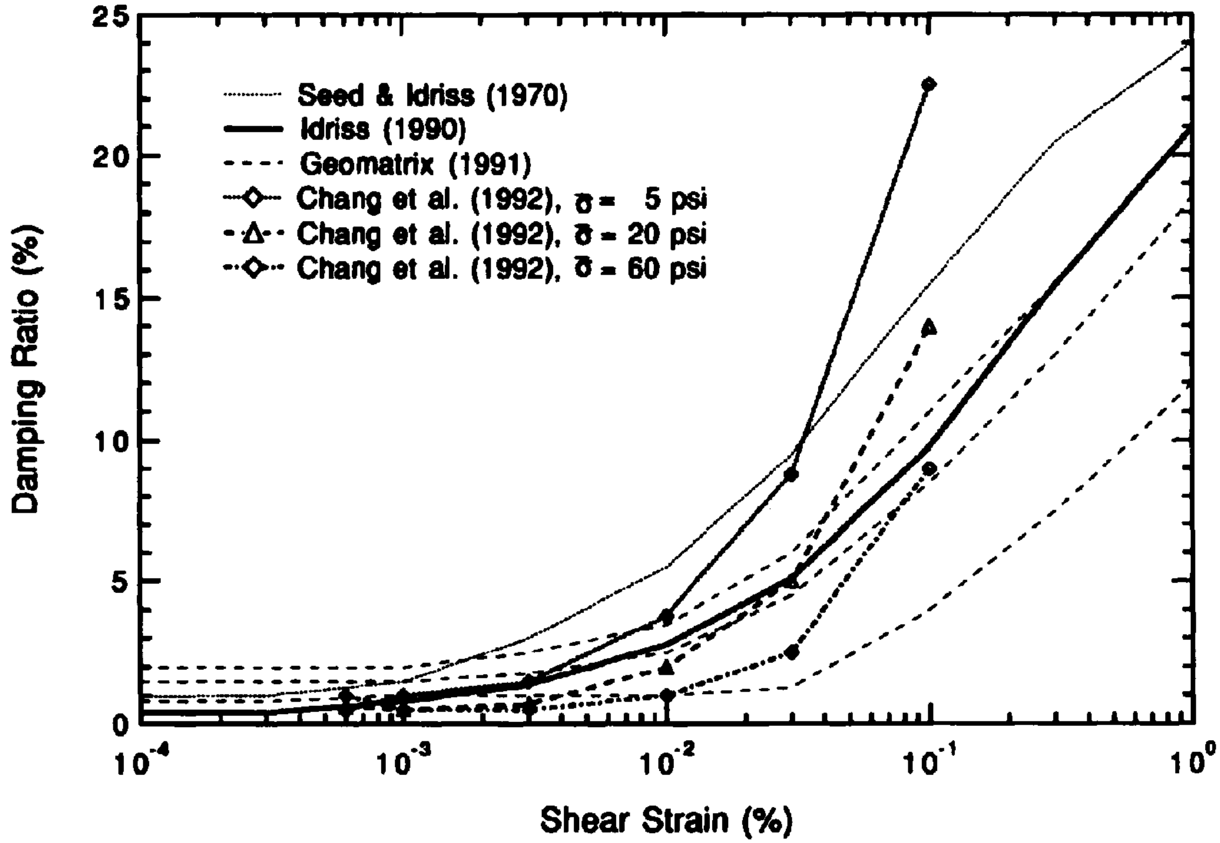

FIGURE A-7(c) Comparison of the Damping Ratio Curves for Jackson Fine Sand from Chang et al. (1992) and Other Experimental Results

The test data of sands in the Memphis area cannot be used to determine the variation of the damping ratio because the available data are limited. Figure A-8 shows the test data collected by Seed and Idriss (1970). Even though the mean curve in Figure A-8 has been modified (Idriss 1990), the range of the test data does not change very much. Thus, the range shown in Figure A-8 is used to determine the variability of the damping ratio for sand. The standard deviation of the damping ratio at each level of shear strain is determined by assuming that the upper- and lower-bound values shown in Figure A-8 correspond to mean plus or minus two standard deviations. The probabilistic characteristics of the damping ratio for sands in the Memphis area are listed in Table A-III. The mean, and mean ± 2SD curves are also plotted in Figure A-9.

A.3 Shear Modulus Reduction Curve for Clays

Various studies such as Zen et al. (1978), Sun et al. (1988), and Vucetic and Dobry (1991) have demonstrated that the plasticity index (PI) is the most dominant factor affecting the shape of the shear modulus reduction curve for clays. The shear modulus reduction curves gradually shift to the right as PI increases. The testing of clays in the Memphis area has been documented in Hwang et al. (1990) and Chang et al. (1992). Figure A-10 shows the shear modulus reduction curve for the Peabody clayey silt with the PI value estimated as 5 - 10 (Hwang et al. 1990). Chang et al. (1992) conducted the dynamic tests for two types of local clays, silty to sandy clay (CL) and Jackson clay (CL-CH). The test results are shown in Figures A-11(a) and A-11(b), respectively. The PI values of these two types of clays were not determined.

TABLE A-III Probabilistic Characteristics of Damping Ratio for Sands

Strain (%)	Mean (%)	SD (%)	COV
1×10^{-4}	1.04	0.26	0.25
3×10^{-4}	1.31	0.27	0.21
1×10^{-3}	1.65	0.36	0.22
3×10^{-3}	2.00	0.63	0.32
1×10^{-2}	2.80	0.78	0.28
3×10^{-2}	5.10	1.41	0.28
1×10^{-1}	9.80	2.33	0.23
3×10^{-1}	15.50	2.27	0.15
1×10^{0}	21.00	1.72	0.08

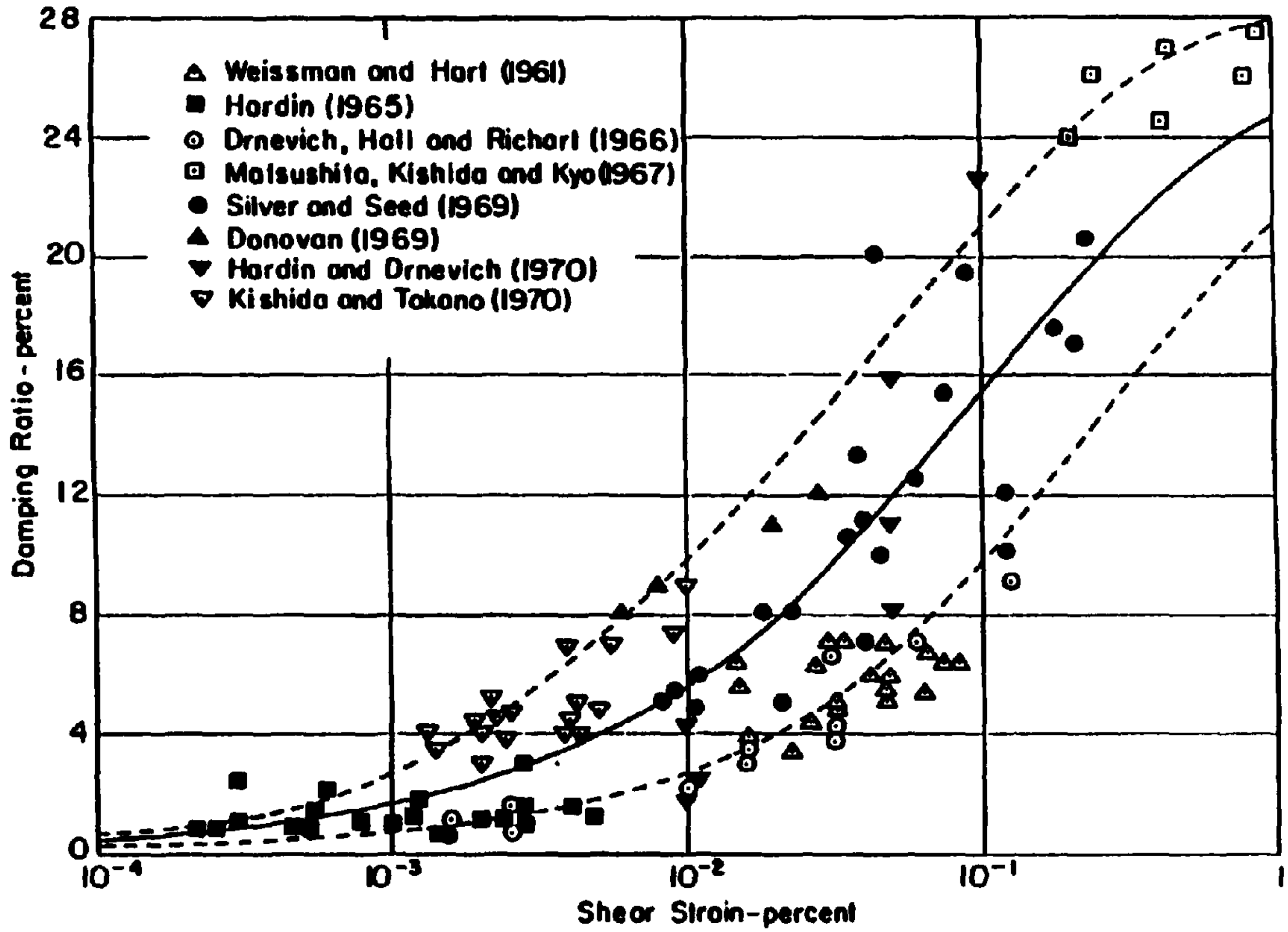

FIGURE A-8 Variation of Damping Ratio for Sand (after Seed and Idriss 1970)

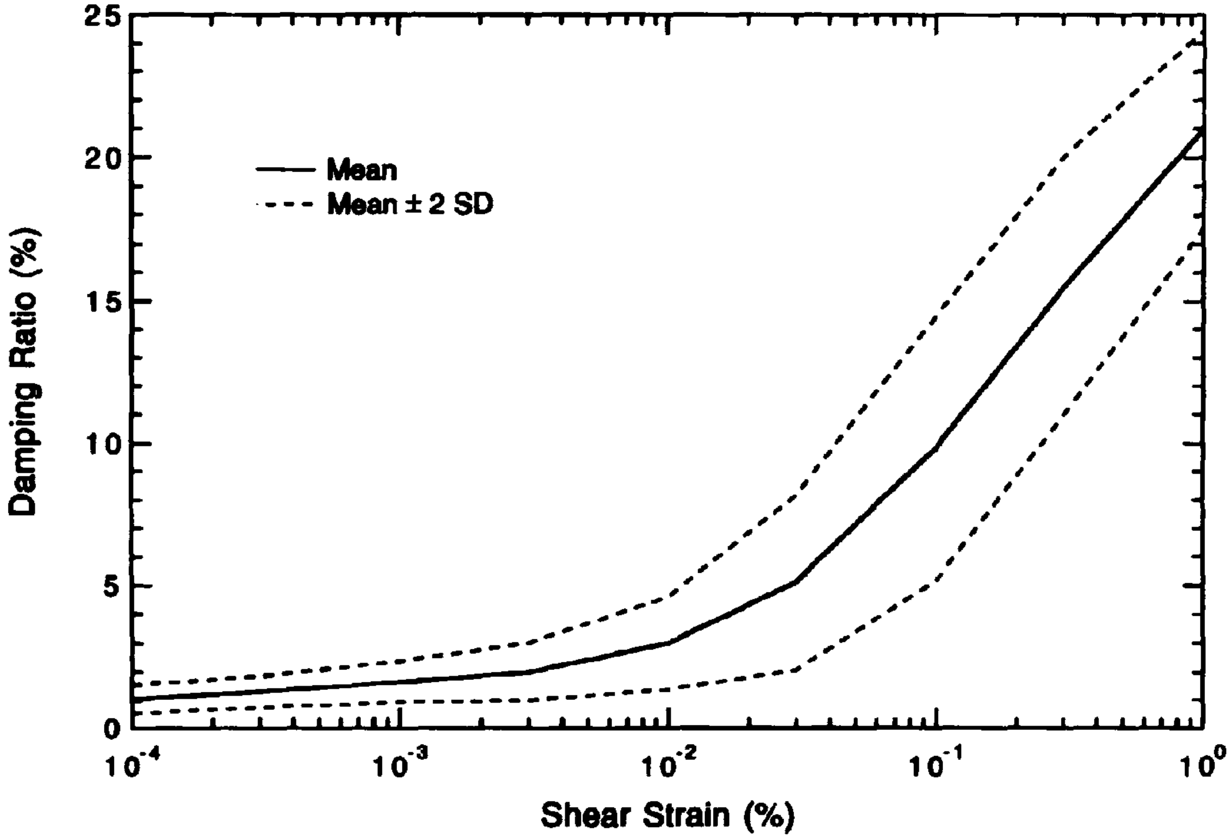

FIGURE A-9 Recommended Damping Ratio Curves for Sand in the Memphis Area

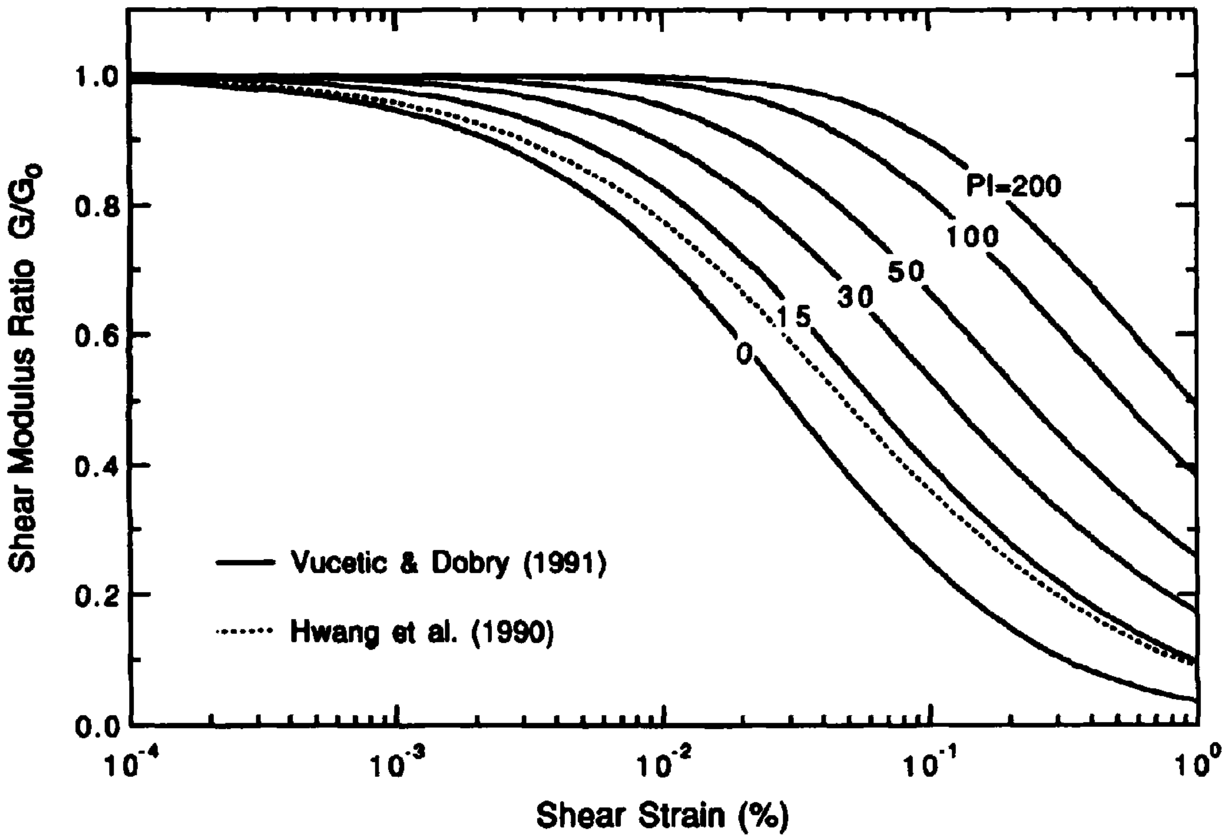

FIGURE A-10 Shear Modulus Reduction Curve for Peabody Clayey Silt (after Hwang et al. 1990)

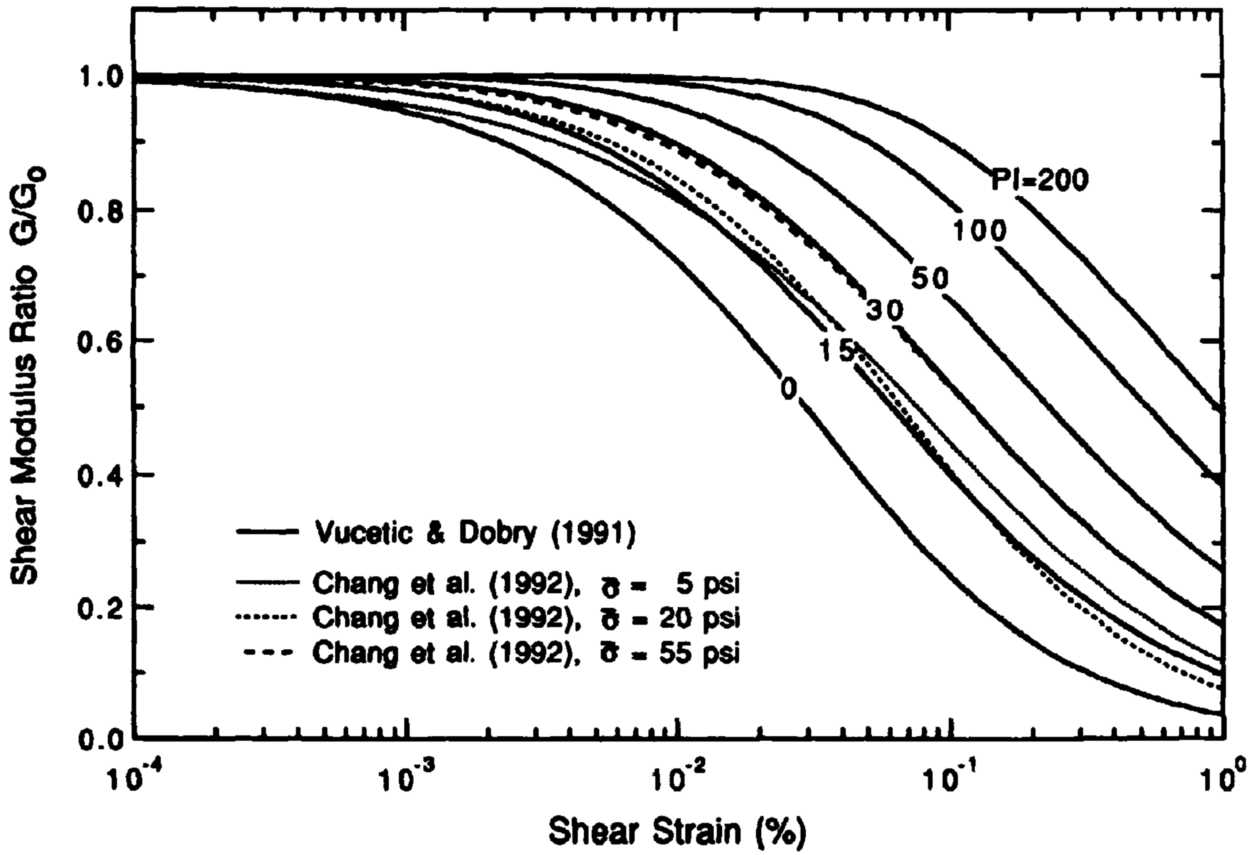

FIGURE A-11(a) Mean Shear Modulus Reduction Curves for Silty to Sandy Clay (after Chang et al. 1992)

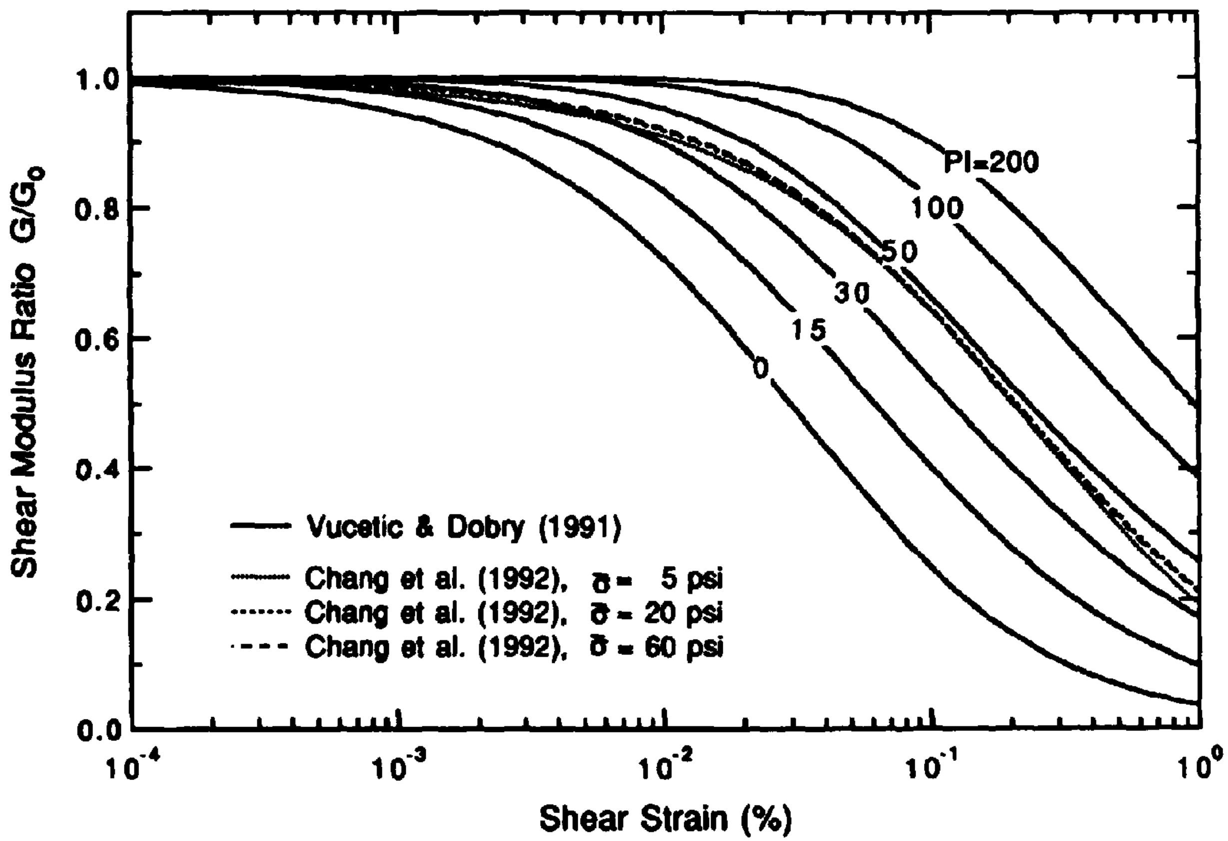

FIGURE A-11(b) Mean Shear Modulus Reduction Curves for Jackson Clay (after Chang et al. 1992)

Sun et al. (1988) and Vucetic and Dobry (1991) summarized the dynamic characteristics of clays according to PI values using the data available in the literature. The results from these two studies are similar. In this study, the results from Vucetic and Dobry (1991) are used and the shear modulus reduction curves corresponding to PI of 0, 15, 30, 50, 100, 200 are also shown in Figures A-10 and A-11. From these figures, it can be found that the testing results for clays in the Memphis area are close to the curves determined by Vucetic and Dobry (1991). Since the shear modulus reduction curves for clays from Vucetic and Dobry (1991) cover the entire range of PI value, these curves are used to represent the dynamic characteristics of clays in the Memphis area.

The shear modulus reduction curves for clay are also expressed using Equation (A.1), in which G_o, γ_o, A and B are four parameters. The low-strain shear modulus G_o of clay is computed as

$$G_o = 2500\ S_u \tag{A.5}$$

where S_u is the undrained shear strength of clay. The reference strain γ_o is taken as 0.0004 (Hwang and Lee 1991). Table A-IV shows the values of parameters A and B corresponding to various PI values. These values are determined from a regression analysis of the curves by Vucetic and Dobry (1991). Using the parameters discussed above, the shear modulus ratios at various levels of shear strain for PI of 15 and 50 are listed in Table A-V.

Because of limited local test data, the test data at shear strains of 0.01%,

TABLE A-IV Parameter Values of A and B for Clays

PI	A	B
0	0.824	0.478
15	1.284	0.385
30	1.796	0.341
50	2.479	0.320
100	3.715	0.306
200	5.055	0.301

TABLE A-V Probabilistic Characteristics of Shear Modulus Ratio for Clays

Strain (%)	PI = 15			PI = 50		
	Mean	SD	COV	Mean	SD	COV
1×10^{-4}	1.00	0.00	0.00	1.00	0.00	0.00
3×10^{-4}	0.99	0.00	0.00	1.00	0.00	0.00
1×10^{-3}	0.98	0.01	0.01	1.00	0.00	0.00
3×10^{-3}	0.93	0.02	0.02	0.99	0.00	0.00
1×10^{-2}	0.83	0.04	0.05	0.95	0.02	0.02
3×10^{-2}	0.65	0.06	0.09	0.86	0.04	0.04
1×10^{-1}	0.40	0.08	0.20	0.67	0.06	0.09
3×10^{-1}	0.22	0.05	0.23	0.45	0.05	0.11
1×10^{0}	0.10	0.03	0.30	0.26	0.04	0.15

0.1%, and 1.0% collected by Vucetic and Dobry (1991) as shown in Figure A-12 are used to calculate the standard deviations of the shear modulus ratio for clays. The lower and upper bounds of the data are taken as the mean minus and plus three standard deviations. The standard deviations at other levels of shear strain are obtained from interpolation or extrapolation of the above results. The probabilistic characteristics of the shear modulus ratio for clays with PI equal to 15 and 50 are listed in Table A-V. The mean and mean ± 2SD shear modulus reduction curves are also shown in Figure A-13.

A.4 Damping Ratio for Clays

Chang et al. (1992) measured the damping of two types of clays in the Memphis area in the range of shear strain from about 0.001% to 0.1%. The mean damping ratio curves for silty to sandy clay and Jackson clay are shown in Figures A-14(a) and A-14(b), respectively. The damping ratio curves corresponding to various PI values from Vucetic and Dobry (1991) are also shown in Figures A-14. The test results of silty to sandy clay at confining pressures of 0.14 and 0.38 MPa (20 and 55 psi) by Chang et al. (1992) agree with the results by Vucetic and Dobry (1991), but the result by Chang et al. has a trend of sharp increase at the high level of shear strain (see Figure A-14(a)). The damping ratio of Jackson clay is much higher than those by Vucetic and Dobry (1991) at the low to middle level of shear strain (see Figure A-14 (b)). Furthermore, Chang et al. (1992) did not measure the damping at the shear strain lower than 0.001% or higher than 0.1%. In this study, the results by Vucetic and Dobry (1991) are employed to establish the damping ratio curves for clays in the Memphis

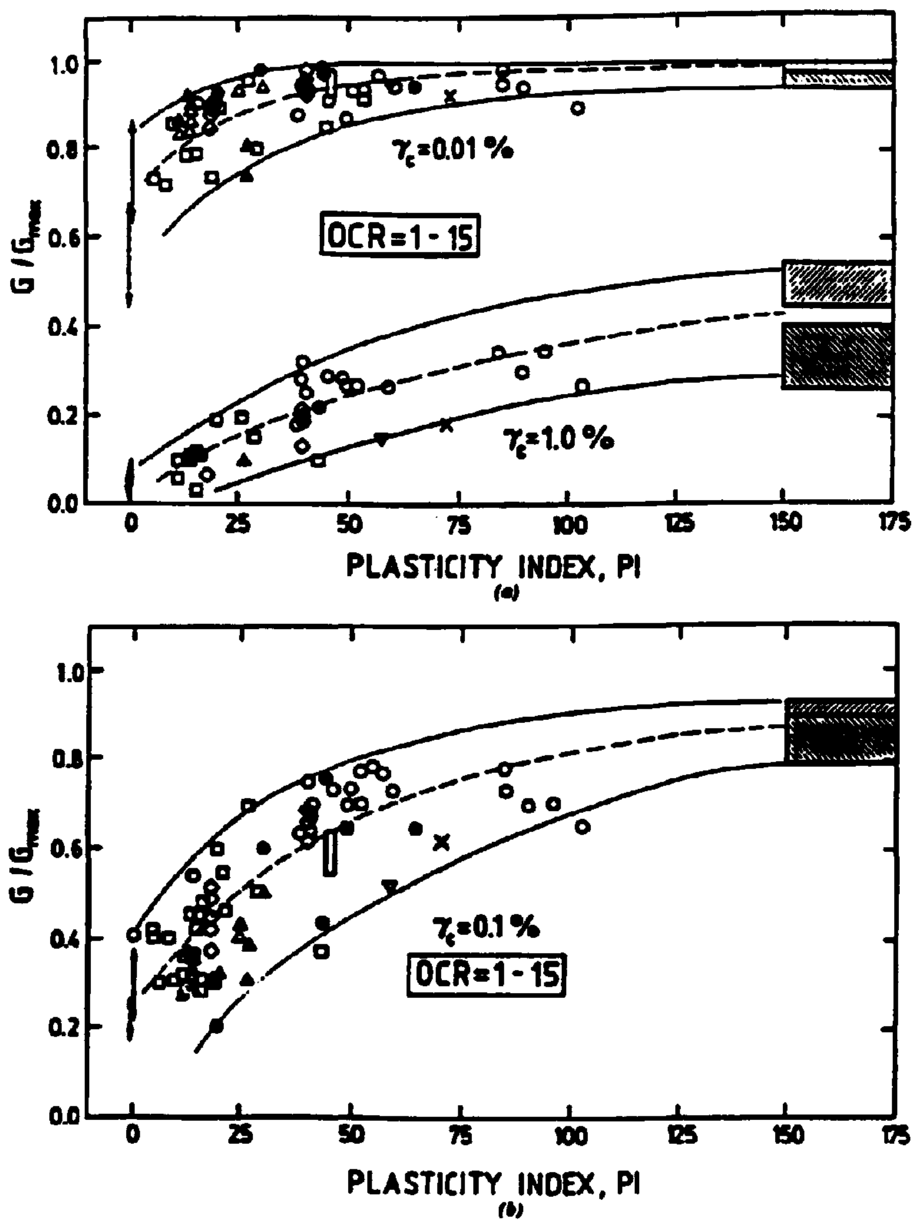

FIGURE A-12 **Variation of Shear Modulus Ratio for Clay (after Vucetic and Dobry 1991)**

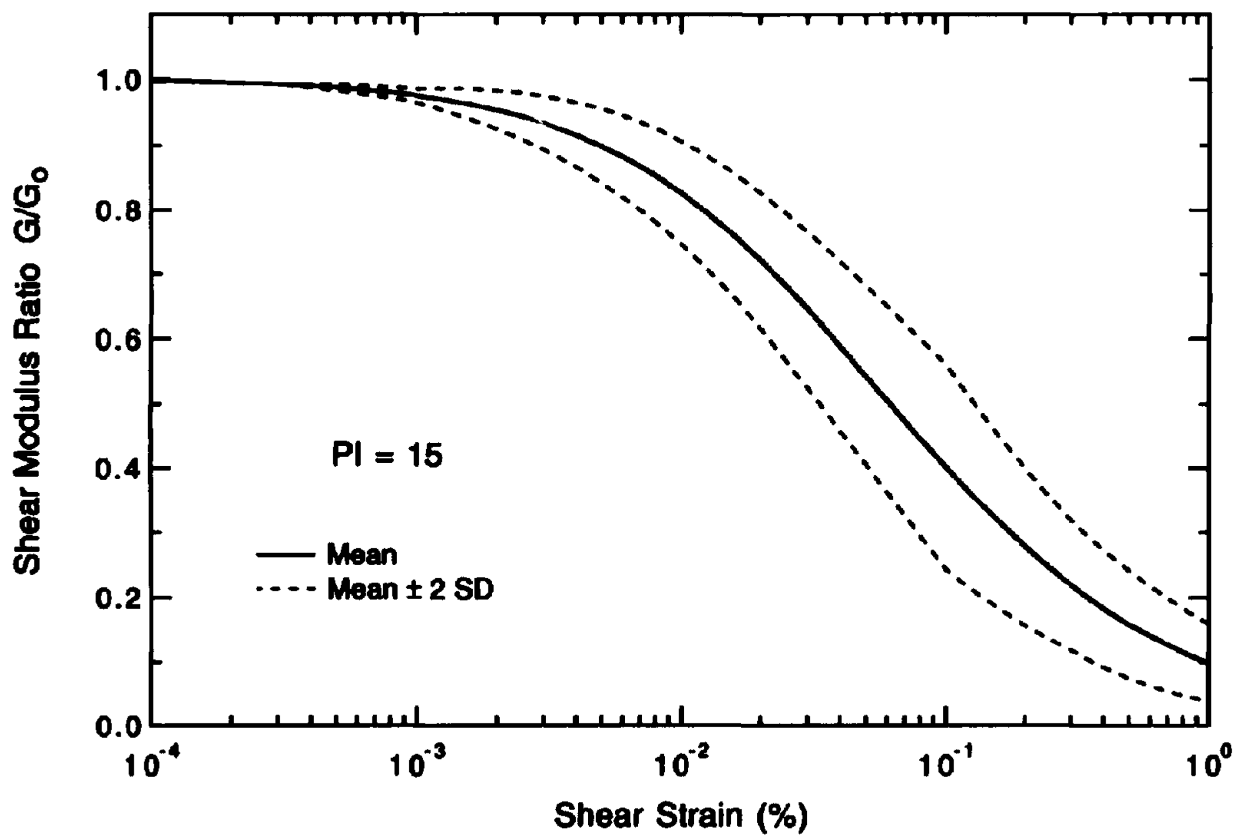

FIGURE A-13(a) Recommended Shear Modulus Reduction Curve for Clay with PI = 15 in the Memphis Area

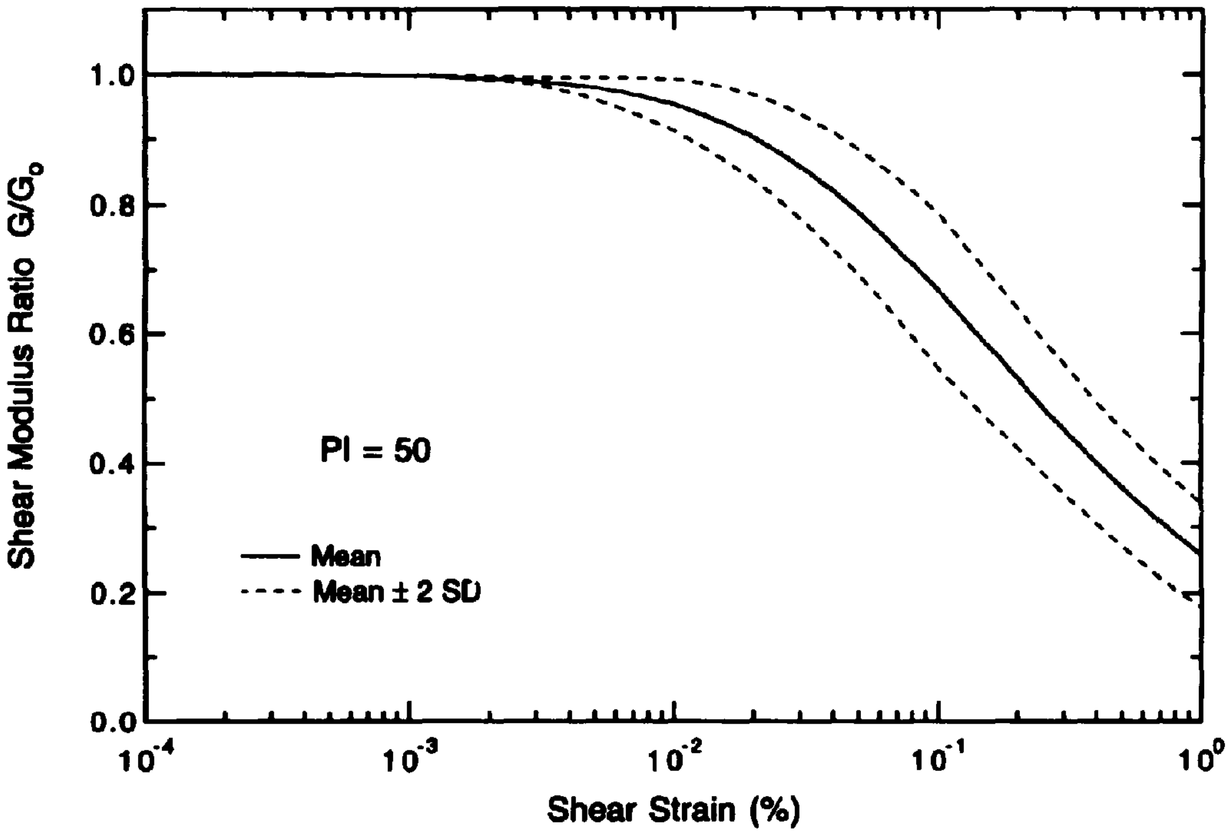

FIGURE A-13(b) Recommended Shear Modulus Reduction Curve for Clay with PI = 50 in the Memphis Area

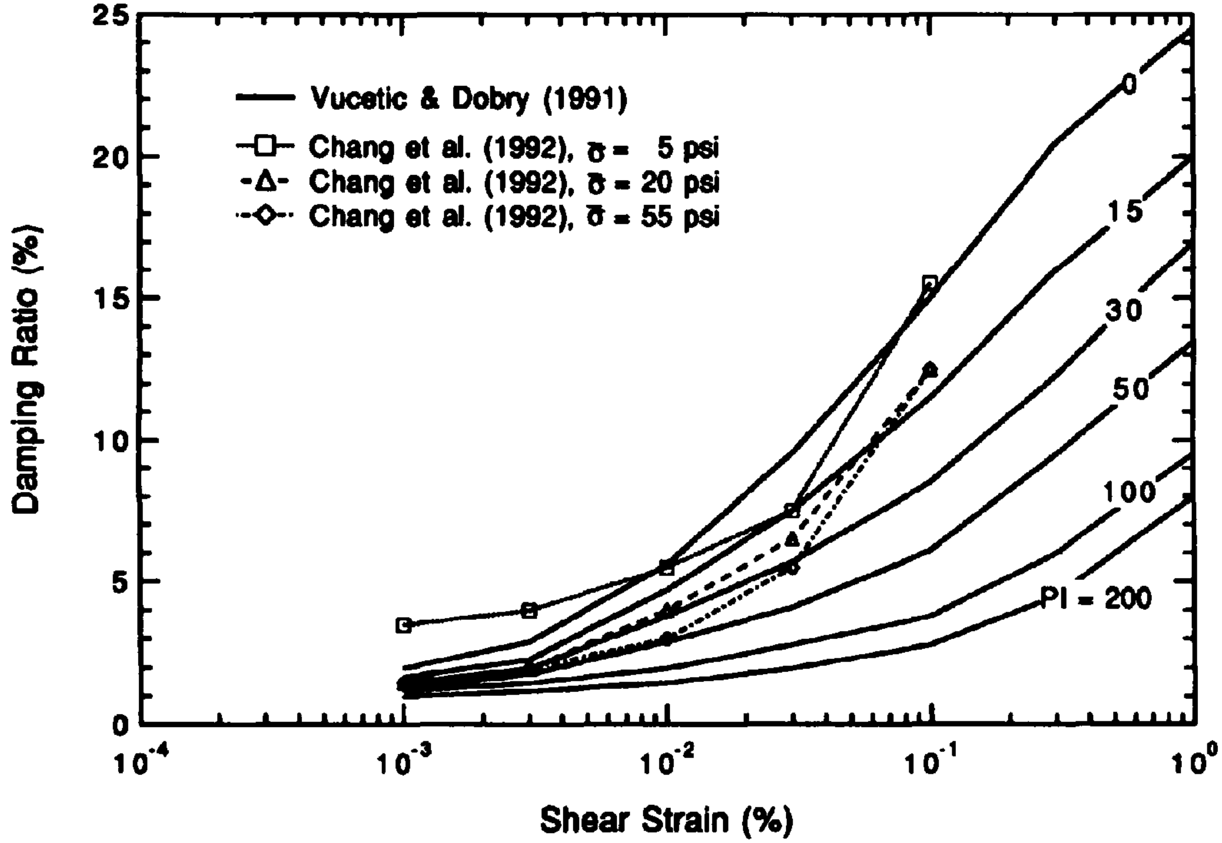

FIGURE A-14(a) Mean Damping Ratio Curves for Silty to Sandy Clay (after Chang et al. 1992)

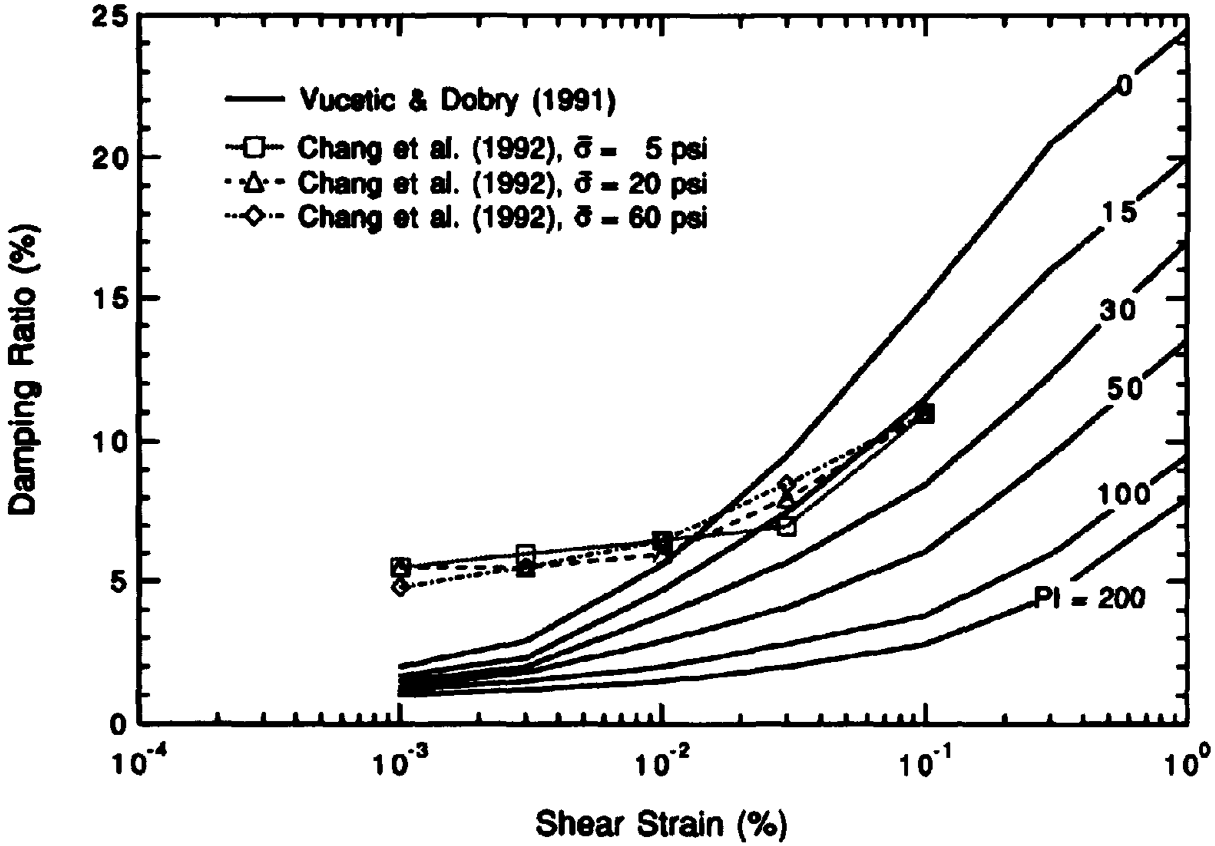

FIGURE A-14(b) Mean Damping Ratio Curves for Jackson Clay (after Chang et al. 1992) area. The mean values of damping ratio at various shear strains for clays with PI of 15 and 50 are listed in Table A-VI. It is noted that the damping ratios at shear strain below 0.001% are extended according to the recommendation by Vucetic and Dobry (1991).

Figure A-15 snows the range of damping ratio for clays corresponding to various PI values at the shear strain of 0.01%, 0.1%, and 1.0% (Vucetic and Dobry 1991). The standard deviations of the damping ratio at these three levels of shear strain are obtained by considering the lower and upper-bound values of the test data as the mean minus and plus three standard deviations. The results for other levels of shear strain are obtained from interpolation and extrapolation. The probabilistic characteristics for clays with PI equal to 15 and 50 in the Memphis area are listed in Table A-VI. The mean and mean ± 2SD damping ratio curves are shown in Figure A-16.

REFERENCES

Chang, T.-S., Teh, L.K., and Zhang, Y. (1992). "Seismic Characteristics of Sediments in the New Madrid Seismic Zone." Technical Report, Center for Earthquake Research and Information, Memphis State University, Memphis, Tennessee.

Geomatrix Consultants, Inc. (1991). "Ground Motion Following Selection of SRS Design Basis Earthquake and Associated Deterministic Approach." Project No. 1724, Draft Final Report for Westinghouse Savannah River Company.

Hardin, B.O. and Drnevich, V.P. (1972). "Shear Modulus and Damping in Soils: Design Equations and Curves." *Journal of the Soil Mechanics and*

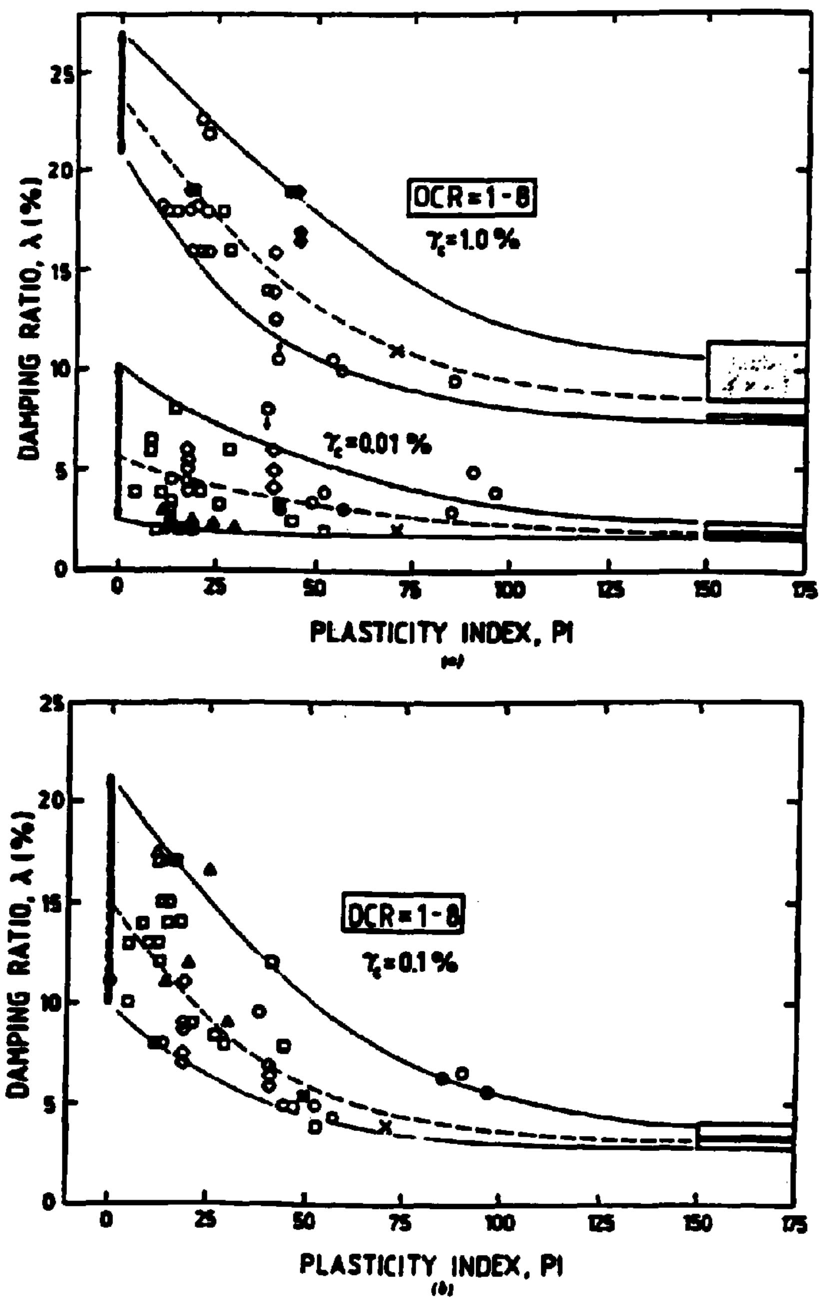

FIGURE A-15 Variation of Damping Ratio for Clay (after Vucetic and Dobry 1991)

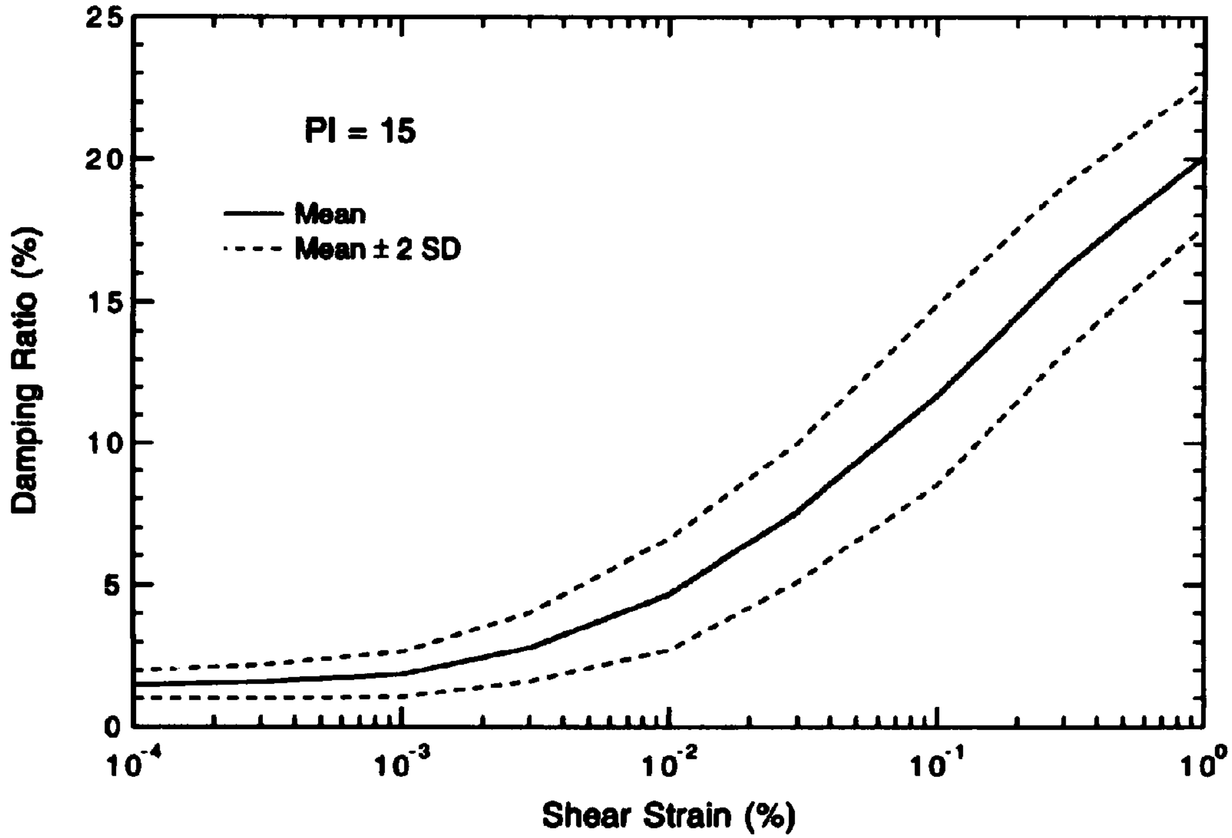

FIGURE A-16(a) Recommended Damping Ratio Curve for Clay with PI = 15 in the Memphis Area

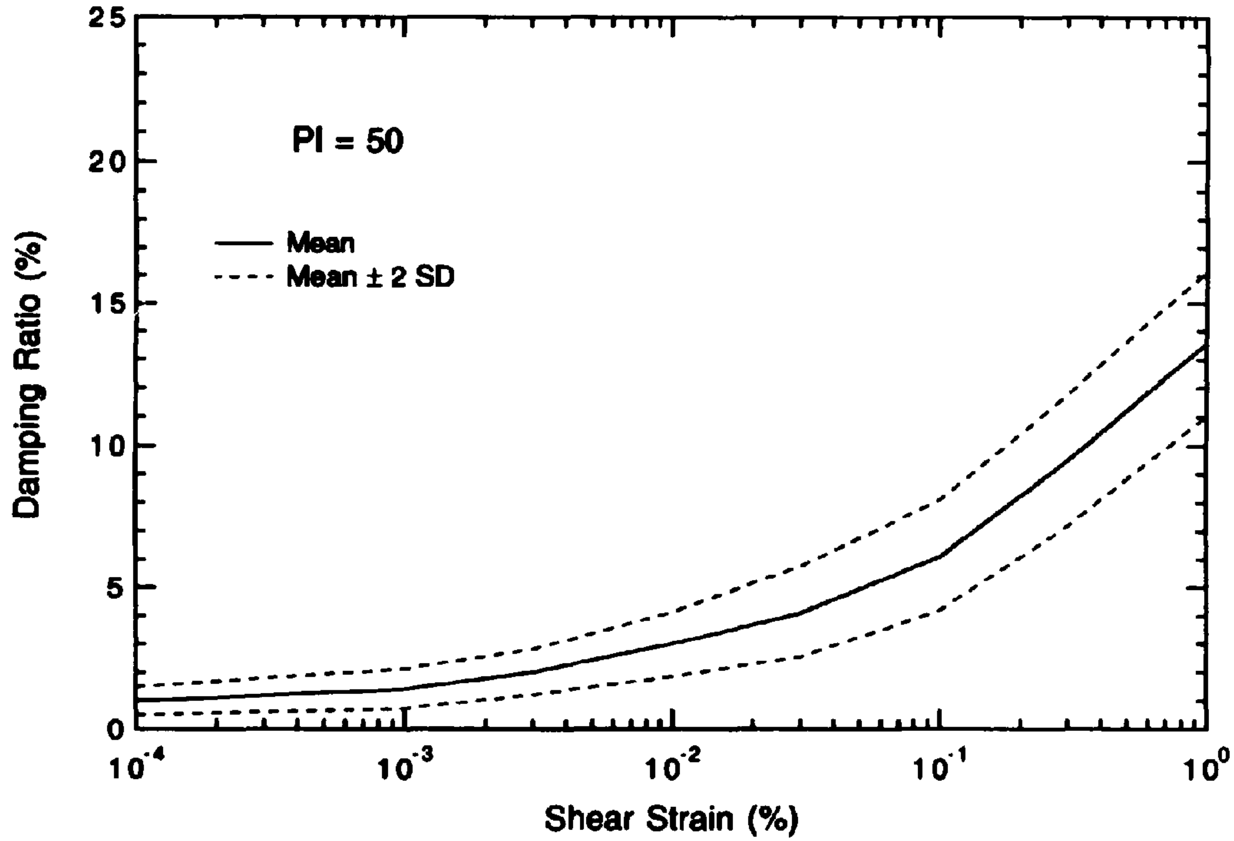

FIGURE A-16(b) Recommended Damping Ratio Curve for Clay with PI = 50 in the Memphis Area

TABLE A-VI Probabilistic Characteristics of Damping Ratio for Clays

Strain (%)	PI = 15			PI = 50		
	Mean (%)	SD (%)	COV	Mean (%)	SD (%)	COV
1×10^{-4}	1.50	0.25	0.17	1.00	0.25	0.25
3×10^{-4}	1.60	0.30	0.19	1.20	0.30	0.25
1×10^{-3}	1.85	0.40	0.22	1.42	0.35	0.25
3×10^{-3}	2.81	0.60	0.21	2.01	0.40	0.20
1×10^{-2}	4.65	0.97	0.21	3.00	0.57	0.19
3×10^{-2}	7.51	1.22	0.16	4.13	0.80	0.19
1×10^{-1}	11.69	1.61	0.14	6.14	0.97	0.14
3×10^{-1}	16.16	1.45	0.09	9.47	1.15	0.12
1×10^{0}	20.17	1.28	0.06	13.59	1.28	0.09

Foundations Division, ASCE, Vol. 98, No. SM7, 667-692.

Hwang, H., Lee, C.S., and Ng, K.W. (1990). "Soil Effects on Earthquake Ground Motions in the Memphis Area." Technical Resort NCEER-90-0029, National Center for Earthquake Engineering Research, State University of New York at Buffalo, Buffalo, New York.

Hwang, H., and Lee, C.S. (1991). "Parametric Study of Site Response Analysis." *International Journal of Soil Dynamics and Earthquake Engineering*, Vol. 10, No. 6, 282-290.

Idriss, I.M. (1990). "Response of Soft Soil Sites During Earthquakes", *Proceedings of the H. B. Seed Memorial Symposium*, Berkeley, California, Vol. 2, 273-289.

Johnson, L.R. and Silva, W. (1981). "The Effects of Unconsolidated Sediments upon the Ground Motion During Local Earthquakes." *Bulletin of Seismological Society of America*, Vol. 71, 127-142.

Joyner, W.B., Warrick, R.E., and Oliver, A.A. (1976). "Analysis of Seismograms from a Downhole Array in Sediments near San Francisco Bay." *Bulletin of Seismological Society of America*, Vol. 66, 937-958.

Joyner, W.B., Warrick, R.E., and Fumal, T.E. (1981). "The Effects of Quaternary Alluvium on Strong Ground Motion in the Coyote Lake, California, Earthquake of 1979." *Bulletin of Seismological Society of America*, Vol. 71, 1333-1349.

Martin, P.P. (1976). "Nonlinear Methods for Dynamic Analysis of Ground Motion.", Ph. D. Dissertation, Dept. of Civil Engineering, University of California, Berkeley, California.

Lee, C.S., Hwang, H., and Chang, T.-S. (1991). "Subsurface Exploration at Pipeline Crossing near the Wolf River." Technical Report, Center for

Lee, C.S., Hwang, H., and Chang, T.-S. (1991). "Subsurface Exploration at Pipeline Crossing near the Wolf River." Technical Report, Center for Earthquake Research and Information, Memphis State University, Memphis, Tennessee.

Schnabel, P.B., Lysmer, J., and Seed, H.B. (1972). "SHAKE, A Computer Program for Earthquake Response Analysis of Horizontally Layered Sites." Report No. UCB/EERC 72/12, Earthquake Engineering Research Center, University of California, Berkeley, California.

Seed, H. B. and Idriss, I.M. (1970). "Soil Moduli and Damping Factors for Dynamic Response Analysis." Report No. UCB/EERC 70/10, University of California, Berkeley, California.

Sun, J.I., Golesorkhi, R., and Seed, H.B. (1988). "Dynamic Moduli and Damping Ratios for Cohesive Soils." Report No. UCB/EERC-88/15, Earthquake Engineering Research Center, University of California, Berkeley, California.

Vucetic, M. and Dobry, R. (1991). "Effect of Soil Plasticity on Cyclic Response." *Journal of Geotechnical Engineering*, ASCE, Vol. 117, No. GE1, 89-107.

Zen, K., Umehara, Y., and Hamada, K. (1978). "Laboratory Tests and In-Situ Seismic Survey on Vibratory Shear Modulus of Clayey Soils with Various Plasticies." *Proceedings of Fifth Japan Earthquake Engineering Symposium*, Tokyo, Japan, 721-728.

NATIONAL CENTER FOR EARTHQUAKE ENGINEERING RESEARCH
LIST OF TECHNICAL REPORTS

The National Center for Earthquake Engineering Research (NCEER) publishes technical reports on a variety of subjects related to earthquake engineering written by authors funded through NCEER. These reports are available from both NCEER's Publications Department and the National Technical Information Service (NTIS). Requests for reports should be directed to the Publications Department, National Center for Earthquake Engineering Research, State University of New York at Buffalo, Red Jacket Quadrangle, Buffalo, New York 14261. Reports can also be requested through NTIS, 5285 Port Royal Road, Springfield, Virginia 22161. NTIS accession numbers are shown in parenthesis, if available.

NCEER-87-0001 "First-Year Program in Research, Education and Technology Transfer," 3/5/87, (PB88-134275).

NCEER-87-0002 "Experimental Evaluation of Instantaneous Optimal Algorithms for Structural Control," by R.C. Lin, T.T. Soong and A.M. Reinhorn, 4/20/87, (PB88-134341).

NCEER-87-0003 "Experimentation Using the Earthquake Simulation Facilities at University at Buffalo," by A.M. Reinhorn and R.L. Ketter, to be published.

NCEER-87-0004 "The System Characteristics and Performance of a Shaking Table," by J.S. Hwang, K.C. Chang and G.C. Lee, 6/1/87, (PB88-134259). This report is available only through NTIS (see address given above).

NCEER-87-0005 "A Finite Element Formulation for Nonlinear Viscoplastic Material Using a Q Model," by O. Gyebi and G. Dasgupta, 11/2/87, (PB88-213764).

NCEER-87-0006 "Symbolic Manipulation Program (SMP) - Algebraic Codes for Two and Three Dimensional Finite Element Formulations," by X. Lee and G. Dasgupta, 11/9/87, (PB88-218522).

NCEER-87-0007 "Instantaneous Optimal Control Laws for Tall Buildings Under Seismic Excitations," by J.N. Yang, A. Akbarpour and P. Ghaemmaghami, 6/10/87, (PB88-134333). This report is only available through NTIS (see address given above).

NCEER-87-0008 "IDARC: Inelastic Damage Analysis of Reinforced Concrete Frame - Shear-Wall Structures," by Y.J. Park, A.M. Reinhorn and S.K. Kunnath, 7/20/87, (PB88-134325).

NCEER-87-0009 "Liquefaction Potential for New York State: A Preliminary Report on Sites in Manhattan and Buffalo," by M. Budhu, V. Vijayakumar, R.F. Giese and L. Baumgras, 8/31/87, (PB88-163704). This report is available only through NTIS (see address given above).

NCEER-87-0010 "Vertical and Torsional Vibration of Foundations in Inhomogeneous Media," by A.S. Veletsos and K.W. Dotson, 6/1/87, (PB88-134291).

NCEER-87-0011 "Seismic Probabilistic Risk Assessment and Seismic Margins Studies for Nuclear Power Plants," by Howard H.M. Hwang, 6/15/87, (PB88-134267).

NCEER-87-0012 "Parametric Studies of Frequency Response of Secondary Systems Under Ground-Acceleration Excitations," by Y. Yong and Y.K. Lin, 6/10/87, (PB88-134309).

NCEER-87-0013 "Frequency Response of Secondary Systems Under Seismic Excitation," by J.A. HoLung, J. Cai and Y.K. Lin, 7/31/87, (PB88-134317).

NCEER-87-0014 "Modelling Earthquake Ground Motions in Seismically Active Regions Using Parametric Time Series Methods," by G.W. Ellis and A.S. Cakmak, 8/25/87, (PB88-134283).

NCEER-87-0015 "Detection and Assessment of Seismic Structural Damage," by E. DiPasquale and A.S. Cakmak, 8/25/87, (PB88-163712).

NCEER-87-0016 "Pipeline Experiment at Parkfield, California," by J. Isenberg and E. Richardson, 9/15/87, (PB88-163720). This report is available only through NTIS (see address given above).

NCEER-87-0017 "Digital Simulation of Seismic Ground Motion," by M. Shinozuka, G. Deodatis and T. Harada, 8/31/87, (PB88-155197). This report is available only through NTIS (see address given above).

NCEER-87-0018 "Practical Considerations for Structural Control: System Uncertainty, System Time Delay and Truncation of Small Control Forces," J.N. Yang and A. Akbarpour, 8/10/87, (PB88-163738).

NCEER-87-0019 "Modal Analysis of Nonclassically Damped Structural Systems Using Canonical Transformation," by J.N. Yang, S. Sarkani and F.X. Long, 9/27/87, (PB88-187851).

NCEER-87-0020 "A Nonstationary Solution in Random Vibration Theory," by J.R. Red-Horse and P.D. Spanos, 11/3/87, (PB88-163746).

NCEER-87-0021 "Horizontal Impedances for Radially Inhomogeneous Viscoelastic Soil Layers," by A.S. Veletsos and K.W. Dotson, 10/15/87, (PB88-150859).

NCEER-87-0022 "Seismic Damage Assessment of Reinforced Concrete Members," by Y.S. Chung, C. Meyer and M. Shinozuka, 10/9/87, (PB88-150867). This report is available only through NTIS (see address given above).

NCEER-87-0023 "Active Structural Control in Civil Engineering," by T.T. Soong, 11/11/87, (PB88-187778).

NCEER-87-0024 "Vertical and Torsional Impedances for Radially Inhomogeneous Viscoelastic Soil Layers," by K.W. Dotson and A.S. Veletsos, 12/87, (PB88-187786).

NCEER-87-0025 "Proceedings from the Symposium on Seismic Hazards, Ground Motions, Soil-Liquefaction and Engineering Practice in Eastern North America," October 20-22, 1987, edited by K.H. Jacob, 12/87, (PB88-188115).

NCEER-87-0026 "Report on the Whittier-Narrows, California, Earthquake of October 1, 1987," by J. Pantelic and A. Reinhorn, 11/87, (PB88-187752). This report is available only through NTIS (see address given above).

NCEER-87-0027 "Design of a Modular Program for Transient Nonlinear Analysis of Large 3-D Building Structures," by S. Srivastav and J.F. Abel, 12/30/87, (PB88-187950).

NCEER-87-0028 "Second-Year Program in Research, Education and Technology Transfer," 3/8/88, (PB88-219480).

NCEER-88-0001 "Workshop on Seismic Computer Analysis and Design of Buildings With Interactive Graphics," by W. McGuire, J.F. Abel and C.H. Conley, 1/18/88, (PB88-187760).

NCEER-88-0002 "Optimal Control of Nonlinear Flexible Structures," by J.N. Yang, F.X. Long and D. Wong, 1/22/88, (PB88-213772).

NCEER-88-0003 "Substructuring Techniques in the Time Domain for Primary-Secondary Structural Systems," by G.D. Manolis and G. Juhn, 2/10/88, (PB88-213780).

NCEER-88-0004 "Iterative Seismic Analysis of Primary-Secondary Systems," by A. Singhal, L.D. Lutes and P.D. Spanos, 2/23/88, (PB88-213798).

NCEER-88-0005 "Stochastic Finite Element Expansion for Random Media," by P.D. Spanos and R. Ghanem, 3/14/88, (PB88-213806).

NCEER-88-0006 "Combining Structural Optimization and Structural Control," by F.Y. Cheng and C.P. Pantelides, 1/10/88, (PB88-213814).

NCEER-88-0007 "Seismic Performance Assessment of Code-Designed Structures," by H.H-M. Hwang, J-W. Jaw and H-J. Shau, 3/20/88, (PB88-219423).

NCEER-88-0008 "Reliability Analysis of Code-Designed Structures Under Natural Hazards," by H.H-M. Hwang, H. Ushiba and M. Shinozuka, 2/29/88, (PB88-229471).

NCEER-88-0009 "Seismic Fragility Analysis of Shear Wall Structures," by J-W Jaw and H.H-M. Hwang, 4/30/88, (PB89-102867).

NCEER-88-0010 "Base Isolation of a Multi-Story Building Under a Harmonic Ground Motion - A Comparison of Performances of Various Systems," by F-G Fan, G. Ahmadi and I.G. Tadjbakhsh, 5/18/88, (PB89-122238).

NCEER-88-0011 "Seismic Floor Response Spectra for a Combined System by Green's Functions," by F.M. Lavelle, L.A. Bergman and P.D. Spanos, 5/1/88, (PB89-102875).

NCEER-88-0012 "A New Solution Technique for Randomly Excited Hysteretic Structures," by G.Q. Cai and Y.K. Lin, 5/16/88, (PB89-102883).

NCEER-88-0013 "A Study of Radiation Damping and Soil-Structure Interaction Effects in the Centrifuge," by K. Weissman, supervised by J.H. Prevost, 5/24/88, (PB89-144703).

NCEER-88-0014 "Parameter Identification and Implementation of a Kinematic Plasticity Model for Frictional Soils," by J.H. Prevost and D.V. Griffiths, to be published.

NCEER-88-0015 "Two- and Three- Dimensional Dynamic Finite Element Analyses of the Long Valley Dam," by D.V. Griffiths and J.H. Prevost, 6/17/88, (PB89-144711).

NCEER-88-0016 "Damage Assessment of Reinforced Concrete Structures in Eastern United States," by A.M. Reinhorn, M.J. Seidel, S.K. Kunnath and Y.J. Park, 6/15/88, (PB89-122220).

NCEER-88-0017 "Dynamic Compliance of Vertically Loaded Strip Foundations in Multilayered Viscoelastic Soils," by S. Ahmad and A.S.M. Israil, 6/17/88, (PB89-102891).

NCEER-88-0018 "An Experimental Study of Seismic Structural Response With Added Viscoelastic Dampers," by R.C. Lin, Z. Liang, T.T. Soong and R.H. Zhang, 6/30/88, (PB89-122212). This report is available only through NTIS (see address given above).

NCEER-88-0019 "Experimental Investigation of Primary - Secondary System Interaction," by G.D. Manolis, G. Juhn and A.M. Reinhorn, 5/27/88, (PB89-122204).

NCEER-88-0020 "A Response Spectrum Approach For Analysis of Nonclassically Damped Structures," by J.N. Yang, S. Sarkani and F.X. Long, 4/22/88, (PB89-102909).

NCEER-88-0021 "Seismic Interaction of Structures and Soils: Stochastic Approach," by A.S. Veletsos and A.M. Prasad, 7/21/88, (PB89-122196).

NCEER-88-0022 "Identification of the Serviceability Limit State and Detection of Seismic Structural Damage," by E. DiPasquale and A.S. Cakmak, 6/15/88, (PB89-122188). This report is available only through NTIS (see address given above).

NCEER-88-0023 "Multi-Hazard Risk Analysis: Case of a Simple Offshore Structure," by B.K. Bhartia and E.H. Vanmarcke, 7/21/88, (PB89-145213).

NCEER-88-0024 "Automated Seismic Design of Reinforced Concrete Buildings," by Y.S. Chung, C. Meyer and M. Shinozuka, 7/5/88, (PB89-122170). This report is available only through NTIS (see address given above).

NCEER-88-0025 "Experimental Study of Active Control of MDOF Structures Under Seismic Excitations," by L.L. Chung, R.C. Lin, T.T. Soong and A.M. Reinhorn, 7/10/88, (PB89-122600).

NCEER-88-0026 "Earthquake Simulation Tests of a Low-Rise Metal Structure," by J.S. Hwang, K.C. Chang, G.C. Lee and R.L. Ketter, 8/1/88, (PB89-102917).

NCEER-88-0027 "Systems Study of Urban Response and Reconstruction Due to Catastrophic Earthquakes," by F. Kozin and H.K. Zhou, 9/22/88, (PB90-162348).

NCEER-88-0028 "Seismic Fragility Analysis of Plane Frame Structures," by H.H-M. Hwang and Y.K. Low, 7/31/88, (PB89-131445).

NCEER-88-0029 "Response Analysis of Stochastic Structures," by A. Kardara, C. Bucher and M. Shinozuka, 9/22/88, (PB89-174429).

NCEER-88-0030 "Nonnormal Accelerations Due to Yielding in a Primary Structure," by D.C.K. Chen and L.D. Lutes, 9/19/88, (PB89-131437).

NCEER-88-0031 "Design Approaches for Soil-Structure Interaction," by A.S. Veletsos, A.M. Prasad and Y. Tang, 12/30/88, (PB89-174437). This report is available only through NTIS (see address given above).

NCEER-88-0032 "A Re-evaluation of Design Spectra for Seismic Damage Control," by C.J. Turkstra and A.G. Tallin, 11/7/88, (PB89-145221).

NCEER-88-0033 "The Behavior and Design of Noncontact Lap Splices Subjected to Repeated Inelastic Tensile Loading," by V.E. Sagan, P. Gergely and R.N. White, 12/8/88, (PB89-163737).

NCEER-88-0034 "Seismic Response of Pile Foundations," by S.M. Mamoon, P.K. Banerjee and S. Ahmad, 11/1/88, (PB89-145239).

NCEER-88-0035 "Modeling of R/C Building Structures With Flexible Floor Diaphragms (IDARC2)," by A.M. Reinhorn, S.K. Kunnath and N. Panahshahi, 9/7/88, (PB89-207153).

NCEER-88-0036 "Solution of the Dam-Reservoir Interaction Problem Using a Combination of FEM, BEM with Particular Integrals, Modal Analysis, and Substructuring," by C-S. Tsai, G.C. Lee and R.L. Ketter, 12/31/88, (PB89-207146).

NCEER-88-0037 "Optimal Placement of Actuators for Structural Control," by F.Y. Cheng and C.P. Pantelides, 8/15/88, (PB89-162846).

NCEER-88-0038 "Teflon Bearings in Aseismic Base Isolation: Experimental Studies and Mathematical Modeling," by A. Mokha, M.C. Constantinou and A.M. Reinhorn, 12/5/88, (PB89-218457). This report is available only through NTIS (see address given above).

NCEER-88-0039 "Seismic Behavior of Flat Slab High-Rise Buildings in the New York City Area," by P. Weidlinger and M. Ettouney, 10/15/88, (PB90-145681).

NCEER-88-0040 "Evaluation of the Earthquake Resistance of Existing Buildings in New York City," by P. Weidlinger and M. Ettouney, 10/15/88, to be published.

NCEER-88-0041 "Small-Scale Modeling Techniques for Reinforced Concrete Structures Subjected to Seismic Loads," by W. Kim, A. El-Attar and R.N. White, 11/22/88, (PB89-189625).

NCEER-88-0042 "Modeling Strong Ground Motion from Multiple Event Earthquakes," by G.W. Ellis and A.S. Cakmak, 10/15/88, (PB89-174445).

NCEER-88-0043 "Nonstationary Models of Seismic Ground Acceleration," by M. Grigoriu, S.E. Ruiz and E. Rosenblueth, 7/15/88, (PB89-189617).

NCEER-88-0044 "SARCF User's Guide: Seismic Analysis of Reinforced Concrete Frames," by Y.S. Chung, C. Meyer and M. Shinozuka, 11/9/88, (PB89-174452).

NCEER-88-0045 "First Expert Panel Meeting on Disaster Research and Planning," edited by J. Pantelic and J. Stoyle, 9/15/88, (PB89-174460).

NCEER-88-0046 "Preliminary Studies of the Effect of Degrading Infill Walls on the Nonlinear Seismic Response of Steel Frames," by C.Z. Chrysostomou, P. Gergely and J.F. Abel, 12/19/88, (PB89-208383).

NCEER-88-0047 "Reinforced Concrete Frame Component Testing Facility - Design, Construction, Instrumentation and Operation," by S.P. Pessiki, C. Conley, T. Bond, P. Gergely and R.N. White, 12/16/88, (PB89-174478).

NCEER-89-0001 "Effects of Protective Cushion and Soil Compliancy on the Response of Equipment Within a Seismically Excited Building," by J.A. HoLung, 2/16/89, (PB89-207179).

NCEER-89-0002 "Statistical Evaluation of Response Modification Factors for Reinforced Concrete Structures," by H.H-M. Hwang and J-W. Jaw, 2/17/89, (PB89-207187).

NCEER-89-0003 "Hysteretic Columns Under Random Excitation," by G-Q. Cai and Y.K. Lin, 1/9/89, (PB89-196513).

NCEER-89-0004 "Experimental Study of 'Elephant Foot Bulge' Instability of Thin-Walled Metal Tanks," by Z-H. Jia and R.L. Ketter, 2/22/89, (PB89-207195).

NCEER-89-0005 "Experiment on Performance of Buried Pipelines Across San Andreas Fault," by J. Isenberg, E. Richardson and T.D. O'Rourke, 3/10/89, (PB89-218440). This report is available only through NTIS (see address given above).

NCEER-89-0006 "A Knowledge-Based Approach to Structural Design of Earthquake-Resistant Buildings," by M. Subramani, P. Gergely, C.H. Conley, J.F. Abel and A.H. Zaghw, 1/15/89, (PB89-218465).

NCEER-89-0007 "Liquefaction Hazards and Their Effects on Buried Pipelines," by T.D. O'Rourke and P.A. Lane, 2/1/89, (PB89-218481).

NCEER-89-0008 "Fundamentals of System Identification in Structural Dynamics," by H. Imai, C-B. Yun, O. Maruyama and M. Shinozuka, 1/26/89, (PB89-207211).

NCEER-89-0009 "Effects of the 1985 Michoacan Earthquake on Water Systems and Other Buried Lifelines in Mexico," by A.G. Ayala and M.J. O'Rourke, 3/8/89, (PB89-207229).

NCEER-89-R010 "NCEER Bibliography of Earthquake Education Materials," by K.E.K. Ross, Second Revision, 9/1/89, (PB90-125352).

NCEER-89-0011 "Inelastic Three-Dimensional Response Analysis of Reinforced Concrete Building Structures (IDARC-3D), Part I - Modeling," by S.K. Kunnath and A.M. Reinhorn, 4/17/89, (PB90-114612).

NCEER-89-0012 "Recommended Modifications to ATC-14," by C.D. Poland and J.O. Malley, 4/12/89, (PB90-108648).

NCEER-89-0013 "Repair and Strengthening of Beam-to-Column Connections Subjected to Earthquake Loading," by M. Corazao and A.J. Durrani, 2/28/89, (PB90-109885).

NCEER-89-0014 "Program EXKAL2 for Identification of Structural Dynamic Systems," by O. Maruyama, C-B. Yun, M. Hoshiya and M. Shinozuka, 5/19/89, (PB90-109877).

NCEER-89-0015 "Response of Frames With Bolted Semi-Rigid Connections, Part I - Experimental Study and Analytical Predictions," by P.J. DiCorso, A.M. Reinhorn, J.R. Dickerson, J.B. Radziminski and W.L. Harper, 6/1/89, to be published.

NCEER-89-0016 "ARMA Monte Carlo Simulation in Probabilistic Structural Analysis," by P.D. Spanos and M.P. Mignolet, 7/10/89, (PB90-109893).

NCEER-89-P017 "Preliminary Proceedings from the Conference on Disaster Preparedness - The Place of Earthquake Education in Our Schools," Edited by K.E.K. Ross, 6/23/89, (PB90-108606).

NCEER-89-0017 "Proceedings from the Conference on Disaster Preparedness - The Place of Earthquake Education in Our Schools," Edited by K.E.K. Ross, 12/31/89, (PB90-207895). This report is available only through NTIS (see address given above).

NCEER-89-0018 "Multidimensional Models of Hysteretic Material Behavior for Vibration Analysis of Shape Memory Energy Absorbing Devices, by E.J. Graesser and F.A. Cozzarelli, 6/7/89, (PB90-164146).

NCEER-89-0019 "Nonlinear Dynamic Analysis of Three-Dimensional Base Isolated Structures (3D-BASIS)," by S. Nagarajaiah, A.M. Reinhorn and M.C. Constantinou, 8/3/89, (PB90-161936). This report is available only through NTIS (see address given above).

NCEER-89-0020 "Structural Control Considering Time-Rate of Control Forces and Control Rate Constraints," by F.Y. Cheng and C.P. Pantelides, 8/3/89, (PB90-120445).

NCEER-89-0021 "Subsurface Conditions of Memphis and Shelby County," by K.W. Ng, T-S. Chang and H-H.M. Hwang, 7/26/89, (PB90-120437).

NCEER-89-0022 "Seismic Wave Propagation Effects on Straight Jointed Buried Pipelines," by K. Elhmadi and M.J. O'Rourke, 8/24/89, (PB90-162322).

NCEER-89-0023 "Workshop on Serviceability Analysis of Water Delivery Systems," edited by M. Grigoriu, 3/6/89, (PB90-127424).

NCEER-89-0024 "Shaking Table Study of a 1/5 Scale Steel Frame Composed of Tapered Members," by K.C. Chang, J.S. Hwang and G.C. Lee, 9/18/89, (PB90-160169).

NCEER-89-0025 "DYNA1D: A Computer Program for Nonlinear Seismic Site Response Analysis - Technical Documentation," by Jean H. Prevost, 9/14/89, (PB90-161944). This report is available only through NTIS (see address given above).

NCEER-89-0026 "1:4 Scale Model Studies of Active Tendon Systems and Active Mass Dampers for Aseismic Protection," by A.M. Reinhorn, T.T. Soong, R.C. Lin, Y.P. Yang, Y. Fukao, H. Abe and M. Nakai, 9/15/89, (PB90-173246).

NCEER-89-0027 "Scattering of Waves by Inclusions in a Nonhomogeneous Elastic Half Space Solved by Boundary Element Methods," by P.K. Hadley, A. Askar and A.S. Cakmak, 6/15/89, (PB90-145699).

NCEER-89-0028 "Statistical Evaluation of Deflection Amplification Factors for Reinforced Concrete Structures," by H.H.M. Hwang, J-W. Jaw and A.L. Ch'ng, 8/31/89, (PB90-164633).

NCEER-89-0029 "Bedrock Accelerations in Memphis Area Due to Large New Madrid Earthquakes," by H.H.M. Hwang, C.H.S. Chen and G. Yu, 11/7/89, (PB90-162330).

NCEER-89-0030 "Seismic Behavior and Response Sensitivity of Secondary Structural Systems," by Y.Q. Chen and T.T. Soong, 10/23/89, (PB90-164658).

NCEER-89-0031 "Random Vibration and Reliability Analysis of Primary-Secondary Structural Systems," by Y. Ibrahim, M. Grigoriu and T.T. Soong, 11/10/89, (PB90-161951).

NCEER-89-0032 "Proceedings from the Second U.S. - Japan Workshop on Liquefaction, Large Ground Deformation and Their Effects on Lifelines, September 26-29, 1989," Edited by T.D. O'Rourke and M. Hamada, 12/1/89, (PB90-209388).

NCEER-89-0033 "Deterministic Model for Seismic Damage Evaluation of Reinforced Concrete Structures," by J.M. Bracci, A.M. Reinhorn, J.B. Mander and S.K. Kunnath, 9/27/89.

NCEER-89-0034 "On the Relation Between Local and Global Damage Indices," by E. DiPasquale and A.S. Cakmak, 8/15/89, (PB90-173865).

NCEER-89-0035 "Cyclic Undrained Behavior of Nonplastic and Low Plasticity Silts," by A.J. Walker and H.E. Stewart, 7/26/89, (PB90-183518).

NCEER-89-0036 "Liquefaction Potential of Surficial Deposits in the City of Buffalo, New York," by M. Budhu, R. Giese and L. Baumgrass, 1/17/89, (PB90-208455).

NCEER-89-0037 "A Deterministic Assessment of Effects of Ground Motion Incoherence," by A.S. Veletsos and Y. Tang, 7/15/89, (PB90-164294).

NCEER-89-0038 "Workshop on Ground Motion Parameters for Seismic Hazard Mapping," July 17-18, 1989, edited by R.V. Whitman, 12/1/89, (PB90-173923).

NCEER-89-0039 "Seismic Effects on Elevated Transit Lines of the New York City Transit Authority," by C.J. Costantino, C.A. Miller and E. Heymsfield, 12/26/89, (PB90-207887).

NCEER-89-0040 "Centrifugal Modeling of Dynamic Soil-Structure Interaction," by K. Weissman, Supervised by J.H. Prevost, 5/10/89, (PB90-207879).

NCEER-89-0041 "Linearized Identification of Buildings With Cores for Seismic Vulnerability Assessment," by I-K. Ho and A.E. Aktan, 11/1/89, (PB90-251943).

NCEER-90-0001 "Geotechnical and Lifeline Aspects of the October 17, 1989 Loma Prieta Earthquake in San Francisco," by T.D. O'Rourke, H.E. Stewart, F.T. Blackburn and T.S. Dickerman, 1/90, (PB90-208596).

NCEER-90-0002 "Nonnormal Secondary Response Due to Yielding in a Primary Structure," by D.C.K. Chen and L.D. Lutes, 2/28/90, (PB90-251976).

NCEER-90-0003 "Earthquake Education Materials for Grades K-12," by K.E.K. Ross, 4/16/90, (PB91-251984).

NCEER-90-0004 "Catalog of Strong Motion Stations in Eastern North America," by R.W. Busby, 4/3/90, (PB90-251984).

NCEER-90-0005 "NCEER Strong-Motion Data Base: A User Manual for the GeoBase Release (Version 1.0 for the Sun3)," by P. Friberg and K. Jacob, 3/31/90 (PB90-258062).

NCEER-90-0006 "Seismic Hazard Along a Crude Oil Pipeline in the Event of an 1811-1812 Type New Madrid Earthquake," by H.H.M. Hwang and C-H.S. Chen, 4/16/90(PB90-258054).

NCEER-90-0007 "Site-Specific Response Spectra for Memphis Sheahan Pumping Station," by H.H.M. Hwang and C.S. Lee, 5/15/90, (PB91-108811).

NCEER-90-0008 "Pilot Study on Seismic Vulnerability of Crude Oil Transmission Systems," by T. Ariman, R. Dobry, M. Grigoriu, F. Kozin, M. O'Rourke, T. O'Rourke and M. Shinozuka, 5/25/90, (PB91-108837).

NCEER-90-0009 "A Program to Generate Site Dependent Time Histories: EQGEN," by G.W. Ellis, M. Srinivasan and A.S. Cakmak, 1/30/90, (PB91-108829).

NCEER-90-0010 "Active Isolation for Seismic Protection of Operating Rooms," by M.E. Talbott, Supervised by M. Shinozuka, 6/8/9, (PB91-110205).

NCEER-90-0011 "Program LINEARID for Identification of Linear Structural Dynamic Systems," by C-B. Yun and M. Shinozuka, 6/25/90, (PB91-110312).

NCEER-90-0012 "Two-Dimensional Two-Phase Elasto-Plastic Seismic Response of Earth Dams," by A.N. Yiagos, Supervised by J.H. Prevost, 6/20/90, (PB91-110197).

NCEER-90-0013 "Secondary Systems in Base-Isolated Structures: Experimental Investigation, Stochastic Response and Stochastic Sensitivity," by G.D. Manolis, G. Juhn, M.C. Constantinou and A.M. Reinhorn, 7/1/90, (PB91-110320).

NCEER-90-0014 "Seismic Behavior of Lightly-Reinforced Concrete Column and Beam-Column Joint Details," by S.P. Pessiki, C.H. Conley, P. Gergely and R.N. White, 8/22/90, (PB91-108795).

NCEER-90-0015 "Two Hybrid Control Systems for Building Structures Under Strong Earthquakes," by J.N. Yang and A. Danielians, 6/29/90, (PB91-125393).

NCEER-90-0016 "Instantaneous Optimal Control with Acceleration and Velocity Feedback," by J.N. Yang and Z. Li, 6/29/90, (PB91-125401).

NCEER-90-0017 "Reconnaissance Report on the Northern Iran Earthquake of June 21, 1990," by M. Mehrain, 10/4/90, (PB91-125377).

NCEER-90-0018 "Evaluation of Liquefaction Potential in Memphis and Shelby County," by T.S. Chang, P.S. Tang, C.S. Lee and H. Hwang, 8/10/90, (PB91-125427).

NCEER-90-0019 "Experimental and Analytical Study of a Combined Sliding Disc Bearing and Helical Steel Spring Isolation System," by M.C. Constantinou, A.S. Mokha and A.M. Reinhorn, 10/4/90, (PB91-125385).

NCEER-90-0020 "Experimental Study and Analytical Prediction of Earthquake Response of a Sliding Isolation System with a Spherical Surface," by A.S. Mokha, M.C. Constantinou and A.M. Reinhorn, 10/11/90, (PB91-125419).

NCEER-90-0021 "Dynamic Interaction Factors for Floating Pile Groups," by G. Gazetas, K. Fan, A. Kaynia and E. Kausel, 9/10/90, (PB91-170381).

NCEER-90-0022 "Evaluation of Seismic Damage Indices for Reinforced Concrete Structures," by S. Rodriguez-Gomez and A.S. Cakmak, 9/30/90, PB91-171322).

NCEER-90-0023 "Study of Site Response at a Selected Memphis Site," by H. Desai, S. Ahmad, E.S. Gazetas and M.R. Oh, 10/11/90, (PB91-196857).

NCEER-90-0024 "A User's Guide to Strongmo: Version 1.0 of NCEER's Strong-Motion Data Access Tool for PCs and Terminals," by P.A. Friberg and C.A.T. Susch, 11/15/90, (PB91-171272).

NCEER-90-0025 "A Three-Dimensional Analytical Study of Spatial Variability of Seismic Ground Motions," by L-L. Hong and A.H.-S. Ang, 10/30/90, (PB91-170399).

NCEER-90-0026 "MUMOID User's Guide - A Program for the Identification of Modal Parameters," by S. Rodriguez-Gomez and E. DiPasquale, 9/30/90, (PB91-171298).

NCEER-90-0027 "SARCF-II User's Guide - Seismic Analysis of Reinforced Concrete Frames," by S. Rodriguez-Gomez, Y.S. Chung and C. Meyer, 9/30/90, (PB91-171280).

NCEER-90-0028 "Viscous Dampers: Testing, Modeling and Application in Vibration and Seismic Isolation," by N. Makris and M.C. Constantinou, 12/20/90 (PB91-190561).

NCEER-90-0029 "Soil Effects on Earthquake Ground Motions in the Memphis Area," by H. Hwang, C.S. Lee, K.W. Ng and T.S. Chang, 8/2/90, (PB91-190751).

NCEER-91-0001 "Proceedings from the Third Japan-U.S. Workshop on Earthquake Resistant Design of Lifeline Facilities and Countermeasures for Soil Liquefaction, December 17-19, 1990," edited by T.D. O'Rourke and M. Hamada, 2/1/91, (PB91-179259).

NCEER-91-0002 "Physical Space Solutions of Non-Proportionally Damped Systems," by M. Tong, Z. Liang and G.C. Lee, 1/15/91, (PB91-179242).

NCEER-91-0003 "Seismic Response of Single Piles and Pile Groups," by K. Fan and G. Gazetas, 1/10/91, (PB92-174994).

NCEER-91-0004 "Damping of Structures: Part 1 - Theory of Complex Damping," by Z. Liang and G. Lee, 10/10/91, (PB92-197235).

NCEER-91-0005 "3D-BASIS - Nonlinear Dynamic Analysis of Three Dimensional Base Isolated Structures: Part II," by S. Nagarajaiah, A.M. Reinhorn and M.C. Constantinou, 2/28/91, (PB91-190553).

NCEER-91-0006 "A Multidimensional Hysteretic Model for Plasticity Deforming Metals in Energy Absorbing Devices," by E.J. Graesser and F.A. Cozzarelli, 4/9/91, (PB92-108364).

NCEER-91-0007 "A Framework for Customizable Knowledge-Based Expert Systems with an Application to a KBES for Evaluating the Seismic Resistance of Existing Buildings," by E.G. Ibarra-Anaya and S.J. Fenves, 4/9/91, (PB91-210930).

NCEER-91-0008 "Nonlinear Analysis of Steel Frames with Semi-Rigid Connections Using the Capacity Spectrum Method," by G.G. Deierlein, S-H. Hsieh, Y-J. Shen and J.F. Abel, 7/2/91, (PB92-113828).

NCEER-91-0009 "Earthquake Education Materials for Grades K-12," by K.E.K. Ross, 4/30/91, (PB91-212142).

NCEER-91-0010 "Phase Wave Velocities and Displacement Phase Differences in a Harmonically Oscillating Pile," by N. Makris and G. Gazetas, 7/8/91, (PB92-108356).

NCEER-91-0011 "Dynamic Characteristics of a Full-Size Five-Story Steel Structure and a 2/5 Scale Model," by K.C. Chang, G.C. Yao, G.C. Lee, D.S. Hao and Y.C. Yeh," 7/2/91, (PB93-116648).

NCEER-91-0012 "Seismic Response of a 2/5 Scale Steel Structure with Added Viscoelastic Dampers," by K.C. Chang, T.T. Soong, S-T. Oh and M.L. Lai, 5/17/91, (PB92-110816).

NCEER-91-0013 "Earthquake Response of Retaining Walls; Full-Scale Testing and Computational Modeling," by S. Alampalli and A-W.M. Elgamal, 6/20/91, to be published.

NCEER-91-0014 "3D-BASIS-M: Nonlinear Dynamic Analysis of Multiple Building Base Isolated Structures," by P.C. Tsopelas, S. Nagarajaiah, M.C. Constantinou and A.M. Reinhorn, 5/28/91, (PB92-113885).

NCEER-91-0015 "Evaluation of SEAOC Design Requirements for Sliding Isolated Structures," by D. Theodossiou and M.C. Constantinou, 6/10/91, (PB92-114602).

NCEER-91-0016 "Closed-Loop Modal Testing of a 27-Story Reinforced Concrete Flat Plate-Core Building," by H.R. Somaprasad, T. Toksoy, H. Yoshiyuki and A.E. Aktan, 7/15/91, (PB92-129980).

NCEER-91-0017 "Shake Table Test of a 1/6 Scale Two-Story Lightly Reinforced Concrete Building," by A.G. El-Attar, R.N. White and P. Gergely, 2/28/91, (PB92-222447).

NCEER-91-0018 "Shake Table Test of a 1/8 Scale Three-Story Lightly Reinforced Concrete Building," by A.G. El-Attar, R.N. White and P. Gergely, 2/28/91, (PB93-116630).

NCEER-91-0019 "Transfer Functions for Rigid Rectangular Foundations," by A.S. Veletsos, A.M. Prasad and W.H. Wu, 7/31/91.

NCEER-91-0020 "Hybrid Control of Seismic-Excited Nonlinear and Inelastic Structural Systems," by J.N. Yang, Z. Li and A. Danielians, 8/1/91, (PB92-143171).

NCEER-91-0021 "The NCEER-91 Earthquake Catalog: Improved Intensity-Based Magnitudes and Recurrence Relations for U.S. Earthquakes East of New Madrid," by L. Seeber and J.G. Armbruster, 8/28/91, (PB92-176742).

NCEER-91-0022 "Proceedings from the Implementation of Earthquake Planning and Education in Schools: The Need for Change - The Roles of the Changemakers," by K.E.K. Ross and F. Winslow, 7/23/91, (PB92-129998).

NCEER-91-0023 "A Study of Reliability-Based Criteria for Seismic Design of Reinforced Concrete Frame Buildings," by H.H.M. Hwang and H-M. Hsu, 8/10/91, (PB92-140235).

NCEER-91-0024 "Experimental Verification of a Number of Structural System Identification Algorithms," by R.G. Ghanem, H. Gavin and M. Shinozuka, 9/18/91, (PB92-176577).

NCEER-91-0025 "Probabilistic Evaluation of Liquefaction Potential," by H.H.M. Hwang and C.S. Lee," 11/25/91, (PB92-143429).

NCEER-91-0026 "Instantaneous Optimal Control for Linear, Nonlinear and Hysteretic Structures - Stable Controllers," by J.N. Yang and Z. Li, 11/15/91, (PB92-163807).

NCEER-91-0027 "Experimental and Theoretical Study of a Sliding Isolation System for Bridges," by M.C. Constantinou, A. Kartoum, A.M. Reinhorn and P. Bradford, 11/15/91, (PB92-176973).

NCEER-92-0001 "Case Studies of Liquefaction and Lifeline Performance During Past Earthquakes, Volume 1: Japanese Case Studies," Edited by M. Hamada and T. O'Rourke, 2/17/92, (PB92-197243).

NCEER-92-0002 "Case Studies of Liquefaction and Lifeline Performance During Past Earthquakes, Volume 2: United States Case Studies," Edited by T. O'Rourke and M. Hamada, 2/17/92, (PB92-197250).

NCEER-92-0003 "Issues in Earthquake Education," Edited by K. Ross, 2/3/92, (PB92-222389).

NCEER-92-0004 "Proceedings from the First U.S. - Japan Workshop on Earthquake Protective Systems for Bridges," Edited by I.G. Buckle, 2/4/92, (PB94-142239, A99, MF-A06).

NCEER-92-0005 "Seismic Ground Motion from a Haskell-Type Source in a Multiple-Layered Half-Space," A.P. Theoharis, G. Deodatis and M. Shinozuka, 1/2/92, to be published.

NCEER-92-0006 "Proceedings from the Site Effects Workshop," Edited by R. Whitman, 2/29/92, (PB92-197201).

NCEER-92-0007 "Engineering Evaluation of Permanent Ground Deformations Due to Seismically-Induced Liquefaction," by M.H. Baziar, R. Dobry and A-W.M. Elgamal, 3/24/92, (PB92-222421).

NCEER-92-0008 "A Procedure for the Seismic Evaluation of Buildings in the Central and Eastern United States," by C.D. Poland and J.O. Malley, 4/2/92, (PB92-222439).

NCEER-92-0009 "Experimental and Analytical Study of a Hybrid Isolation System Using Friction Controllable Sliding Bearings," by M.Q. Feng, S. Fujii and M. Shinozuka, 5/15/92, (PB93-150282).

NCEER-92-0010 "Seismic Resistance of Slab-Column Connections in Existing Non-Ductile Flat-Plate Buildings," by A.J. Durrani and Y. Du, 5/18/92.

NCEER-92-0011 "The Hysteretic and Dynamic Behavior of Brick Masonry Walls Upgraded by Ferrocement Coatings Under Cyclic Loading and Strong Simulated Ground Motion," by H. Lee and S.P. Prawel, 5/11/92, to be published.

NCEER-92-0012 "Study of Wire Rope Systems for Seismic Protection of Equipment in Buildings," by G.F. Demetriades, M.C. Constantinou and A.M. Reinhorn, 5/20/92.

NCEER-92-0013 "Shape Memory Structural Dampers: Material Properties, Design and Seismic Testing," by P.R. Witting and F.A. Cozzarelli, 5/26/92.

NCEER-92-0014 "Longitudinal Permanent Ground Deformation Effects on Buried Continuous Pipelines," by M.J. O'Rourke, and C. Nordberg, 6/15/92.

NCEER-92-0015 "A Simulation Method for Stationary Gaussian Random Functions Based on the Sampling Theorem," by M. Grigoriu and S. Balopoulou, 6/11/92, (PB93-127496).

NCEER-92-0016 "Gravity-Load-Designed Reinforced Concrete Buildings: Seismic Evaluation of Existing Construction and Detailing Strategies for Improved Seismic Resistance," by G.W. Hoffmann, S.K. Kunnath, A.M. Reinhorn and J.B. Mander, 7/15/92, (PB94-142007, A08, MF-A02).

NCEER-92-0017 "Observations on Water System and Pipeline Performance in the Limón Area of Costa Rica Due to the April 22, 1991 Earthquake," by M. O'Rourke and D. Ballantyne, 6/30/92, (PB93-126811).

NCEER-92-0018 "Fourth Edition of Earthquake Education Materials for Grades K-12," Edited by K.E.K. Ross, 8/10/92.

NCEER-92-0019 "Proceedings from the Fourth Japan-U.S. Workshop on Earthquake Resistant Design of Lifeline Facilities and Countermeasures for Soil Liquefaction," Edited by M. Hamada and T.D. O'Rourke, 8/12/92, (PB93-163939).

NCEER-92-0020 "Active Bracing System: A Full Scale Implementation of Active Control," by A.M. Reinhorn, T.T. Soong, R.C. Lin, M.A. Riley, Y.P. Wang, S. Aizawa and M. Higashino, 8/14/92, (PB93-127512).

NCEER-92-0021 "Empirical Analysis of Horizontal Ground Displacement Generated by Liquefaction-Induced Lateral Spreads," by S.F. Bartlett and T.L. Youd, 8/17/92, (PB93-188241).

NCEER-92-0022 "IDARC Version 3.0: Inelastic Damage Analysis of Reinforced Concrete Structures," by S.K. Kunnath, A.M. Reinhorn and R.F. Lobo, 8/31/92, (PB93-227502, A07, MF-A02).

NCEER-92-0023 "A Semi-Empirical Analysis of Strong-Motion Peaks in Terms of Seismic Source, Propagation Path and Local Site Conditions, by M. Kamiyama, M.J. O'Rourke and R. Flores-Berrones, 9/9/92, (PB93-150266).

NCEER-92-0024 "Seismic Behavior of Reinforced Concrete Frame Structures with Nonductile Details, Part I: Summary of Experimental Findings of Full Scale Beam-Column Joint Tests," by A. Beres, R.N. White and P. Gergely, 9/30/92, (PB93-227783, A05, MF-A01).

NCEER-92-0025 "Experimental Results of Repaired and Retrofitted Beam-Column Joint Tests in Lightly Reinforced Concrete Frame Buildings," by A. Beres, S. El-Borgi, R.N. White and P. Gergely, 10/29/92, (PB93-227791, A05, MF-A01).

NCEER-92-0026 "A Generalization of Optimal Control Theory: Linear and Nonlinear Structures," by J.N. Yang, Z. Li and S. Vongchavalitkul, 11/2/92, (PB93-188621).

NCEER-92-0027 "Seismic Resistance of Reinforced Concrete Frame Structures Designed Only for Gravity Loads: Part I - Design and Properties of a One-Third Scale Model Structure," by J.M. Bracci, A.M. Reinhorn and J.B. Mander, 12/1/92, (PB94-104502, A08, MF-A02).

NCEER-92-0028 "Seismic Resistance of Reinforced Concrete Frame Structures Designed Only for Gravity Loads: Part II - Experimental Performance of Subassemblages," by L.E. Aycardi, J.B. Mander and A.M. Reinhorn, 12/1/92, (PB94-104510, A08, MF-A02).

NCEER-92-0029 "Seismic Resistance of Reinforced Concrete Frame Structures Designed Only for Gravity Loads: Part III - Experimental Performance and Analytical Study of a Structural Model," by J.M. Bracci, A.M. Reinhorn and J.B. Mander, 12/1/92, (PB93-227528, A09, MF-A01).

NCEER-92-0030 "Evaluation of Seismic Retrofit of Reinforced Concrete Frame Structures: Part I - Experimental Performance of Retrofitted Subassemblages," by D. Choudhuri, J.B. Mander and A.M. Reinhorn, 12/8/92, (PB93-198307, A07, MF-A02).

NCEER-92-0031 "Evaluation of Seismic Retrofit of Reinforced Concrete Frame Structures: Part II - Experimental Performance and Analytical Study of a Retrofitted Structural Model," by J.M. Bracci, A.M. Reinhorn and J.B. Mander, 12/8/92, (PB93-198315, A09, MF-A03).

NCEER-92-0032 "Experimental and Analytical Investigation of Seismic Response of Structures with Supplemental Fluid Viscous Dampers," by M.C. Constantinou and M.D. Symans, 12/21/92, (PB93-191435).

NCEER-92-0033 "Reconnaissance Report on the Cairo, Egypt Earthquake of October 12, 1992," by M. Khater, 12/23/92, (PB93-188621).

NCEER-92-0034 "Low-Level Dynamic Characteristics of Four Tall Flat-Plate Buildings in New York City," by H. Gavin, S. Yuan, J. Grossman, E. Pekelis and K. Jacob, 12/28/92, (PB93-188217).

NCEER-93-0001 "An Experimental Study on the Seismic Performance of Brick-Infilled Steel Frames With and Without Retrofit," by J.B. Mander, B. Nair, K. Wojtkowski and J. Ma, 1/29/93, (PB93-227510, A07, MF-A02).

NCEER-93-0002 "Social Accounting for Disaster Preparedness and Recovery Planning," by S. Cole, E. Pantoja and V. Razak, 2/22/93, (PB94-142114, A12, MF-A03).

NCEER-93-0003 "Assessment of 1991 NEHRP Provisions for Nonstructural Components and Recommended Revisions," by T.T. Soong, G. Chen, Z. Wu, R-H. Zhang and M. Grigoriu, 3/1/93, (PB93-188639).

NCEER-93-0004 "Evaluation of Static and Response Spectrum Analysis Procedures of SEAOC/UBC for Seismic Isolated Structures," by C.W. Winters and M.C. Constantinou, 3/23/93, (PB93-198299).

NCEER-93-0005 "Earthquakes in the Northeast - Are We Ignoring the Hazard? A Workshop on Earthquake Science and Safety for Educators," edited by K.E.K. Ross, 4/2/93, (PB94-103066, A09, MF-A02).

NCEER-93-0006 "Inelastic Response of Reinforced Concrete Structures with Viscoelastic Braces," by R.F. Lobo, J.M. Bracci, K.L. Shen, A.M. Reinhorn and T.T. Soong, 4/5/93, (PB93-227486, A05, MF-A02).

NCEER-93-0007 "Seismic Testing of Installation Methods for Computers and Data Processing Equipment," by K. Kosar, T.T. Soong, K.L. Shen, J.A. HoLung and Y.K. Lin, 4/12/93, (PB93-198299).

NCEER-93-0008 "Retrofit of Reinforced Concrete Frames Using Added Dampers," by A. Reinhorn, M. Constantinou and C. Li, to be published.

NCEER-93-0009 "Seismic Behavior and Design Guidelines for Steel Frame Structures with Added Viscoelastic Dampers," by K.C. Chang, M.L. Lai, T.T. Soong, D.S. Hao and Y.C. Yeh, 5/1/93, (PB94-141959, A07, MF-A02).

NCEER-93-0010 "Seismic Performance of Shear-Critical Reinforced Concrete Bridge Piers," by J.B. Mander, S.M. Waheed, M.T.A. Chaudhary and S.S. Chen, 5/12/93, (PB93-227494, A08, MF-A02).

NCEER-93-0011 "3D-BASIS-TABS: Computer Program for Nonlinear Dynamic Analysis of Three Dimensional Base Isolated Structures," by S. Nagarajaiah, C. Li, A.M. Reinhorn and M.C. Constantinou, 8/2/93, (PB94-141819, A09, MF-A02).

NCEER-93-0012 "Effects of Hydrocarbon Spills from an Oil Pipeline Break on Ground Water," by O.J. Helweg and H.H.M. Hwang, 8/3/93, (PB94-141942, A06, MF-A02).

NCEER-93-0013 "Simplified Procedures for Seismic Design of Nonstructural Components and Assessment of Current Code Provisions," by M.P. Singh, L.E. Suarez, E.E. Matheu and G.O. Maldonado, 8/4/93, (PB94-141827, A09, MF-A02).

NCEER-93-0014 "An Energy Approach to Seismic Analysis and Design of Secondary Systems," by G. Chen and T.T. Soong, 8/6/93, (PB94-142767, A11, MF-A03).

NCEER-93-0015 "Proceedings from School Sites: Becoming Prepared for Earthquakes - Commemorating the Third Anniversary of the Loma Prieta Earthquake," Edited by F.E. Winslow and K.E.K. Ross, 8/16/93.

NCEER-93-0016 "Reconnaissance Report of Damage to Historic Monuments in Cairo, Egypt Following the October 12, 1992 Dahshur Earthquake," by D. Sykora, D. Look, G. Croci, E. Karaesmen and E. Karaesmen, 8/19/93, (PB94-142221, A08, MF-A02).

NCEER-93-0017 "The Island of Guam Earthquake of August 8, 1993," by S.W. Swan and S.K. Harris, 9/30/93, (PB94-141843, A04, MF-A01).

NCEER-93-0018 "Engineering Aspects of the October 12, 1992 Egyptian Earthquake," by A.W. Elgamal, M. Amer, K. Adalier and A. Abul-Fadl, 10/7/93, (PB94-141983, A05, MF-A01).

NCEER-93-0019 "Development of an Earthquake Motion Simulator and its Application in Dynamic Centrifuge Testing," by I. Krstelj, Supervised by J.H. Prevost, 10/23/93.

NCEER-93-0020 "NCEER-Taisei Corporation Research Program on Sliding Seismic Isolation Systems for Bridges: Experimental and Analytical Study of a Friction Pendulum System (FPS)," by M.C. Constantinou, P. Tsopelas, Y-S. Kim and S. Okamoto, 11/1/93, (PB94-142775, A08, MF-A02).

NCEER-93-0021 "Finite Element Modeling of Elastomeric Seismic Isolation Bearings," by L.J. Billings, Supervised by R. Shepherd, 11/8/93, to be published.

NCEER-93-0022 "Seismic Vulnerability of Equipment in Critical Facilities: Life-Safety and Operational Consequences," by K. Porter, G.S. Johnson, M.M. Zadeh, C. Scawthorn and S. Eder, 11/24/93.

NCEER-93-0023 "Hokkaido Nansei-oki, Japan Earthquake of July 12, 1993, by P.I. Yanev and C.R. Scawthorn, 12/23/93.

NCEER-94-0001 "An Evaluation of Seismic Serviceability of Water Supply Networks with Application to the San Francisco Auxiliary Water Supply System," by I. Markov, Supervised by M. Grigoriu and T. O'Rourke, 1/21/94.

NCEER-94-0002 "NCEER-Taisei Corporation Research Program on Sliding Seismic Isolation Systems for Bridges: Experimental and Analytical Study of Systems Consisting of Sliding Bearings, Rubber Restoring Force Devices and Fluid Dampers," Volumes I and II, by P. Tsopelas, S. Okamoto, M.C. Constantinou, D. Ozaki and S. Fujii, 2/4/94.

NCEER-94-0003 "A Markov Model for Local and Global Damage Indices in Seismic Analysis," by S. Rahman and M. Grigoriu, 2/18/94.

NCEER-94-0004 "Proceedings from the NCEER Workshop on Seismic Response of Masonry Infills," edited by D.P. Abrams, 3/1/94.

NCEER-94-0005 "The Northridge, California Earthquake of January 17, 1994: General Reconnaissance Report," edited by J.D. Goltz, 3/11/94.

NCEER-94-0006 "Seismic Energy Based Fatigue Damage Analysis of Bridge Columns: Part I - Evaluation of Seismic Capacity," by G.A. Chang and J.B. Mander, 3/14/94.

NCEER-94-0007 "Seismic Isolation of Multi-Story Frame Structures Using Spherical Sliding Isolation Systems," by T.M. Al-Hussaini, V.A. Zayas and M.C. Constantinou, 3/17/94.

NCEER-94-0008 "The Northridge, California Earthquake of January 17, 1994: Performance of Highway Bridges," edited by I.G. Buckle, 3/24/94.

NCEER-94-0009 "Proceedings of the Third U.S.-Japan Workshop on Earthquake Protective Systems for Bridges," edited by I.G. Buckle and I. Friedland, 3/31/94.

NCEER-94-0010 "3D-BASIS-ME: Computer Program for Nonlinear Dynamic Analysis of Seismically Isolated Single and Multiple Structures and Liquid Storage Tanks," by P.C. Tsopelas, M.C. Constantinou and A.M. Reinhorn, 4/12/94.

NCEER-94-0011 "The Northridge, California Earthquake of January 17, 1994: Performance of Gas Transmission Pipelines," by T.D. O'Rourke and M.C. Palmer, 5/16/94.

NCEER-94-0012 "Feasibility Study of Replacement Procedures and Earthquake Performance Related to Gas Transmission Pipelines," by T.D. O'Rourke and M.C. Palmer, 5/25/94.

NCEER-94-0013 "Seismic Energy Based Fatigue Damage Analysis of Bridge Columns: Part II - Evaluation of Seismic Demand," by G.A. Chang and J.B. Mander, 6/1/94, to be published.

NCEER-94-0014 "NCEER-Taisei Corporation Research Program on Sliding Seismic Isolation Systems for Bridges: Experimental and Analytical Study of a System Consisting of Sliding Bearings and Fluid Restoring Force/Damping Devices," by P. Tsopelas and M.C. Constantinou, 6/13/94.

NCEER-94-0015 "Generation of Hazard-Consistent Fragility Curves for Seismic Loss Estimation Studies," by H. Hwang and J-R. Huo, 6/14/94.